Distributed Event Triggered Control, Estimation, and Optimization for Cyber-Physical Systems

by

Xiangyu Meng

A thesis submitted in partial fulfillment of the requirements for the degree of

Doctor of Philosophy

in

CONTROL SYSTEMS

Department of Electrical and Computer Engineering

University of Alberta

Abstract

A cyber-physical system (CPS) is a system in which computational systems interact with physical processes. Control systems in a CPS application often include algorithms that react to sensor data by issuing control signals via actuators to the physical components of the CPS. Communication over wireless networks is the most energy-consuming function performed by the cyber components of a CPS; thus communication frequencies need to be minimized. Event triggered communication has been recognized as an efficient means to reduce communication rates between different cyber components.

In this thesis, event triggered schemes serve as a communication protocol to mediate data exchange in distributed control, estimation, and optimization for CPSs. Firstly, it is established that event triggered communication outperforms time triggered communication based on a finite time quadratic optimal control problem for first order stochastic systems. Secondly, it is demonstrated that event triggered impulse control still outperforms periodic impulse control for second order systems in terms of mean-square state variations, while both having the same average control rate. Thirdly, a synchronization problem is considered for multi-agent systems with distributed event triggered control updates. Given an undirected and connected network topology, conditions on the feedback gain, the triggering parameters and the maximum sampling period for solving the asymptotic synchronization problem are developed based on the feasibility of local linear matrix inequalities (LMIs). Fourthly, a distributed state estimation method is presented through wireless sensor networks with event triggered communication protocols among the sensors. Homogeneous detection criteria and

consensus filters are designed to determine broadcasting instants and perform state estimation. Lastly, an event triggered communication scheme is used to investigate distributed optimization algorithms for a network utility maximization (NUM) problem. State-dependent thresholds are established under which the proposed event triggered barrier algorithm guarantees convergence to the optimal solution to the NUM problem.

Preface

Chapter 2 of this thesis was published as X. Meng, B.Wang, T. Chen, and M. Darouach, "Sensing and actuation strategies for event triggered stochastic optimal control," *Proc. 52nd IEEE Conference on Decision and Control*, pp. 3097-3102, Florence, Italy, December 10-13, 2013. I was responsible for the analysis and design as well as the manuscript composition with the assistance of B. Wang. Professor Chen was the supervisory author and was involved with concept formation and manuscript composition. Professor Darouach contributed to manuscript edits.

Chapter 3 of this thesis was published as X. Meng and T. Chen, "Optimal sampling and performance comparison of periodic and event based impulse control," *IEEE Transactions on Automatic Control*, vol. 57, no. 12, pp. 3252-3259, December 2012.

Chapter 5 of this thesis was published as X. Meng and T. Chen, "Optimality and stability of event triggered consensus state estimation for wireless sensor networks," *Proc. American Control Conference*, pp. 3565-3570, Portland, Oregon, USA, June 4-6, 2014.

The analysis in Chapter 4 and Chapter 6, the concluding remarks in Chapter 7, as well as the literature review in Chapter 1 are my original work.

Acknowledgements

This thesis is a milestone on my path to obtaining the PhD degree at the University of Alberta. At the end of my PhD program, I would like to thank the guidance of my supervisor, help from colleagues, and support from my family.

First and foremost, I would like to express my sincere gratitude to my supervisor, Professor Tongwen Chen for his excellent guidance and continued support. He helped me come up with the thesis topic - event triggered sampling whilst allowing me the room to work in my own way. I am grateful to Professor Chen for his support of trips to several international conferences. At conferences, I disseminated my research results and met people who were interested in the same topic of research. I also want to give my gratitude to Professor Chen for his precious critique and proofreading for this thesis.

Besides my supervisor, I would like to thank the rest of my candidacy exam committee: Professor Horacio Marquez, Associate Professor Qing Zhao, Professor Alan Lynch, and Associate Professor Mahdi Tavakoli, for their insight comments, and difficult questions, which made me aware of my weakness and how to improve myself.

I wish to thank my co-authors, Dr. Feng Xiao and Dr. Bingchang Wang, for academic collaborations that have profoundly influenced my way of thinking. I have benefited greatly from the collaboration with Dr. Xiao. Without his inspiration, the idea on event triggered control for multi-agent systems would not be materialized. The discussions with Dr. Bingchang Wang were not only of great importance for the development of my research on event triggered control for stochastic systems, but also helped me confidence in my knowl-

edge of stochastic control.

My sincere thanks also go to Professor Karl Henrik Johansson for offering me a visiting opportunity in his group at the Royal Institute of Technology (KTH), Stockholm, Sweden. Discussions with Professor Joao Pedro Hespanha from the University of California, Santa Barbara, USA, and Assistant Professor Maben Rabi from the Chalmers University of Technology, Sweden, have been illuminating. I would also like to thank Associate Professor Dimos Dimarogonas, Dr. Ziyang Meng, Dr. Junfeng Wu, Dr. Kun Liu, and Dr. Chithrupa Ramesh for discussions regarding topics on event triggered sampling during my visit.

I am indebt to my wife Chunyan Gao, who sacrificed a lot to support me, and took more responsibilities in looking after our daughter Kaylee. Thanks for her unwavering love.

Contents

List of Tables

List of Figures

Chapter 1

Introduction

In this chapter, we will introduce cyber-physical systems (CPSs), discuss event triggered sampling and communication, and review the relevant literature.

1.1 Cyber-Physical Systems and Event Triggered Sampling

The arrival of digital technologies has given rise to a tight combination of, and coordination between, communication, computational, control units and physical processes. A new term has been coined to characterize this generation: *Cyber-Physical Systems* (CPSs) [59]. CPSs refer to the orchestration of networked computational resources and physical processes. CPSs occur naturally in such diverse areas as communication, consumer appliances, energy, civil infrastructure, health care, manufacturing, military, robotics, and transportation. The core of CPSs is networking. The introduction of real-time networks raises some design challenges regarding limited sensor energy, limited communication bandwidth, and limited computational resource. All of these suggest that event triggered sampling should be utilized to provide a solid information exchange mechanism for design, deployment, monitoring and adaptation of CPSs. Event triggered sampling has many advantages compared with periodic sampling, such as control by exception. It is useful in situations when control actions are expensive and it is a prevalent form of control in biological systems. Event triggered sampling provides an alternative way to determine when communication actions should be invoked, which reduces communication bandwidth usages and controller update frequencies. Event triggered sampling is therefore used in many feedback control systems, and various terms are utilized to express this sampling strategy, such as level-crossing sampling, magnitude-driven sampling, sampling in the amplitude domain, and Lebesgue sampling. In the sensor network community, the magnitude-driven/level-crossing sampling is known as the send-on-delta or

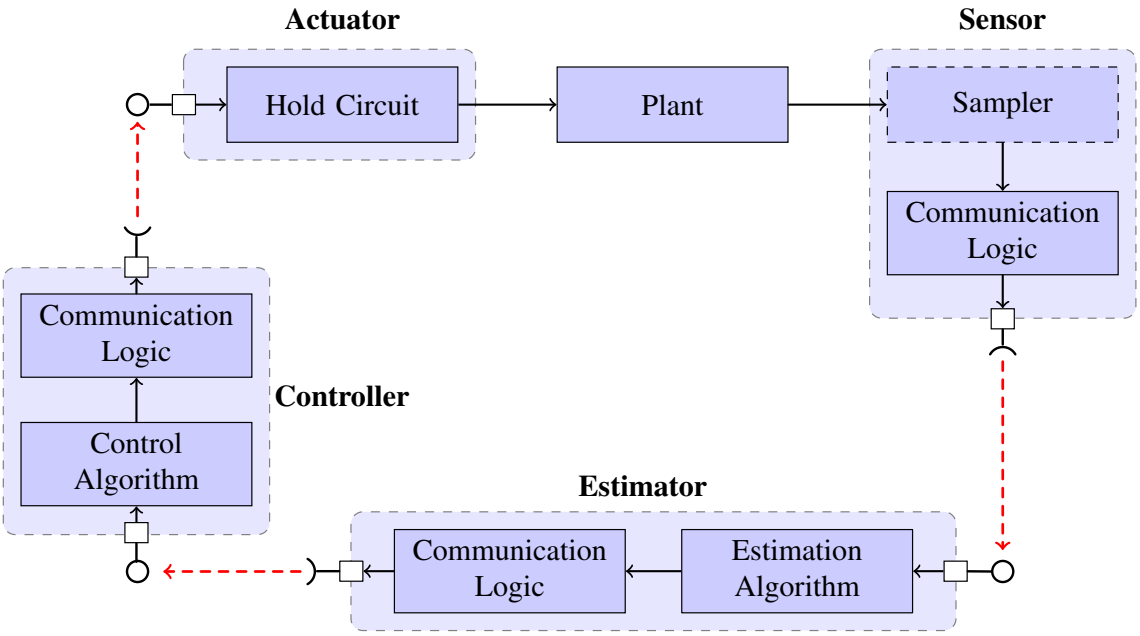

Figure 1.1: Generic model of event triggered control systems

deadbands.

Control systems in a CPS application often include algorithms that react to sensor data by issuing control signals via actuators to physical components of the CPS. Classical control theory assumes a continuous or periodic signaling, where the controller continually or periodically observes the physical subsystem, and continually or periodically provides actuation to the physical component. Continuous communication might be impractical and periodic communication may be inflexible. In a typical CPS architecture, the signaling is mediated by software and networks that do not possess such continuous or periodic behavior. CPSs, however, require extending the classic control theory to embrace the dynamics of software and networks, which can have profound effects on stability and dynamics of the physical subsystems. Detailed overview of event triggered control systems can be found in [4, 111, 62, 44, 15, 66, 85].

The generic structure of a system with event triggered communication is depicted in Figure 1.1. Each cyber subsystem (sensor, estimator, controller, and actuator) is deployed in an intelligent node communicating via processing incoming events and triggering outgoing events according to its communication logic. The sensor measures the output of a continuous plant continuously or periodically. Then it determines if the plant output should be directed to the estimator according to its communication logic. The estimator obtains

an estimate of the state using an estimation algorithm after receiving data from the sensor. Its communication logic determines if the estimated state should be forwarded to the controller. The controller is invoked and then calculates a control value according to a control algorithm. The controller sends the new control value to the actuator according to its own communication logic.

In the event triggered system shown in Figure 1.1, the sensor, estimator, controller, and actuator reside on various nodes in a network. There are many different topologies that can be imagined. The controller could be co-located with the actuator; the estimator could be co-located with the sensor. In addition, the sensor, estimator, and controller nodes could be very simple and contain no communication logic.

1.2 Communication Logic Design

Since an efficient use of network resources is one of the main motive forces for application of event triggered sampling, design of communication protocols is a central issue. For implementation, the communication protocol should admit a strictly positive lower bound of inter-event times. The commonly used communication logics are discussed as follows.

Level Crossing Sampling

Level crossing sampling, also known as Lebesgue sampling, is a threshold based encoding scheme [56].

Let $\mathcal{L}$ be a given infinite set of levels:

$$\mathcal{L} = \{\ldots, l_{-2}, l_{-1}, l_0, l_1, l_2, \ldots\}$$

with $l_0 = 0$, $l_i \in \mathbb{R}$, and $l_i < l_{i+1}$ for $\forall i \in \mathbb{Z}$. If a set of levels with all non-zero levels is desirable, l_0 can be removed from the set $\mathcal{L}$. The sampling instants triggered by $\mathcal{L}$ for signal $x(t)$ are defined through fresh crossings of levels:

$$t_0 = 0, \qquad t_{k+1} = \inf\left\{t \,|t > t_k, x\left(t\right) \in \mathcal{L}, x\left(t\right) \neq x\left(t_k\right)\right\}.$$

Error based communication logic conditions can be generalized by introducing a generic function $g : \mathbb{R}^n \times \mathbb{R}^n \times [0, \infty) \to \mathbb{R}$, which must have the following properties:

1. $g\left(x, e, t\right)$ is a piecewise continuous function in t;

2. $g(x, e, t) \geq 0$ for almost all t except event instants;

3. $g(x, e, t) < 0 \Rightarrow e(t^+) = 0 \Rightarrow g(x, e, t^+) \geq 0$.

The initial event instant is assumed to be t_0. Property 2 must be ensured for almost all t. It is natural to set the next event instant t_{k+1} equal to the first time when $g(x, e, t) < 0$. This observation is condensed in the following lemma:

Lemma 1 *If the event instants are set according to*

$$t_{k+1} = \inf\{t : t > t_k,\ g(x(t), e(t), t) < 0\},$$

then we have

$$g(x, e, t) \geq 0, \qquad \textit{for } \forall t \in [t_k, t_{k+1}).$$

This lemma is easy to prove by the property that $g(x(t), e(t), t)$ is a continuous function in $t \in [t_k, t_{k+1})$.

Send-on-Delta Triggering Logic

Send-on-delta sampling is a principle of non-equidistant sampling, in which not all sampled values will be sent, but only those which have sufficiently large differences to the previously transmitted value. The commonly used communication logic strategies based on errors are summarized in Table 1.1 [103]. Here AE denotes the absolution error between the current state and the state at the last event time; IAE denotes the integrated absolute error from the last event times; APE denotes the error between a prediction of the state and its current state; IAPE denotes the integral of the error between the prediction and the state; and IAEE denotes the energy of the error between the current state and the state at the last event time.

Table 1.1: Error based conditions of communication strategies applied to the sensor

Error Based Condition	Label	Definition of Error
$g(e) = \delta - \|e(t)\|$	AE	$e(t) = x(t_k) - x(t)$
$g(e) = \delta - \int_{t_k}^{t} \|e(\tau)\| d\tau$	IAE	$e(t) = x(t_k) - x(t)$
$g(e) = \delta - \|e(t)\|$	APE	$e(t) = \hat{x}(t) - x(t)$
$g(e) = \delta - \int_{t_k}^{t} \|e(\tau)\| d\tau$	IAPE	$e(t) = \hat{x}(t) - x(t)$
$g(e) = \delta - \int_{t_k}^{t} \|e(\tau)\|^2 d\tau$	IAEE	$e(t) = x(t_k) - x(t)$

Adaptive Triggering Logic

The general form of adaptive triggering conditions can be formulated as

$$g\left(x,e\right)=\delta+\sigma x^{T}\left(t\right)\Phi x\left(t\right)-e^{T}\left(t\right)\Psi e\left(t\right),$$

which includes most existing triggering conditions as special cases. For example, if we take $\delta=0$, $\Phi=\Psi=I$, it reduces to the event triggering mechanism that was proposed in [108]. Also it includes the send-on-delta triggering rule as a special case by taking $\sigma=0$, and $\Psi=I$.

Triggering Logic Based on Sampled Data

Sampled-data triggering logic is constructed to determine whether the newly sampled data should be sent out by using the following triggering condition:

$$g\left(x,e\right)=\delta+\sigma x^{T}\left(kh\right)\Phi x\left(kh\right)-e^{T}\left(kh\right)\Psi e\left(kh\right),$$

where h is the sampling period. Event detectors based on sampled data do not need to monitor the state and test the triggering condition continuously. The triggering condition is supervised only at sampling instants. Therefore, the inter-event interval is at least lower bounded by the sampling period, which is particularly useful in multi-agent systems [78].

Triggering Logic Based on Relative Entropy

Let probability density function (PDF) $p_1\left(x\right)$ be a posterior distribution while $p_2\left(x\right)$ a prior distribution. The Kullback-Keibler divergence or relative entropy is defined as

$$D_{KL}\left(p_1\left(x\right)||p_2\left(x\right)\right)=\int_{-\infty}^{+\infty}p_1\left(x\right)\log\frac{p_1\left(x\right)}{p_2\left(x\right)}dx.$$

The communication logic is defined as

$$g\left(x\right)=\delta-D_{KL}\left(p_1\left(x\right)||p_2\left(x\right)\right),$$

where D_{KL} is known as the information gain [73].

Triggering Logic Based on Variance

Let $v(k)$ denote the state prediction variance. A measurement is transmitted if and only if $\gamma(v(k))$ exceeds a tolerable bound, that is,

$$g\left(v\right)=\delta-\gamma(v(k)),$$

where $\gamma(v(k))$ is a function of $v(k)$ [110].

1.3 Actuator Options

Control algorithm design is essentially the problem of finding an open loop control signal that drives the system from its state at the time of event to a desired state. Many methods from control system design can be used for designing control signal generating circuits. For regulation problems, a dead-beat controller can be used which drives the state to zero in a finite time. Optimal control [9, 10] and model predictive control [72, 14, 100, 37] are other alternatives that are particularly useful when there are restriction on the control signal. The design of hold circuits will be discussed as follows for event triggered control systems.

Zero-Order Hold

Since computer control is widely used, zero-order hold becomes a standard solution [5]. The causal reconstruction of a zero-order hold is given by

$$\hat{x}(t) = x(t_k), \qquad t_k \leq t < t_{k+1}.$$

This means that the reconstructed signal is piecewise constant, continuous from the right, and equal to the sampled signal at event instants. Because of its simplicity, the zero-order hold is very common in event triggered control systems, which is not only used at actuators, but also at sensors, estimators, and controllers. The standard D-A converters are often designed in such a way that the old value is held constant until a new value is received.

Higher-Order Hold

The zero-order hold can be regarded as an extrapolation using a polynomial of degree zero. For smooth functions, it is possible to obtain smaller reconstruction errors by extrapolation with higher-order polynomials. A first-order causal polynomial extrapolation gives

$$\hat{x}(t) = x(t_k) + \frac{t - t_k}{t_k - t_{k-1}} \left(x(t_k) - x(t_{k-1}) \right), \qquad t_k \leq t < t_{k+1}.$$

Differences between different holds are illustrated by a simple example in [4], which shows that the hold circuit has important implication to system performance. The impulse hold where the control signal is an impulse is an extreme case [4, 77]. Since the hold circuit is important, it is natural that it should be matched to the process [83].

1.4 Modeling Event Triggered Control Systems

Let us take an event triggered state feedback control of linear time-invariant systems as an example for illustration. Consider the system described by

$$\dot{x}(t) = Ax(t) + Bu(t), \tag{1.1}$$

with $x(t) \in \mathbb{R}^n$, and $u(t) \in \mathbb{R}^p$. The control signal $u(t)$ is kept constant between two consecutive event instants, that is,

$$u(t) = Kx(t_k), \tag{1.2}$$

for $t \in [t_k, t_{k+1})$.

Systems with event triggered control can be modeled in different ways, relating to various tools and theories which are potentially applicable. We will look into this in more detail below.

Systems with Measurement Errors

Define the measurement error $e(t)$ to be

$$e(t) = x(t_k) - x(t),$$

for $t \in [t_k, t_{k+1})$. The evolution of the system in (1.1) under the implementation of the control law in (1.2) is thus described by

$$\dot{x}(t) = Ax(t) + BK[x(t) + e(t)] = (A + BK)x(t) + BKe(t). \tag{1.3}$$

The notion of *Input-to-State Stability* (ISS) can be used to characterize the stability of the closed-loop system in (1.3).

Systems with Input Delay

Define a function $\tau(t)$ as

$$\tau(t) = t - t_k$$

for $t \in [t_k, t_{k+1})$. Obviously

$$0 \leq \tau(t) < t_{k+1} - t_k$$

and

$$\dot{\tau}(t) = 1.$$

Utilizing $\tau(t)$, one can rewrite the system in (1.1) as

$$\dot{x}(t) = Ax(t) + BKx(t - \tau(t)). \tag{1.4}$$

Therefore, the behavior of the closed-loop system in (1.4) can be described by a system with input delay.

Impulsive Systems

Let

$$e(t) = x(t_k) - x(t)$$

denote the error at time t. Define $\chi = \begin{bmatrix} x^T & e^T \end{bmatrix}^T$, which yields the dynamics of the system

$$\begin{aligned} \dot{\chi}(t) &= \bar{A}\chi(t), \qquad \text{when } \chi(t) \in \mathcal{F}, \\ \chi\left(t^+\right) &= \bar{C}\chi(t), \qquad \text{when } \chi(t) \in \mathcal{J}, \end{aligned} \tag{1.5}$$

where

$$\bar{A} = \begin{bmatrix} A + BK & BK \\ -A - BK & -BK \end{bmatrix}, \qquad \bar{C} = \begin{bmatrix} I & 0 \\ 0 & 0 \end{bmatrix}.$$

Here $\mathcal{F}$ and $\mathcal{J}$ denote the flow and jump sets, respectively. Note that the event times t_k are now related to the time at which the jumps of χ take place, in which a reset occurs according to $e\left(t_k^+\right) = 0$, but $x\left(t_k^+\right) = x(t_k)$ remains the same. The system flows between two consecutive event instants. This yields an impulsive system of the form in (1.5).

Hybrid Systems

The hybrid representation is more formally written as follows:

$$\begin{cases} \dot{x}(t) = Ax(t) + Bu(t) \\ \dot{u}(t) = 0 \end{cases} \qquad \text{when } x(t) \in \mathcal{F},$$

$$\begin{cases} x(t^+) = x(t) \\ u(t^+) = Kx(t) \end{cases} \qquad \text{when } x(t) \in \mathcal{J},$$

where $\mathcal{F}$ and $\mathcal{J}$ are the flow and jump sets, respectively.

The definition of stability and sufficient conditions to guarantee the stability for different systems can be found in Appendix A.

1.5 Literature Survey

1.5.1 Event Triggered Control

There are two main research streams concerning event triggered control: event triggered control for stochastic systems, and event triggered control for deterministic systems.

A. Event Triggered Control for Stochastic Systems

Event triggered control for stochastic systems focuses on obtaining optimal or sub-optimal event triggering mechanisms for a predefined performance index. The research in this line was sparked by the pioneering work [4]. This paper considered a scalar diffusion process where the control signal was an impulse signal. Under an event triggered scheme, the control action was taken whenever the state magnitude exceeded a specified level; while under the periodic manner, the control action was taken at every sampling instant. Reference [4] showed that event triggered systems had better performance than periodically triggered systems in terms of the steady-state variance while operating at the same mean control frequency. This work was extended to the sporadic control with a well-defined minimum inter-event time [46] and generalized to a class of symmetric second-order systems [77]. In [46], two sporadic control schemes, sporadic control with continuous and discrete measurements, were explored for first-order linear stochastic systems. The results showed that sporadic control could give better performance than periodic control in terms of both reduced process state variance and reduced control action frequency. In [77], it was demonstrated that the event triggered impulse control still outperformed periodic impulse control for higher-order systems in terms of mean-square state variations while both having the same average control rate. The authors in [87] showed that the certainty equivalence controller was optimal for an extended linear-quadratic-Gaussian (LQG) framework that incorporated communication constraints. A similar result was also given in [99].

B. Event Triggered Control for Deterministic Systems

On the other hand, event triggered control for deterministic systems focuses on closed-loop system stability. The literature on stability of event triggered control algorithms is by now extensive. The line of research is further divided into the following branches.

B1. Event Triggered Control for Linear/Nonlinear Systems

The work in [108] proposed adaptive triggering rules to update control actions whenever it was necessary to ensure a certain decrease in a Lyapunov function. This paper showed that the zero-order hold implementation of a simple state feedback controller based on the event triggered paradigm could guarantee a desired performance while relaxing periodic execution requirements. Later on, the idea was extended to trajectory tracking for nonlinear systems [109] and generalized in [26]. The assumption that system states are perfectly measured is very important in monitoring and control of event triggered control systems. However, in many applications only partial state variables are directly measured. Thus, it is natural to design output feedback controllers. The output feedback control incorporating event triggered communication was studied in [32, 23, 120]. The primary challenge of extending existing results from event triggered state feedback to output feedback is how to derive a strictly positive lower bound of the inter-event times; and some strategies have been proposed. In [23], the performance degenerated from asymptotic stability to ultimate bounded stability in order to guarantee a minimum inter-event time.

It is noted that all the work above is based on continuous event detection. The sampled-data event detection approach is introduced to relax the continuous monitoring. Periodic event triggered control is a control strategy that combines ideas from conventional periodic sampled-data control and event triggered control [79, 43, 80]. In [80], events were triggered by using only the sensor output information to achieve asymptotic stability and a positive constant lower bound of inter-event times simultaneously. These references are all based on Lyapunov techniques. A continuous Lyapunov function is required to be monotonically decreasing in the event based control system as it is in continuous feedback systems; this, however, is not necessary as shown in [114, 19].

Although the Lyapunov technique is the workhorse for recent studies on event triggered control systems, there were also other methods in the literature. By modeling event triggered control systems as piecewise linear systems [45], event-driven PID, state feedback, and output feedback control schemes were considered. The use of a generalized hold instead of a zero-order hold to generate inter-sample open-loop control signals was studied in [32]. Similarly, a model-based approach was proposed in [71] for event-based state feedback control in which a control input generator mimicked a continuous feedback between two consecutive event times; then this approach was extended to coping with communication delays and packet losses in the feedback link in [60]. The discrete counterpart was addressed in [28], which also incorporated an on-line parameter estimation of dynamical systems. Com-

bining the sampled-data communication logic and model-based approach was done in [42]. The stabilization problem of linear, discrete-time, time-varying systems in the context of supervised control was considered in [53].

B2. Event Triggered Control for Networked Control Systems

Event triggered control for networked control systems with time-varying delays was studied in [122, 94, 95] based on a sampled-data communication logic. The packet disorder was not considered by the authors. However, there exist packet disorders in event triggered control systems. A solution to avoid the phenomenon of packet disorder was provided in [76]. Other solutions to deal with communication delays and packet losses can be found in [61, 29]. Later on, the idea was extended to wireless sensor networks [74]. In [74], a decentralized event triggered implementation of centralized controllers over wireless sensor networks was presented. Event triggered data transmission in distributed networked control systems with packet losses and transmission delays was examined in [113]. A control design problem for uncertain event triggered networked control systems with both state and input quantizations was investigated in [51].

B3. Event Triggered Control for Multi-Agent Systems

Event triggered communication is also proved especially useful in multi-agent systems, such as consensus algorithms [67, 21, 117], and tracking control [49]. A challenging issue posed to this problem is the minimum inter-event interval. Unlike linear systems, there exist few results which derive a strictly positive lower bound of inter-event times for multi-agent systems, although the consensus can always be guaranteed with reduced control updates [25, 30]. Currently, the only solution is based on sampled-data event detection [78]. Note that existing results on distributed event triggered multi-agent systems focus on single- or double-integrator dynamics mostly. Event triggered methods for linear multi-agent systems were presented in [124, 127]; output synchronization of multi-agent systems was presented in [121].

1.5.2 Event Triggered Estimation

When the state of a process is not measured directly, we can construct an estimator to provide an estimate of system state [2, 106]. The estimation problem with event triggered communication is not a standard problem. If no event occurs, the information can only be inferred

from the communication logic; when an event occurs, a precise measurement of the output is obtained.

For systems subject to energy bounded disturbances, the $\mathcal{H}_\infty$ filter could be used to minimize the $\mathcal{H}_\infty$ norm of filtering error systems. Full order linear dynamic filters with communication logic for continuous-time systems can be found in [52, 123]. The work in [81] introduced a general event triggered framework of state estimation for discrete-time systems with parameter uncertainties residing in a polytope. A robust filter was designed to ensure the ℓ_2 stability from disturbance to the estimation error and to minimize the ℓ_2 gain subject to both packet rate and size constraints.

For systems with Gaussian noise, modified Kalman filter algorithms are usually used to solve networked estimation problems with reduced communication. Early work on this problem focused on modifying the standard Kalman filter algorithm to solve networked estimation problems. Under the send-on-delta method, there was no sensor data transmission if the sensor value did not change more than the specified value from the previously transmitted one. This way, sensor data traffic could be reduced with relative small estimation performance degradation [107]. The estimation performance was improved by [88], where the states were periodically estimated by the estimator node regardless of whether the sensor nodes transmitted data or not. The idea was also used to design fault isolation filters to improve resource utilization with graceful fault estimation performance degradation [63], and was generalized in [7]. An optimal estimator for a chosen process model can be derived by finding the conditional probability density of the process state given available information. The amount of computation involved makes the optimal filter intractable in general [116]. The optimal filter is approximated by different techniques, such as the Gaussian sum filter [105], and the particle filter [35, 16]. Distributed consensus state estimation with event triggered communication protocols among sensors in a wireless sensor network was presented in [82].

1.5.3 Event Triggered Optimization

Many problems in control engineering can be formulated as optimization problems. Distributed algorithms that solve network optimization problems are distributed gradient-based algorithms that converge to the optimal point provided that the communication between subsystems is sufficiently frequent. Event triggered distributed algorithms were introduced in a scenario where multiple agents cooperated to control their individual state so as to optimize a common objective while communicating with each other to exchange state information

[126]. The distributed event triggered optimization was also well suited for solving the active optimal power flow problem [75]. These results confirm that approximated solutions can be obtained with significantly less communication while they have the same accuracy as solutions computed without event triggered communication.

1.6 Thesis Outline

The rest of this thesis is organized as follows.

In Chapter 2, the problem of optimal control for first order stochastic systems with a quadratic performance index over a finite time horizon is studied. The performance of three messaging policies for sensing combined with two hold circuits for actuation is compared based on optimization over the parameters of event detection and feedback control. The sampling rules include deterministic sampling (DS), level-crossing sampling (LCS) and optimal sampling (OS), and the hold circuits include zero order hold (ZOH) and generalized hold (GH). Some general results are established that level-crossing sampling performs more effectively than deterministic sampling and generalized hold outperforms zero order hold. Chapter 2 is based on the following publication:

- **X. Meng**, B.Wang, T. Chen and M. Darouach, "Sensing and actuation strategies for event triggered stochastic optimal control," *Proc. 52nd IEEE Conference on Decision and Control*, pp. 3097-3102, Florence, Italy, December 10-13, 2013.

In Chapter 3, several issues of periodic and event based impulse control for a class of second order stochastic systems are considered, including the optimal sampling and performance comparison. The procedures are provided to design the optimal sampling period for periodic sampling and optimal threshold for event based sampling. It is demonstrated that event based impulse control outperforms periodic impulse control in terms of mean square state variations, while both having the same average control rate. Chapter 3 is based on the following publication:

- **X. Meng** and T. Chen, "Optimal sampling and performance comparison of periodic and event based impulse control," *IEEE Transactions on Automatic Control*, vol. 57, no. 12, pp. 3252-3259, December 2012.

Chapter 4 considers the synchronization problem for multi-agent systems with event based control updates, where all agents share the same dynamic model of any order, including single- and double-integrator dynamics as special cases. Controller updating instants are

determined by distributed event detectors in individual agents. Whenever an event condition is violated, the agent and one neighbor involved in the event will update their own control action individually. The problem is formulated so that event conditions need to be checked only at discrete sampling instants; the control update periods are thus at least lower bounded by the synchronous sampling period for all agents. Given an undirected and connected network topology, conditions on the feedback gain, the triggering parameters and the maximum sampling period for solving the asymptotic synchronization problem are developed based on feasibility of local linear matrix inequalities (LMIs). Finally, key design procedures are illustrated by numerical simulations.

Chapter 5 presents distributed state estimation methods through wireless sensor networks with event triggered communication protocols among the sensors. Homogeneous detection criteria are designed on each sensor node to determine the broadcasting instants. Thus, a consensus on state estimates is reached with all estimator sensors for a suboptimal consensus filter. The purpose of event detection is to achieve energy efficient operation by reducing unnecessary interactions among the neighboring sensors. In addition, the performance of the proposed state estimation algorithm is validated using a simulation example. Part of Chapter 5 is based on the following publication:

- **X. Meng** and T. Chen, "Optimality and stability of event triggered consensus state estimation for wireless sensor networks," *Proc. American Control Conference*, pp. 3565-3570, Portland, Oregon, USA, June 4-6, 2014.

Chapter 6 is concerned with event triggered distributed optimization for network utility maximization (NUM) problems. Under the event triggering logic, a source broadcasts its information to links when a local signal exceeds a state dependent threshold. A similar communication logic is executed by all links, where the link broadcasts its information to all sources that use the link. The algorithm is based on a sequential barrier method, which can be applied to optimization problems with constraints. The efficiency of the proposed scheme is verified via simulations. The simulation result shows that the proposed algorithm reduces the number of message exchanges while guaranteeing the converge to the optimal solution.

This following publications do not form any part of this thesis, but contribute to the event triggered perspective of this work.

- F. Xiao, **X. Meng** and T. Chen, "Sampled-data consensus in switching networks of integrators based on edge events," Accepted in *International Journal of Control*.

- B. Wang, **X. Meng** and T. Chen, "Event based pulse-modulated control of linear stochastic systems," *IEEE Transactions on Automatic Control*, vol. 59, no. 8, pp. 2144-2150, 2014.

- **X. Meng** and T. Chen, "Event detection and control co-design of sampled-data systems," *International Journal of Control*, vol. 87, no. 4, pp. 777-786, 2014.

- **X. Meng** and T. Chen, "Event triggered robust filter design for discrete-time systems," *IET Control Theory & Applications*, vol. 8, no. 2, pp. 104-113, January 2014.

- **X. Meng** and T. Chen, "Event based agreement protocols for multi-agent networks," *Automatica*, vol. 49, no. 7, pp. 2123-2132, July 2013

- **X. Meng** and T. Chen, "Event-based stabilization over networks with transmission delays," *Journal of Control Science and Engineering*, vol. 2012, article ID 212035, 8 pages, 2012. doi:10.1155/2012/212035

- **X. Meng**, and T. Chen, "Event-driven communication for sampled-data control systems," *Proc. 2013 American Control Conference*, pp. 3008-3013, Washington, DC, USA, June 17-19, 2013.

- F. Xiao, **X. Meng**, and T. Chen, "Average sampled-data consensus driven by edge events," *Proc. 31st Chinese Control Conference*, pp. 6239-6244, Hefei, China, July 25-27, 2012.

Chapter 2

Sensing and Actuation Strategies for Event Triggered Optimal Control

In the chapter, the problem of optimal control for first order stochastic systems with a quadratic performance index over a finite time horizon is studied. The performances of three messaging policies for sensing combined with two hold circuits for actuation are compared based on optimization over the parameters of event detection and feedback control.

2.1 Introduction

The defining feature of networked control systems is reflected in limited channel capacities, which are characterized by constrained data rates through shared or wireless networks, thus reducing the average number of transmissions, and limiting the minimum time interval between transmissions. From practical considerations, it is natural that the sampling frequency must be high relative to the rate of change of the signals of interest, such as level-crossing sampling, send-on-delta, adaptive sampling, and model based sampling.

This chapter discusses the problem of event triggered sampling and control co-design for first order stochastic systems. The problem setup was originally considered in [97]; but this chapter is different in the following aspects: (1) A quadratic performance index involving control cost is considered as the criterion for designing event detectors and controllers in a finite time horizon; (2) instead of deterministic sampling and optimal sampling, level-crossing sampling [56] is also presented based on the work in [98] for the estimation problem with an emphasis here more on jointly optimizing the control and threshold; (3) the impact of generalized hold rather than just ZOH used in earlier papers is analyzed. The generalized hold scheme could be justified by the choice of the network topology that the controller co-locates with the actuator but resides on a separate node with the sensor and recent results

on the structure of joint optimal event triggered control/estimation [99, 65, 87]. For zero order hold, these measurements are directly used for feedback; whereas for generalized hold, these measurements permit us to perform a mean square estimation of the state, and the estimated state is subsequently used for feedback. The feedback gain and the parameter of the event detector are optimized based on a quadratic performance index. By comparing the different event triggered sensing and actuation schemes, it is demonstrated that level-crossing sampling improves the performance significantly, and generalized hold is desirable for event based control.

2.2 Problem Formulation

Consider a first order linear diffusion process $x(t)$ described by the stochastic differential equation

$$dx(t) = ax(t)\,dt + u(t)\,dt + d\omega(t), \qquad x(0) = 0, \tag{2.1}$$

where $\omega(t)$ is a standard Wiener process or Brownian motion process, the drift coefficient a is known, and $u(t)$ is the control input.

The goal here is to minimize the quadratic performance criterion

$$J = \mathbb{E}\left[\int_0^T x^2(t)\,dt\right] + \rho\mathbb{E}\left[\int_0^T u^2(t)\,dt\right] \tag{2.2}$$

with only one sample allowed over the finite interval $[0, T]$ by using different sampling strategies and hold circuits, respectively. Here the positive ρ is the relative weight. Because of the important Markov property for diffusions, the control signals depend only on the received sample at the stopping time in the time interval $[0, T]$. For zero order hold, the control signals are given by

$$u(t) = \begin{cases} 0 & \text{if } 0 \le t < \tau, \\ Kx(\tau) & \text{if } \tau \le t \le T. \end{cases} \tag{2.3}$$

For generalized hold, the control signals are given by

$$u(t) = \begin{cases} 0 & \text{if } 0 \le t < \tau, \\ K\hat{x}(t) & \text{if } \tau \le t \le T, \end{cases} \tag{2.4}$$

where $\hat{x}(t)$ is the mean square estimation of $x(t)$ and obeys a linear ordinary differential equation

$$\frac{d\hat{x}(t)}{dt} = a\hat{x}(t) + u(t) \tag{2.5}$$

for $\tau \leq t \leq T$, and $\hat{x}(\tau) = x(\tau)$. Here the switching time τ is a stopping time determined by sampling mechanisms including deterministic sampling, level-crossing sampling, and optimal sampling, which will be explained subsequently.

2.3 Optimal Design for Zero Order Hold

To facilitate the notation, define functions

$$h(t) \triangleq \frac{e^{2at} - 2at - 1}{4a^2}, \text{ and } g(t) \triangleq \frac{e^{2at} - 1}{2a}.$$

Assume $a \neq 0$. Using the zero order hold in (2.3), split the aggregate quadratic cost into two parts as follows:

$$J = J_1 + J_2, \tag{2.6}$$

where

$$\begin{aligned} J_1 &\triangleq \mathbb{E}\left[\int_0^\tau x^2(t)\,dt\right], \\ J_2 &\triangleq \mathbb{E}\left[\int_\tau^T x^2(t)\,dt\right] + \rho\mathbb{E}\left[\int_\tau^T K^2 x^2(\tau)\,dt\right]. \end{aligned}$$

The first term of the expression above is given by

$$J_1 = \mathbb{E}\left[\int_0^\tau \int_0^t e^{2a\theta} d\theta dt\right] = \mathbb{E}\left[\frac{e^{2a\tau} - 2a\tau - 1}{4a^2}\right].$$

The second term represents the part of the cost incurred on $[\tau, T]$, which can be expressed as

$$\begin{aligned} J_2 =& \mathbb{E}\left[h(T-\tau) + x^2(\tau)\, g(T-\tau) - x^2(\tau)(4\alpha)^{-1}\beta^2\right] \\ &+ \mathbb{E}\left[x^2(\tau)\,\alpha\left(K + (2\alpha)^{-1}\beta\right)^2\right] \end{aligned}$$

where

$$\begin{aligned} \alpha &= \rho(T-\tau) + \frac{e^{2a(T-\tau)} - 4e^{a(T-\tau)} + 3 + 2a(T-\tau)}{2a^3}, \\ \beta &= \frac{e^{2a(T-\tau)} - 2e^{a(T-\tau)} + 1}{a^2}. \end{aligned}$$

From the expression above and the fact $\alpha > 0$, the optimal choice of the feedback gain K^* is

$$K^* = -\frac{\beta}{2\alpha}. \tag{2.7}$$

Remark 2 *For zero order hold, the optimal feedback gain K^* cannot be predetermined; it is closely related to the sampling instant τ but does not depend on the state $x(\tau)$ at the sampling instant directly. Whatever triggers the sampling, the controller has to wait for the sampling time to compute the optimal feedback gain.*

Let K^* given by equation (2.7) be the optimal feedback gain. Thus, the original optimization problem is reduced to choose the pair $(\tau, x(\tau))$ such that the objective function

$$J = \mathbb{E}\left[h(\tau) + h(T-\tau) + x^2(\tau)\, g(T-\tau) - x^2(\tau)\,\frac{\beta^2}{4\alpha}\right]$$

is minimized.

Next, two different classes of sampling strategies are going to be considered and the optimal design will be conducted within each class to minimize the above performance measure. The classes are deterministic sampling and level-crossing sampling.

2.3.1 Optimal Deterministic Sampling

Let us first minimize the above performance measure over the class of deterministic sampling times. For deterministic sampling

$$\mathbb{E}\left[x^2(\tau)\right] = \frac{e^{2a\tau} - 1}{2a}.$$

The above performance measure then can be written as follows:

$$J = \frac{e^{2aT} - 2aT - 1}{4a^2} - \mathbb{E}\left[\frac{e^{2a\tau} - 1}{4a^2}\frac{\beta^2}{4\alpha}\right].$$

The optimal deterministic sampling time τ is the one that minimizes the above performance for a given weight ρ:

$$\tau^* = \arg\min_{0\le\tau\le T} J.$$

The Brownian Motion Process Case

Now let us detail the drift coefficient $a = 0$ which brings about a Brownian motion process. For $a = 0$, the performance in (2.2) takes the form

$$\begin{aligned} J =& \mathbb{E}\left[\tau(T-\tau) + K\tau(T-\tau)^2 + \rho K^2 \tau(T-\tau)\right] \\ &+ \mathbb{E}\left[\frac{\tau^2}{2} + \frac{(T-\tau)^2}{2} + K^2\frac{\tau(T-\tau)^3}{3}\right]. \end{aligned}$$

The expression above permits us to determine that the optimal solution to the feedback gain is

$$K^* = -\frac{3\left(T-\tau\right)}{2\left(T-\tau\right)^2+6\rho}$$

and the objective function thus becomes

$$J = \frac{T^2}{2} - \mathbb{E}\left[\frac{3\tau\left(T-\tau\right)^3}{4\left(\left(T-\tau\right)^2+3\rho\right)}\right]. \tag{2.8}$$

It is easy to check out that the optimal sampling time falls into the interval

$$\frac{T}{4} \leq \tau^* \leq \frac{T}{2}.$$

The optimal design is to choose τ to minimize the aggregate performance for a given weight ρ:

$$\tau^* = \arg\min_{\frac{T}{4}\leq\tau\leq\frac{T}{2}} \frac{T^2}{2} - \frac{3\tau\left(T-\tau\right)^3}{4\left(\left(T-\tau\right)^2+3\rho\right)}$$

and the optimal feedback gain is given by

$$K^* = -\frac{3\left(T-\tau^*\right)}{2\left(T-\tau^*\right)^2+6\rho}.$$

Remark 3 *For the special case of $\rho = 0$, the solution to this optimization problem is given in [97] with*

$$\tau^* = 0.5T, \quad K^* = -3T^{-1}, \quad J^* = 0.3125T^2.$$

Figure 2.1 depicts the optimal performance and sampling time as a function of ρ for values of the parameter $a = -1, 0, 1$.

2.3.2 Optimal Level-Crossing Sampling for the Brownian Motion Process

Level-crossing sampling is a threshold based encoding scheme in which a new sample is taken whenever $|x\left(t\right)|$ exceeds a specified threshold δ with the corresponding sampling instant defined as

$$\tau_\delta = \inf_t \left\{t \mid |x\left(t\right)| = \delta,\ x\left(0\right) = x_0 \in \left(-\delta, \delta\right)\right\}.$$

Since a finite horizon problem is considered, it may happen that $\tau_\delta > T$. Therefore, a time-out at the end of the time horizon is used and the sampling time is defined as $\tau = \tau_\delta \wedge T$. Definitely sampling at the end time $\tau = T$ has nothing effect on the performance

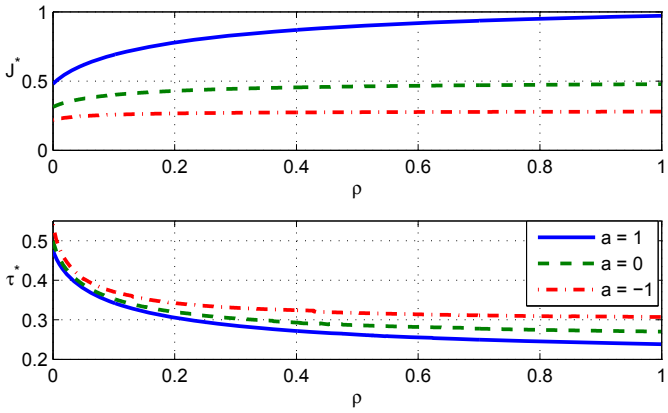

Figure 2.1: The optimal performance and sampling time of the deterministic sampling and ZOH hold scheme.

improvement since it is equivalent to not sampling at all. It is important to find the level-crossing probability that the process exceeds a threshold before the time-out T. The density function of τ_δ can be obtained by derivation of the moment generating function.

Lemma 4 *Let τ_δ denote the first passage time of $|x(t)|$ at the threshold δ. The moment generating function is then given by*

$$F_{\tau_\delta}(s) \triangleq \mathbb{E}\left[e^{-s\tau_\delta}\right] = \frac{\cosh\left(x_0\sqrt{2s}\right)}{\cosh\left(\delta\sqrt{2s}\right)}.$$

Proof. From Lemma 5.7.4 in [54], it follows that

$$\mathbb{E}\left[\tau_\delta\right] < \infty.$$

Let

$$u(x_0) \triangleq \mathbb{E}\left[e^{-s\tau_\delta}\right].$$

Then by Proposition 5.7.2 in [54], the function $u(x_0)$ satisfies the elliptic equation

$$\frac{1}{2}\frac{\partial^2 u(x_0)}{\partial x_0^2} - su(x_0) = 0, \quad x_0 \in (-\delta, \delta)$$

as well as the boundary condition

$$u(\delta) = u(-\delta) = 1.$$

By solving the *Dirichlet problem*, the solution is given by

$$u(x_0) = \frac{e^{x_0\sqrt{2s}} + e^{-x_0\sqrt{2s}}}{e^{\delta\sqrt{2s}} + e^{-\delta\sqrt{2s}}},$$

from which the desired relation is obtained immediately. ■

Recalling that the initial condition $x_0 = 0$, the probability density function of the random variable τ_δ is given by the following line integral, an integral formula for the inverse Laplace transform:

$$\begin{aligned} f(t) &= \mathcal{L}^{-1}\left(F_{\tau_\delta}(s)\right) = \frac{1}{2\pi j}\oint F_{\tau_\delta}(s)\, e^{st} ds \\ &= \frac{1}{2\pi j}\lim_{l\to\infty}\int_{\gamma-jl}^{\gamma+jl} \frac{e^{st}}{\cosh\left(\delta\sqrt{2s}\right)} ds. \end{aligned}$$

Since $\cosh(x) = \cos(jx)$, the singularities of $F_{\tau_\delta}(s)$ which are also zeros of $\cosh\left(\delta\sqrt{2s}\right)$ are

$$s_k = -(2k+1)^2 \frac{\pi^2}{8\delta^2},\ k = 0, 1, 2, \ldots,$$

then γ can be set to zero. The threshold crossing probability before the time-out T can be computed as

$$\begin{aligned} \mathbb{P}[\tau_\delta < T] &= \int_0^T f(t)\, dt = \frac{1}{2\pi j}\oint F_{\tau_\delta}(s)\left[\int_0^T e^{st} dt\right] ds \\ &= \frac{1}{2\pi j}\lim_{l\to\infty}\int_{-jl}^{jl} \frac{e^{sT}-1}{s\cosh\left(\delta\sqrt{2s}\right)} ds. \end{aligned}$$

Note that the integrand does not in any way affect the status of the poles since $s = 0$ is canceled by a single zero at zero on the numerator. In order to calculate this line integral over the complex plane, the standard methods of contour integration are employed. To wit, take a path that encloses the whole left half of the complex plane so that all the poles lie inside the contour. Then by the Cauchy residue theorem,

$$\mathbb{P}[\tau_\delta < T] = \sum\nolimits_{k\geq 0} \frac{e^{s_k T}-1}{s_k} \lim_{s\to s_k} \frac{s - s_k}{\cosh\left(\delta\sqrt{2s}\right)}.$$

In order to find the limit, apply the L'Hopital's rule to the indeterminate form 0/0. Since $\sinh(x) = -j\sin(jx)$, then it can be shown that

$$\lim_{s\to s_k} \frac{s - s_k}{\cosh\left(\delta\sqrt{2s}\right)} = (-1)^k (2k+1) \frac{\pi}{2\delta^2}.$$

This expression permits the determination of the probability

$$\mathbb{P}[\tau_\delta < T] = \frac{4}{\pi}\sum\nolimits_{k\geq 0} (-1)^k \frac{1 - e^{-(2k+1)^2\lambda}}{2k+1},$$

where

$$\lambda = \frac{T\pi^2}{8\delta^2}.$$

In what follows, write $\frac{1}{2k+1}$ as an integral, and sum a geometric series effortlessly by adopting the technique described in [1]:

$$\sum_{k\geq 0} \frac{(-1)^k}{2k+1} = \sum_{k\geq 0} (-1)^k \int_0^1 x^{2k} dx = \int_0^1 \frac{dx}{1+x^2} = \frac{\pi}{4}.$$

This series converges although very slowly, it produces an interesting value. This leads the probability to

$$\mathbb{P}\left[\tau_\delta < T\right] = 1 - \frac{4}{\pi} \sum\nolimits_{k\geq 0} (-1)^k \frac{e^{-(2k+1)^2 \frac{T\pi^2}{8\delta^2}}}{2k+1}.$$

By letting $T \to \infty$ or $\delta = 0$, it can be obtained that $\mathbb{P}\left[\tau_\delta < T\right] = 1$, which does make sense. The probability that the process exceeds the threshold before the time-out T as a function of the threshold δ is given in Figure 2.2, and it monotonically decreases with the threshold δ as seen from the figure. Note that the probability depends on the ratio of the length of the time horizon T and the square of the threshold δ. This suggests that, without loss of generality, the focus can be limited to $T = 1$. The result for other T can be obtained from $T = 1$ by scaling δ^2 to make the ratio invariant. Now the performance

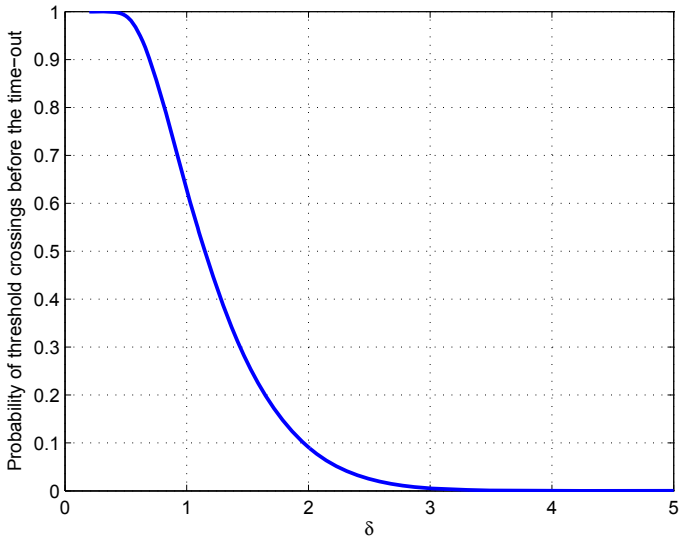

Figure 2.2: Probability that a sample is generated as a function of the parameter δ with $T = 1$

$$J = \mathbb{E}\left[\int_0^{\tau_\delta \wedge T} x^2(t)\, dt\right] + \mathbb{E}\left[\int_{\tau_\delta \wedge T}^{T} x^2(t)\, dt\right] + \rho\mathbb{E}\left[\int_{\tau_\delta \wedge T}^{T} K^2 x^2(\tau)\, dt\right],$$

will be minimized by selecting the optimal threshold δ and feedback gain K.

Applying the Ito differential rule gives

$$d\left[(T-t)\,x^2\,(t)\right] = (T-t)\,(2x\,(t)\,dx(t)+dt) - x^2\,(t)\,dt.$$

Taking the Ito integral and expectation on both sides leads to

$$J_1 = \frac{T^2}{2} - \mathbb{E}\left[\delta^2\,(T-\tau_\delta)^+ + \frac{1}{2}\left[(T-\tau_\delta)^+\right]^2\right],$$

where the property of the Ito integral (see Theorem 3.2.1 in [89]) has been used.

Thus, the corresponding performance becomes

$$J = \frac{T^2}{2} + \frac{1}{3}K^2\delta^2\mathbb{E}\left[\left[(T-\tau_\delta)^+\right]^3\right] + K\delta^2\mathbb{E}\left[\left[(T-\tau_\delta)^+\right]^2\right] + \rho K^2\delta^2\mathbb{E}\left[(T-\tau_\delta)^+\right].$$

The next step is to write the above expression in terms of K and δ alone. This requires an evaluation of the first, second, and third moment: $\mathbb{E}[\,(T-\tau_\delta)^+]$, $\mathbb{E}[[\,(T-\tau_\delta)^+]^2]$, and $\mathbb{E}[[\,(T-\tau_\delta)^+]^3]$, which can be calculated as the way in [98]:

$$\mathbb{E}[\,(T-\tau_\delta)^+] = \frac{T^2\pi^2}{8\delta^2\lambda} + \frac{T^2\pi}{2\delta^2\lambda^2}\sum\nolimits_{k\geq 0}(-1)^k\,\frac{e^{-\lambda(2k+1)^2}}{(2k+1)^3} - \frac{T^2\pi}{2\delta^2\lambda^2}\sum\nolimits_{k\geq 0}\frac{(-1)^k}{(2k+1)^3},$$

$$\mathbb{E}[[\,(T-\tau_\delta)^+]^2] = 512\frac{\delta^4}{\pi^5}\sum_{k\geq 0}(-1)^k\,\frac{1-e^{-(2k+1)^2\lambda}}{(2k+1)^5} - 64\frac{\delta^2 T}{\pi^3}\sum_{k\geq 0}\frac{(-1)^k}{(2k+1)^3} + T^2,$$

$$\begin{aligned}\mathbb{E}[[\,(T-\tau_\delta)^+]^3] = {} & \frac{3\pi T^4}{\lambda^4\delta^2}\sum_{k\geq 0}(-1)^k\,\frac{e^{-(2k+1)^2\lambda}-1}{(2k+1)^7} \\ & + T^3 - \frac{3\pi T^4}{2\lambda^2\delta^2}\sum_{k\geq 0}(-1)^k\,\frac{1}{(2k+1)^3} + \frac{3\pi T^4}{\lambda^3\delta^2}\sum_{k\geq 0}(-1)^k\,\frac{1}{(2k+1)^5}.\end{aligned}$$

For positive integer values n, there is a formula

$$\sum_{k=0}^{\infty}\frac{(-1)^k}{(2k+1)^{2n+1}} = E_n\frac{1}{2\,(2n)!}\left(\frac{\pi}{2}\right)^{2n+1},$$

where the *Euler numbers* E_n are the natural numbers defined according to:

$$\sec x - 1 = \frac{E_1 x^2}{2!} + \frac{E_2 x^4}{4!} + \frac{E_3 x^6}{6!} + \cdots$$

The first three values of Euler numbers are

$$E_1 = 1,\ E_2 = 5,\ E_3 = 61.$$

After substituting the series with their sums, the performance can be further reduced to the expression below:

$$J = \frac{4096\delta^8 K^2}{\pi^7}\sum_{k\geq 0}(-1)^k\frac{e^{-(2k+1)^2\lambda}}{(2k+1)^7} + \frac{5}{3}K\delta^6 + \frac{1}{3}K^2\delta^2\left[T^3 - 3T^2\delta^2 + 5T\delta^4 - \frac{61}{15}\delta^6\right]$$
$$+ \frac{T^2}{2} - 2K\delta^4 T + K\delta^2\left[512\frac{\delta^4}{\pi^5}\sum_{k\geq 0}(-1)^{k+1}\frac{e^{-(2k+1)^2\lambda}}{(2k+1)^5} + T^2\right]$$
$$+ \rho K^2\delta^2\left[T - \delta^2 + \frac{32\delta^2}{\pi^3}\sum\nolimits_{k\geq 0}\frac{(-1)^k e^{-\lambda(2k+1)^2}}{(2k+1)^3}\right].$$

The optimal δ^* will be computed by minimizing the performance for a given weight ρ:

$$\delta^* = \arg\min_{\delta>0,K} J.$$

Remark 5 *Actually the resulting δ optimized in this way is just a sub-optimal threshold for the zero order hold and level-crossing sampling strategies. Given fixed thresholds, the controller waits for the sampling time to compute the feedback gain, which performs better than any predetermined feedback gains. The true optimal threshold and feedback gain should be optimized based on the performance index in (2.8), which are difficult to obtain. However, it is possible to obtain the analytic result for $\rho = 0$ as shown in the following.*

For $\rho = 0$, the optimal feedback gain K^* satisfies

$$K^* = -\frac{3}{2\left(T - \tau_{\delta^*}\right)^+}.$$

The associated quadratic performance index then admits the form

$$J = \frac{T^2}{2} - \frac{3}{4}\delta^2\mathbb{E}\left[\left(T - \tau_\delta\right)^+\right] = \frac{T^2}{2} - \frac{3}{4}\delta^2 T + \frac{3}{4}\delta^4 - 24\frac{\delta^4}{\pi^3}\sum\nolimits_{k\geq 0}\frac{(-1)^k e^{-\lambda(2k+1)^2}}{(2k+1)^3}.$$

The minimum performance obtained proves to be $J^* = 0.2733T^2$ and this is accomplished by choosing the threshold $\delta^* = 0.9389\sqrt{T}$. For this optimal threshold, the probability that the process reaches this threshold before the end time T is 68.59%.

Figure 2.3(a) depicts the sub-optimal performance J as a function of the weight ρ and Figure 2.3(b) the corresponding sub-optimal threshold.

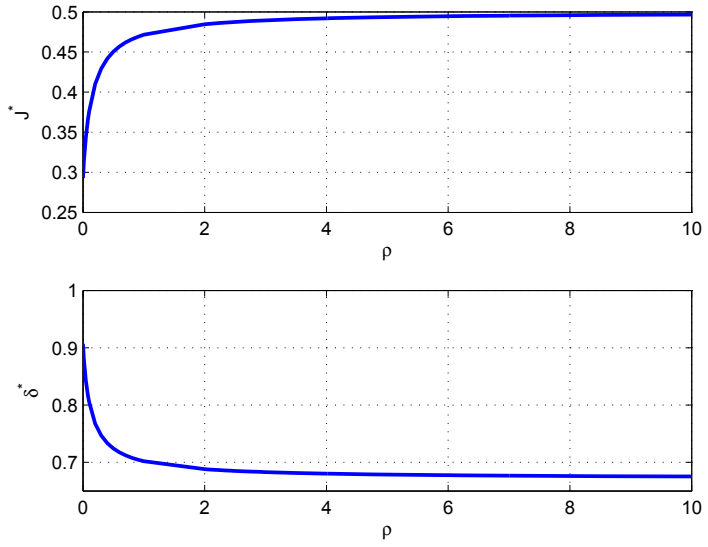

Figure 2.3: The sub-optimal performance and threshold of level-crossing sampling and ZOH hold scheme.

2.4 Optimal Design for Generalized Hold

The state of the controller in (2.5) is

$$\hat{x}(t) = e^{(a+K)(t-\tau)} x(\tau), \qquad \text{for } t \in [\tau, T].$$

Under the generalized hold, the state of (2.1) can be written as

$$x(t) = e^{(a+K)(t-\tau)} x(\tau) + \int_{\tau}^{t} e^{a(t-s)} d\omega(s),$$

for $\tau \leq t \leq T$ [3]. The aggregate quadratic performance can be decomposed as in the ZOH case:

$$J = \mathbb{E}\left[\int_0^{\tau} x^2(t)\, dt\right] + \mathbb{E}\left[\int_{\tau}^{T} x^2(t)\, dt\right] + \rho \mathbb{E}\left[\int_{\tau}^{T} K^2 \hat{x}^2(t)\, dt\right].$$

The second term of the expression above constitutes the part of state variance received from the sampling time τ to the end of the time horizon T, and it could be carried as

$$\mathbb{E}\left[\int_{\tau}^{T} x^2(t)\, dt\right] = \mathbb{E}\left[x^2(\tau) \frac{e^{2(a+K)(T-\tau)} - 1}{2(a+K)}\right] + \mathbb{E}\left[\frac{e^{2a(T-\tau)} - 2a(T-\tau) - 1}{4a^2}\right].$$

As in the case of zero order hold, deterministic sampling and level-crossing sampling strategies are considered and the optimal design will be conducted within each class to minimize the performance.

2.4.1 Optimal Deterministic Sampling

For deterministic sampling, the performance takes the form

$$J = \frac{e^{2a\tau} + e^{2a(T-\tau)}}{4a^2} + \frac{e^{2a\tau} - 1}{2a}\frac{e^{2(a+K)(T-\tau)} - 1}{2(a+K)} - \frac{aT+1}{2a^2} + \rho K^2 \frac{e^{2a\tau} - 1}{2a}\frac{e^{2(a+K)(T-\tau)} - 1}{2(a+K)}.$$

The optimal sampling time τ^* and feedback gain K^* can be found by solving the following optimization problem:

$$\begin{array}{ll} \text{minimize} & J \\ \text{subjec to} & 0 \leq \tau \leq T. \end{array}$$

For $\rho = 0$, the optimal choice of K^* and τ^* is

$$\tau^* = \frac{T}{2}, \text{ and } K^* = -\infty.$$

The corresponding performance cost is

$$J = \frac{T^2}{4}.$$

In this case, the optimal generalized hold becomes the impulse hold where the control signal is an impulse [46, 77]. This is equivalent to reset the state to the origin at $\tau = 0.5T$.

Figure 2.4 depicts the optimal performance, sampling time, and feedback gain for values of the parameter $a = 1, 0, -1$.

2.4.2 Optimal Level-Crossing Sampling for the Brownian Motion Process

Using the previous result yields

$$\begin{aligned} \mathbb{E}\left[\int_0^{\tau_\delta \wedge T} x^2(t)\,dt\right] =& \frac{T^2}{2} - \delta^2 \mathbb{E}[(T-\tau_\delta)^+] - \frac{1}{2}\mathbb{E}\left[\left[(T-\tau_\delta)^+\right]^2\right], \\ \mathbb{E}\left[\int_{\tau_\delta \wedge T}^{T} x^2(t)\,dt\right] =& \mathbb{E}\left[x^2(\tau_\delta \wedge T)\frac{e^{2K(T-\tau_\delta)^+} - 1}{2K}\right] + \frac{1}{2}\mathbb{E}\left[\left[(T-\tau_\delta)^+\right]^2\right]. \end{aligned}$$

Thus, the performance becomes

$$J = \frac{T^2}{2} - \delta^2 \mathbb{E}\left[(T-\tau_\delta)^+\right] + \frac{\delta^2}{2}\left(\frac{1}{K} + \rho K\right)\mathbb{E}\left[e^{2K(T-\tau_\delta)^+} - 1\right].$$

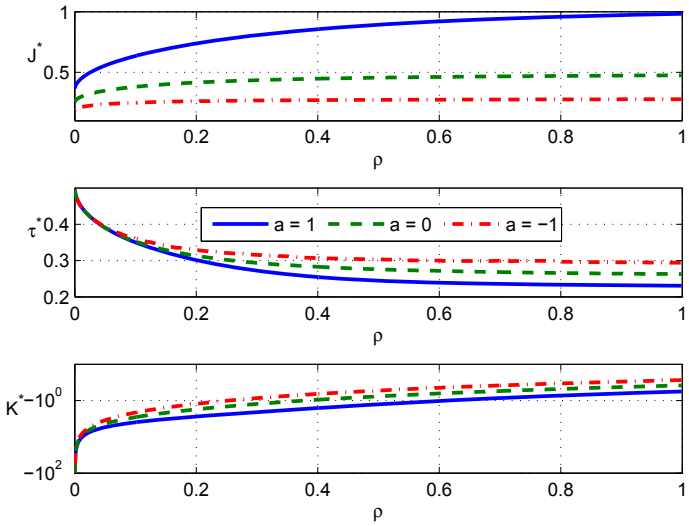

Figure 2.4: The optimal performance, threshold and feedback gain of the deterministic sampling and generalized hold scheme as a function of ρ for systems with $a = 1, 0, -1$, respectively.

A numerical method of computing $\mathbb{E}[e^{2K(T-\tau_\delta)^+} - 1]$ over a fixed finite time interval is provided in [57]. Let $W(x,t)$ be a continuous and bounded function defined on the region $[-\delta, \delta] \times [0, T]$, and satisfy the partial differential equation

$$\frac{\partial W(x,t)}{\partial t} + \frac{1}{2}\frac{\partial^2 W(x,t)}{\partial x^2} + e^{-2Kt} = 0,$$

along with the boundary and initial conditions

$$\begin{cases} W(-\delta, t) = W(\delta, t) = 0 & \text{for } t \in [0, T), \\ W(x, T) = 0 & \text{for } x \in [-\delta, \delta]. \end{cases}$$

Then

$$W(0,0) = \mathbb{E}\left[\int_0^{\tau_\delta \wedge T} e^{-2Kt} dt\right].$$

A brief proof will be shown here. Applying standard Itô calculus on $W(x,t)$ yields

$$\begin{aligned} \mathbb{E}\left[W\left(x\left(\tau_\delta \wedge T\right), \tau_\delta \wedge T\right)\right] - W(0,0) &= \mathbb{E}\left[\int_0^{\tau_\delta \wedge T} dW\left(x(t), t\right)\right] \\ &= \mathbb{E}\left[\int_0^{\tau_\delta \wedge T} \left[\frac{\partial W(x,t)}{\partial t} + \frac{1}{2}\frac{\partial^2 W(x,t)}{\partial x^2}\right] dt\right] \\ &= \mathbb{E}\left[\int_0^{\tau_\delta \wedge T} -e^{-2Kt} dt\right]. \end{aligned}$$

If the process hits the boundary before time T, $x(\tau_\delta \wedge T) = \pm\delta$ in which case

$$W(x(\tau_\delta \wedge T), \tau_\delta \wedge T) = W(\pm\delta, \tau_\delta) = 0.$$

If the process does not exit the boundary of δ before T, then the sampling instant is $\tau_\delta \wedge T = T$ which yields $W(x(\tau_\delta \wedge T), \tau_\delta \wedge T) = W(x(T), T) = 0$. Thus the above relationship can be concluded.

Note that $W(0,0)$ is still a function of δ and K for fixed time horizon T. Therefore, define

$$U(\delta, K) \triangleq W(0,0).$$

Then the performance can be written as

$$J = \frac{T^2}{2} - \delta^2 T + \delta^4 \left(1 - \frac{32}{\pi^3} \sum\nolimits_{k\geq 0} \frac{(-1)^k e^{-\lambda(2k+1)^2}}{(2k+1)^3}\right) + \frac{\delta^2}{2}\left(\frac{1}{K} + \rho K\right)\left[e^{2KT}(1 - 2KU(\delta, K)) - 1\right].$$

The optimal δ and K can be computed by minimizing the performance J. The optimal δ and K derived in this way are sub-optimal threshold, and feedback gain, respectively. Again, the true optimal result will be shown analytically below for the case $\rho = 0$. For $\rho = 0$, the optimal K^* is

$$K^* = -\infty,$$

and then the performance takes the form as

$$J = \frac{T^2}{2} + \delta^4 - \delta^2 T - \frac{32\delta^4}{\pi^3} \sum\nolimits_{k\geq 0} \frac{(-1)^k e^{-\lambda(2k+1)^2}}{(2k+1)^3}.$$

The minimum performance obtained comes out to be

$$J^* = 0.1977T^2,$$

and this is accomplished by choosing the threshold

$$\delta^* = 0.9389\sqrt{T}.$$

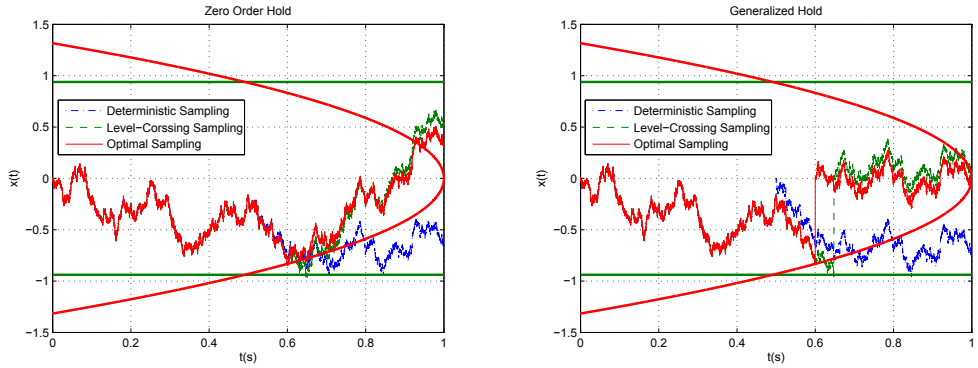

Figure 2.5: Control of a Wiener process with time horizon $T = 1$.

2.5 Performance Comparison for the Brownian Motion Process

To provide some insight, first consider the special case $\rho = 0$; the results for this case are summarized in Table 2.1. The table determines the ranking of the sampling and hold strategies. The optimal sampling is the best among all possible sampling rules, level-crossing sampling outperforms deterministic sampling, and generalized hold outperforms zero order hold, which are not surprising. Another important insight given by this table is that the optimal parameters for each sampling scheme are independent of hold circuits. This table also shows that selecting hold circuits is more effective for performance improvement than selecting sampling strategies.

Table 2.1: Comparison of different sampling and control schemes

	J	Triggering Instant τ^*	K^*
DSZOH	$0.3125T^2$	$t = 0.5T$	$-3T^{-1}$
LCSZOH	$0.2733T^2$	$\inf\{t\| \, \|x(t)\| \geq 0.9389\sqrt{T}\}$	$-1.5\,(T-\tau)^{-1}$
OSZOH	$0.2623T^2$	$\inf\{t\|x^2(t) \geq \sqrt{3}\,(T-t)\}$	$-1.5\,(T-\tau)^{-1}$
DSGH	$0.2500T^2$	$t = 0.5T$	$-\infty$
LCSGH	$0.1977T^2$	$\inf\{t\| \, \|x(t)\| \geq 0.9389\sqrt{T}\}$	$-\infty$
OSGH	$0.1830T^2$	$\inf\{t\|x^2(t) \geq \sqrt{3}\,(T-t)\}$	$-\infty$

The result on the optimal sampling and generalized hold scheme is given below. It is optimal in the sense that (K, τ) minimizes the following performance measure among all

possible sampling policy and feedback gain pairs:

$$J = \frac{T^2}{2} - \mathbb{E}\left[x^2(\tau)(T-\tau)\right] + \frac{\mathbb{E}\left[x^2(\tau)\left(e^{2K(T-\tau)}-1\right)\right]}{2K}.$$

It makes intuitive sense to set K^* to be $-\infty$. Because of this observation that the performance measure takes the form as below:

$$J = \frac{T^2}{2} - \mathbb{E}\left[x^2(\tau)(T-\tau)\right].$$

Next it is clear that in order to minimize the performance it is sufficient to maximize the expected reward function:

$$\mathbb{E}\left[x^2(\tau)(T-\tau)\right].$$

The optimal sampling rule is to sample at the time when the process first reaches the symmetric parabola [97]:

$$\tau^* = \inf\{t | x^2(t) \geq \sqrt{3}(T-t)\}.$$

Now let us calculate the expected performance incurred by the optimal sampling scheme. At the sampling time, the inequality becomes an equality

$$\mathbb{E}\left[x^2(\tau)\right] = \sqrt{3}T - \sqrt{3}\mathbb{E}[\tau] = \mathbb{E}[\tau].$$

Consequently,

$$\mathbb{E}[\tau] = \frac{\sqrt{3}}{\sqrt{3}+1}T,$$

and the expect reward function becomes

$$\mathbb{E}\left[x^2(\tau)(T-\tau)\right] = \sqrt{3}\left\{(\sqrt{3}-2)T^2 + \mathbb{E}\left[\tau^2\right]\right\}.$$

The next step is to evaluate the second moment of the sampling time. According to Theorem 8.5.8 in [24], the function $x^4(t) - 6x^2(t)t + 3t^2$ is a martingale. Since τ is a bounded stopping time, then

$$\mathbb{E}\left[x^4(\tau) - 6x^2(\tau)\tau + 3\tau^2\right] = 0.$$

This relation suggests

$$\mathbb{E}\left[\tau^2\right] = \left(2\sqrt{3}-1\right)T^2 - (2\sqrt{3}+1)\mathbb{E}\left[\tau^2\right],$$

then from which it can be concluded

$$\mathbb{E}\left[\tau^2\right] = \frac{7-3\sqrt{3}}{4}T^2.$$

Finally, the optimal performance becomes

$$J = \frac{T^2}{2} - \frac{3-\sqrt{3}}{4}T^2 = \frac{\sqrt{3}-1}{4}T^2.$$

The realizations of a Wiener process with different event triggered sensing and actuation strategies are shown in Figure 2.5. The simulation was performed by choosing the same Wiener process. The deterministic sampling always samples at the mid-point of the time horizon independent of the state. As seen from the figure the state is very close to the origin at the time $t = 0.5$; therefore there is no need to waste the only sampling budget and take the control action. The difference between level-crossing sampling and optimal sampling is that the threshold of optimal sampling is time-dependent rather than a constant. It is advantageous to depend on the time for thresholds over a finite time horizon. The reason that the impulse hold gives better performance than the zero order hold is because it resets the state back to zero instantaneously; however, the zero order hold takes some time to bring it back.

Figure 2.6 shows the optimal achievable cost J^* for the four different event triggered sampling and control strategies. It is notable that for small weight ρ, the achievable performance of deterministic sampling and generalized hold is better than that of level-crossing sampling and zero-order hold; while the opposite is true when ρ becomes large. It is surprising that sampling plays a more important role than hold in performance improvement for large weights.

2.6 Conclusion

Three sampling schemes typically used for event detection combined with two hold circuits for control actuation have been considered for optimal design and performance comparison. The three sampling schemes consist of deterministic sampling, level-crossing sampling, and optimal sampling; and the two hold circuits include zero order hold and generalized hold. The results obtained in this chapter enable performance ranking among different combinations of sampling and hold strategies.

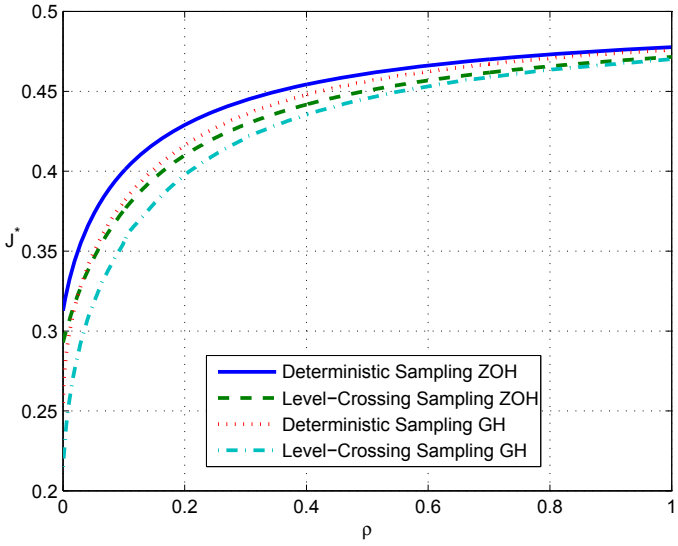

Figure 2.6: Optimal achievable performance J^*

Chapter 3

Optimal Sampling and Performance Comparison of Periodic and Event Based Impulse Control

In this chapter, several issues of periodic and event based impulse control for a class of second order stochastic systems are considered, including the optimal sampling and performance comparison.

3.1 Introduction

Time and event triggered sampling mechanisms, also known as Riemann and Lebesgue sampling schemes, respectively, are two important ways to perform A-to-D conversion in computer controlled systems. Time-triggered digital control systems are most often implemented by periodic sampling of the sensors and zero-order hold of the actuators. The advantage of this approach is its simplicity, that is, the discretization of a linear time-invariant system via step-invariant transformation yields an equivalent time-invariant discrete-time system synchronized at the sampling instants. The time-varying nature of sampled-data systems thus disappears, arriving at a purely discrete-time time-invariant control problem.

Different from periodic sampling, event based mechanism takes control action only when some specific event occurs; for example, the output reaches a boundary or the error function exceeds a limit. This type of sampling is closer to human intelligence and is of interest in situations to reduce the information exchange and network bandwidth usage. The differences between event based sampling and periodic sampling are compared in different settings [6], [97], which turn out to favor the former. It is worth mentioning that such comparisons are only conducted for first order linear stochastic systems or integrating dynamics due to

the ease of calculation in one dimension. The analytic results for higher order systems are difficult to obtain in general. Therefore, it is not clear whether event based impulse control still outperforms periodic impulse control for higher order systems, which motivates us to carry out the present study.

In this chapter, periodic impulse and event based impulse controls are investigated for a class of second order stochastic systems; the contributions of this work include: (a) providing an optimal sampling period for periodic impulse control; (b) determining an optimal threshold for event based impulse control; (c) obtaining a performance ratio between periodic control and event based control. For event based impulse control, the states are reset to zero whenever the magnitude reaches a given level. As mentioned earlier, the partial differential equations with boundary conditions for the mean first passage time and stationary variance are not simple to solve in two dimensions. To make the problem tractable, second order stochastic systems in the Cartesian coordinates are first converted to first order stochastic systems in the polar coordinates at the cost of losing linearity. Next, the Kolmogorov backward equation is constructed based on the derived first order nonlinear stochastic differential equation. It is shown that the average sampling period can be expressed as an absolutely convergent series. Furthermore, the stationary distribution of the state is obtained by solving the Kolmogorov forward equation. Finally, it is shown that for the same average control rate, event based impulse control outperforms periodic impulse control. It is worth noting that all the calculations are performed analytically.

3.2 Problem Formulation

Consider the second order system to be controlled according to the following stochastic differential equations:

$$\begin{aligned} dx_1(t) &= ax_1(t)\,dt + u_1(t)\,dt + dv_1(t) \\ dx_2(t) &= ax_2(t)\,dt + u_2(t)\,dt + dv_2(t) \end{aligned} \tag{3.1}$$

where $x(t)$ is a two-dimensional state vector, a is the pole of the process, and the disturbances $v_1(t)$ and $v_2(t)$ are mutually independent Wiener processes with unit incremental variance. At the sampling instant t_k, the control signal

$$u(t) = -x(t_k)\,\delta(t - t_k)$$

is applied to the system that makes $x(t_k+) = 0$ where δ is a Dirac delta or an impulse function. The control performance is measured by the the mean square variation J^x and the

average control rate J^u:

$$J = \underbrace{\lim_{T\to\infty} \frac{1}{T}\mathbb{E}\int_0^T x^T(t)\,x(t)\,dt}_{J^x} + \rho \underbrace{\lim_{T\to\infty} \frac{1}{T} N_{[0,T]}}_{J^u}, \tag{3.2}$$

where ρ is the relative weight and $N_{[0,T]}$ is the number of control actions in the interval $[0, T]$ [46]. The goal here is threefold: first, to determine the optimal sampling period for periodic impulse control that minimizes J; second, to determine the optimal threshold for event based impulse control that minimizes J; last, to compare the variances of the states between conventional periodic impulse control and event based impulse control while ensuring the same average control frequency.

Remark 6 *Note that the more general model*

$$dx'(t) = ax'(t)\,dt + u'(t)\,dt + \sigma dv(t)$$

can be reduced to (3.1) by the utilization of coordinate scaling. Choosing $x' = \sigma x$, $u' = \sigma u$, *and* $\rho' = \sigma^2\rho$, *the dynamics becomes*

$$\sigma dx(t) = a\sigma x(t)\,dt + \sigma u(t)\,dt + \sigma dv(t),$$

and the cost is weighted by

$$J' = J^{x\prime} + \rho' J^{u\prime} = \sigma^2 J^x + \sigma^2\rho J^u = \sigma^2 J.$$

This suggests that, without loss of generality, the focus here can be limited to the normalized case $\sigma = 1$.

3.3 Optimal Periodic Impulse Control

In this section, the variance of the state, the average control rate as well as the optimal sampling period are given for the general system in (3.1), and specialized for $a = 0$.

Theorem 7 *Consider the stochastic differential equation in (3.1) controlled by periodic impulses with a sampling period* h. *The variance of the state as defined in (3.2) is*

$$J_P^x = \begin{cases} \frac{e^{2ah}-2ah-1}{2a^2h} & a \neq 0, \\ h & a = 0, \end{cases}$$

and the average control rate as defined in (3.2) is

$$J_P^u = \frac{1}{h}.$$

Proof. Under periodic impulse control, reset the states to zero according to a deterministic, periodic sequence $t_k = kh$, for $k \geq 0$. Between impulses, the states evolve as

$$dx(t) = \operatorname{diag}\{a, a\} x(t) dt + dv(t)$$

and the sampled system becomes

$$x(kh + t) = \int_{kh}^{kh+t} e^{\operatorname{diag}\{a,a\}(kh+t-\tau)} dv(\tau),$$

see [3].

The average variance of such a process is

$$J_P^x = \lim_{N\to\infty} \frac{1}{Nh} \sum_{k=0}^{N-1} \int_0^h \int_0^t 2e^{2a\tau} d\tau dt = \frac{2}{h} \int_0^h \int_0^t e^{2a\tau} d\tau dt,$$

and the average control rate is

$$J_P^u = \lim_{T\to\infty} \frac{1}{T} N_{[0,T]} = \lim_{N\to\infty} \frac{1}{Nh} N = \frac{1}{h}.$$

This completes the proof. ■

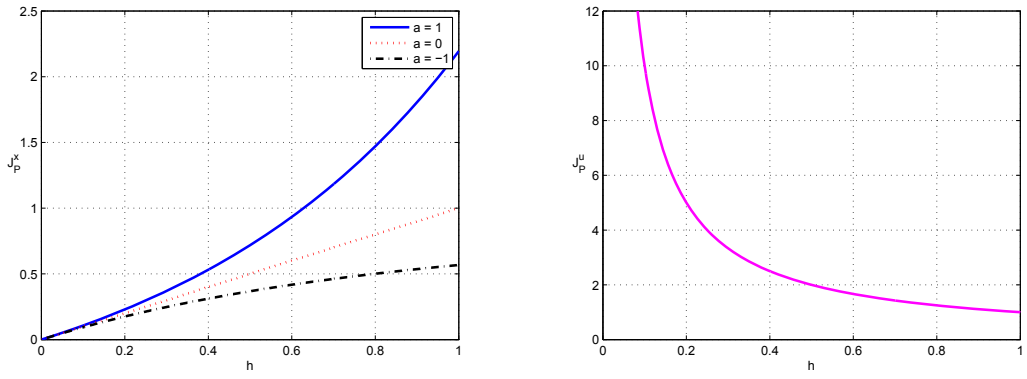

(a) Mean square variation (b) Average control rate

Figure 3.1: The performance with periodic impulse control for $a = -1, 0, 1$.

Figure 3.1 shows the mean square variation J_P^x and the average control rate J_P^u as a function of the sampling period h for different values of the pole a. It is clear that J_P^x is an increasing function of h for each a. The variance cost increases linearly for marginal stable systems $a = 0$, much faster for unstable systems $a = 1$ and slower for stable systems $a = -1$. At the same time, J_P^u decreases monotonically. The variances for marginal stable

and unstable systems approach to infinite as $h \to \infty$. But it can be shown that the variance for stable systems converges by applying the L'Hôpital's rule to the indeterminate form ∞/∞, that is,

$$\lim_{h\to\infty} J_P^x = \lim_{h\to\infty} \frac{e^{2ah} - 2ah - 1}{2a^2 h} = \lim_{h\to\infty} \frac{2ae^{2ah} - 2a}{2a^2} = -\frac{1}{a}.$$

The optimal sampling problem is to choose a fixed sample period to minimize the aggregate performance for a given weight ρ:

$$h^* = \arg\min_{h>0} J_P = \arg\min_{h>0} \left(\frac{e^{2ah} - 2ah - 1}{2a^2 h} + \rho \frac{1}{h} \right).$$

In the following, the optimal sampling problem is specialized to the case of $a = 0$.

Corollary 8 *Consider the stochastic differential equation in (3.1) with $a = 0$ controlled by periodic impulses with a sampling period h. Then the optimal sampling period h^* minimizes the performance in (3.2) is $\sqrt{\rho}$, and the corresponding performance J_P^* is $2\sqrt{\rho}$.*

The optimal sampling period and performance as a function of ρ for different values of the pole a are shown in Figure 3.2. Here it is seen that when the relative weight becomes large for stable systems, the sampling period approaches infinity and the total cost is bounded by $-1/a$, which means that no control action is needed. Overall, a larger sampling period means lower control cost but higher variance cost. Thus, there exists a trade-off between the mean square variation and the average control rate and Figure 3.3 shows the optimal trade-off curves, where stable systems need the fewest control actions for the same variance cost.

3.4 Optimal Event Based Impulse Control

For event based control the region

$$x_1^2(t) + x_2^2(t) < \Delta^2$$

is chosen to limit the states. Impulse control actions are taken only when $\|x(t)\|_2 = \Delta$. With this control law the process becomes an instantaneous return process, which is analogous to a Markov diffusion process.

It is of interest to convert (3.1) from Cartesian to polar coordinates by using the method in [31]. Set

$$x_1(t) = r(t)\cos\phi(t), \qquad x_2(t) = r(t)\sin\phi(t),$$

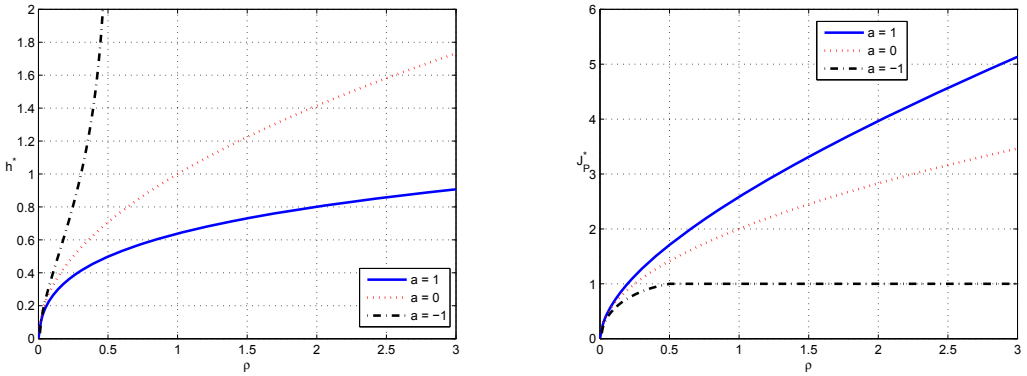

(a) Optimal sampling period (b) Optimal cost

Figure 3.2: The optimal sampling period and performance with periodic impulse control for $a = -1, 0, 1$.

with

$$r(t) = \sqrt{x_1^2(t) + x_2^2(t)},$$

so that

$$\log r(t) + j\phi(t) = \log\left[x_1(t) + jx_2(t)\right].$$

Apply the Ito differentiation rule to derive

$$d\left[\log r(t) + j\phi(t)\right] = adt + e^{-\log r(t) - j\phi(t)}\left[dv_1(t) + jdv_2(t)\right].$$

Take the real part and use the Ito differentiation rule to find

$$dr(t) = \left[ar(t) + \frac{1}{2r(t)}\right]dt + dv_1(t)\cos\phi(t) + dv_2(t)\sin\phi(t).$$

Define

$$d\omega(t) = dv_1(t)\cos\phi(t) + dv_2(t)\sin\phi(t),$$

which is an orthogonal transformation, thus it is also an increment of a standard Wiener process $\omega(t)$.

Here the stochastic differential equation for magnitude between impulses is

$$dr(t) = \left[ar(t) + \frac{1}{2r(t)}\right]dt + d\omega(t). \tag{3.3}$$

Remark 9 *Using the stochastic calculus, it is possible to convert the Cartesian stochastic differential equation in (3.1) to the polar equation in (3.3). Nevertheless, a direct conversion is not possible since the stochastic differential equation does not obey the rule of ordinary calculus. If doing so, the term* $[1/2r(t)]\,dt$ *would not be found.*

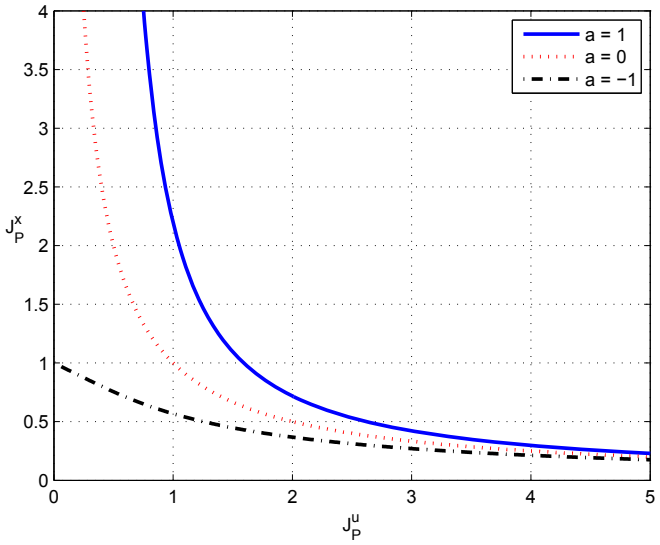

Figure 3.3: The optimal trade-off curves between the mean square variation and the average control rate with periodic impulse control for $a = -1, 0, 1$.

Remark 10 *The mean exit time and steady state probability distribution will be calculated by solving the Kolmogorov backward and forward equations respectively which are partial differential equations for higher order systems. Unfortunately, the closed form solutions do not often exist. However, in dealing with the polar equation in (3.3), it is possible to perform calculations analytically as shown in the following.*

3.4.1 Average Control Rate

The average control rate is derived in the following theorem.

Theorem 11 *Consider the stochastic differential equation in (3.1) controlled by an event based impulse scheme with the bound Δ. The average control rate as defined in (3.2) is*

$$J_E^u = \frac{1}{\sum_{k=1}^{\infty} \frac{(-a)^{k-1}\Delta^{2k}}{2kk!}}.$$

Proof. Consider the interval $(0, \Delta)$, where the endpoint Δ is an absorbing barrier and 0 is a reflecting barrier. The mean exit time from the region $(0, \Delta)$ can be computed by solving the Kolmogorov backward equation

$$\frac{1}{2}\frac{\partial^2 h_E(r)}{\partial r^2} + \left(ar + \frac{1}{2r}\right)\frac{\partial h_E(r)}{\partial r} = -1$$

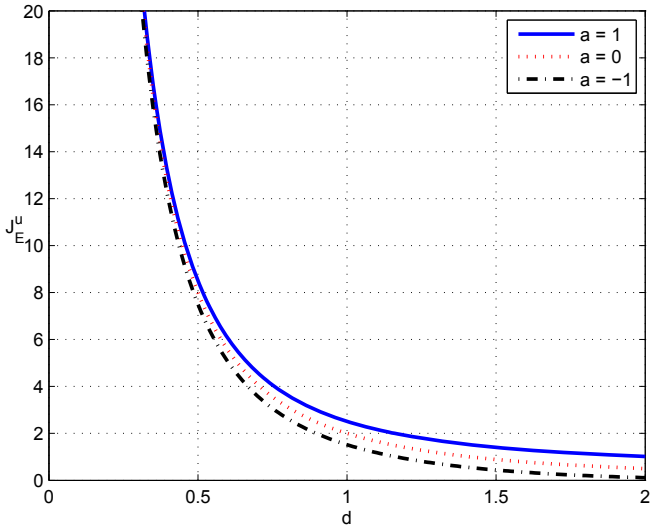

Figure 3.4: The average control rates with event based impulse control for $a = -1, 0, 1$.

with the boundary conditions $h_E(\Delta) = 0$ and $\frac{\partial h_E(0)}{\partial r} = 0$ [31]. The solution is given by

$$h_E(r) = 2\int_r^{\Delta}\int_0^y \frac{z}{y} e^{a\left(z^2-y^2\right)} dz dy,$$

and the average sampling period is the mean exit time when the process starts at $r = 0$

$$h_E(0) = 2\int_0^{\Delta}\int_0^y \frac{z}{y} e^{a\left(z^2-y^2\right)} dz dy.$$

Consider the case $a \neq 0$,

$$h_E(0) = \int_0^{\Delta} \frac{1-e^{-ay^2}}{ay} dy.$$

Using the Taylor series of the function e^{-ay^2}, the integration can be written as

$$h_E(0) = \int_0^{\Delta} \sum_{k=1}^{\infty} \frac{(-a)^{k-1} y^{2k-1}}{k!} dy = \sum_{k=1}^{\infty} \frac{(-a)^{k-1} \Delta^{2k}}{2kk!}.$$

The infinite series $h_E(0)$ converges absolutely, which can be shown as follows:

$$\sum_{k=1}^{\infty} \left| \frac{(-a)^{k-1} \Delta^{2k}}{2kk!} \right| < \frac{1}{2|a|} \sum_{k=0}^{\infty} \frac{\left(|a|\Delta^2\right)^k}{k!} = \frac{1}{2|a|} e^{|a|\Delta^2} < \infty.$$

For the special case of $a = 0$,

$$h_E(0) = \frac{\Delta^2}{2},$$

which is also included in the above infinite series. Therefore, the average control rate can be found as

$$J_E^u = \frac{1}{h_E(0)}.$$

This completes the proof. ■

Figure 3.4 shows the average control rate as a function of Δ for different values of the pole a. Notice that the average control rate decreases as Δ increases for each case. As expected, the average control rate is slower for stable systems $a = -1$, and faster for unstable systems $a = 1$ for the same Δ.

3.4.2 Mean Square Variation

It can be shown that the probability density of r satisfies the forward Kolmogorov equation

$$\begin{aligned}\frac{\partial p(r,t)}{\partial t} &= \frac{\partial}{\partial r}\left[\frac{1}{2}\frac{\partial p(r,t)}{\partial r} - \left(ar + \frac{1}{2r}\right)p(r,t)\right] \\ &\quad - \left[\frac{1}{2}\frac{\partial p(r,t)}{\partial r} - \left(ar + \frac{1}{2r}\right)p(r,t)\right]_{r=\Delta}\delta_r,\end{aligned}$$

where the second term on the right hand side describes the probability flux caused by resetting of the states when the boundary is reached [6]. The probability density of r is given by the stationary solution to the differential equation

$$\frac{1}{2}\frac{\partial^2 p(r)}{\partial r^2} - \left(ar + \frac{1}{2r}\right)\frac{\partial p(r)}{\partial r} + \left(\frac{1}{2r^2} - a\right)p(r) = 0.$$

The equation has the solutions

$$p(r) = (c_1 + c_2 \ln r)\, re^{ar^2} + 2c_2 are^{ar^2}\int_r^\Delta \int_0^y \frac{z}{y}e^{a\left(z^2-y^2\right)}dzdy,$$

which can be written as

$$p(r) = c_1 re^{ar^2} + c_2 re^{ar^2}\ln r + c_2 are^{ar^2}\sum_{k=1}^{\infty}\frac{(-a)^{k-1}\left(\Delta^{2k} - r^{2k}\right)}{2kk!}$$

by the same trick.

The constants c_1 and c_2 are determined by the equations

$$p(\Delta) = 0, \qquad \int_0^\Delta p(r)\,dr = 1.$$

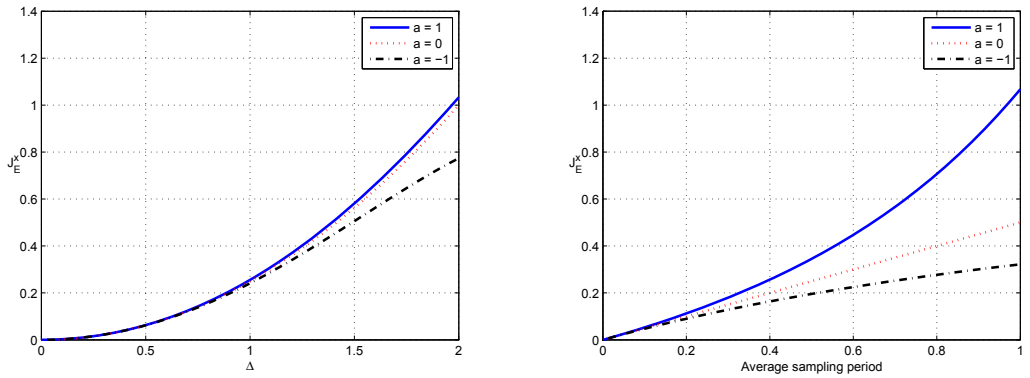

Figure 3.5: The mean square variation with event based impulse control for $a = -1, 0, 1$.

Having obtained the stationary probability distribution of r the variance of the states can be now computed

$$J_E^x = \int_0^{\Delta} r^2 p\,(r)\,dr.$$

For the case $a = 0$, the variance can be explicitly expressed by elementary functions.

Corollary 12 *Consider the stochastic differential equation in (3.1) with $a = 0$ controlled by an event based impulse scheme with the bound Δ. The variance of the state as defined in (3.2) is*

$$J_E^x = \frac{\Delta^2}{4}.$$

Proof. The probability density is given by

$$p\,(r) = c_1 r + c_2 r \ln r,$$

with c_1 and c_2 satisfying

$$c_1 + c_2 \ln \Delta = 0, \qquad \frac{\Delta^2}{2} c_1 + c_2 \left(\frac{\Delta^2 \ln \Delta}{2} - \frac{\Delta^2}{4} \right) = 1.$$

The equations determine that

$$c_1 = \frac{4 \ln \Delta}{\Delta^2}, \qquad c_2 = -\frac{4}{\Delta^2},$$

thus

$$p\,(r) = \frac{4r}{\Delta^2} \ln \frac{\Delta}{r}.$$

The variance of the states is given by

$$J_E^x = \int_0^\Delta r^2 p\left(r\right) dr = \int_0^\Delta \frac{4r^3}{\Delta^2} \ln \frac{\Delta}{r} dr = \frac{\Delta^2}{4}.$$

This completes the proof. ■

Figure 3.5 shows the variances of event based impulse control as a function of Δ and as a function of the average sampling period respectively. The curves exhibit similar behaviors to the variances of periodic impulse control.

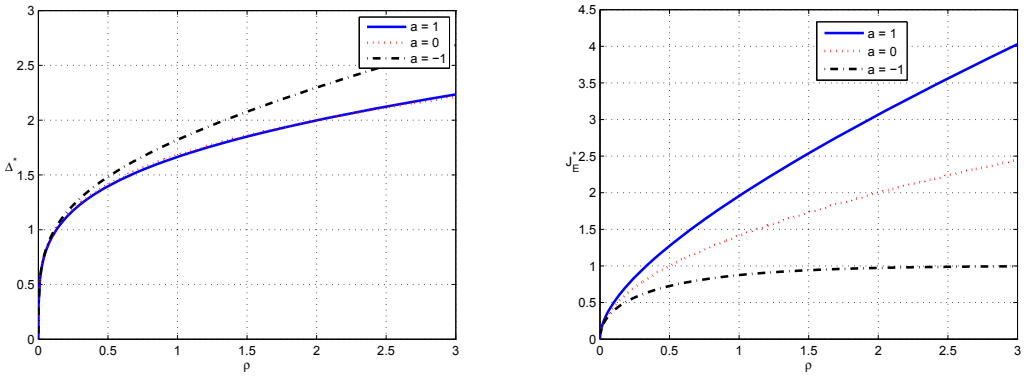

(a) Optimal threshold (b) Optimal cost

Figure 3.6: The optimal threshold and performance with event based impulse control for $a = -1, 0, 1$.

3.4.3 Optimal Threshold

The optimal threshold will be computed by minimizing the aggregate performance for a given weight ρ :

$$\Delta^* = \arg\min_{\Delta>0} J_E = \arg\min_{\Delta>0} \left(J_E^x + \rho J_E^u\right).$$

Again, the previous result is specialized to the case of $a = 0$.

Corollary 13 *Consider the stochastic differential equation in (3.1) with $a = 0$ controlled by an event based impulse scheme with the bound Δ. The optimal boundary Δ^* minimizes the performance in (3.2) is $\sqrt[4]{8\rho}$, and the optimal performance cost J_E^* incurred by the optimal threshold is then $\sqrt{2\rho}$.*

The proof can be done by solving the optimization problem with the objective function $J_E = \frac{\Delta^2}{4} + \rho\frac{2}{\Delta^2}$.

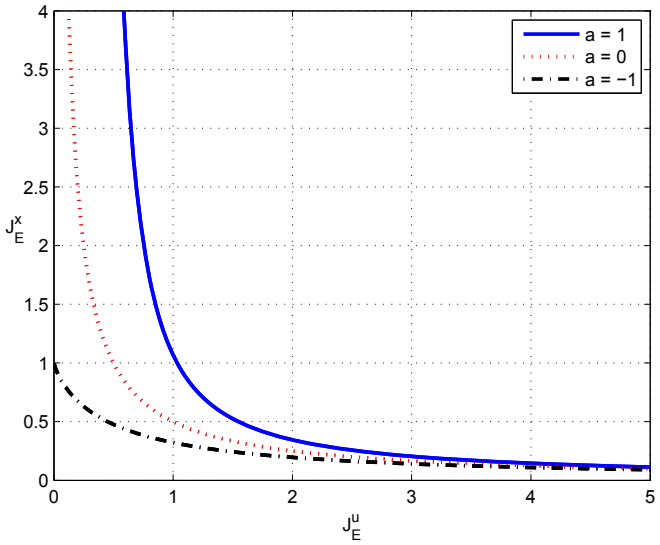

Figure 3.7: The optimal trade-off curve between the mean square variation and the average control rate with event based impulse control for $a = -1, 0, 1$.

The optimal threshold Δ^* and performance J_E^* as a function of the weight ρ are shown in Figure 3.6 for different values of the pole a. It can be seen that the optimal threshold is zero when $\rho = 0$ for each case, which leads to impulse control with continuous sampling. It can also be seen that the optimal cost decreases as a decreases. The optimal trade-off curves between the state variance cost and control rate cost are plotted in Figure 3.7. When a very large ρ is chosen, the most effective way to decrease J_E is to use little control, at the expense of a large variance; when a very small ρ is chosen, the most effective way to decrease J_E is to obtain a very small variance, even if this is achieved at the expense of a high control rate. The large curvature points for unstable and marginal stable systems show that small decreases in the control rate can be accomplished by large increases in the variances. Such point is the proverbial knee of the trade-off curve, and in many applications represents a good compromise solution [12]. However, for stable systems the control rate can be reduced to sufficiently low levels without large increase in the variance.

3.5 Comparison

To provide some insight, first consider the special case $a = 0$; the results for this case are summarized in the following corollary.

Corollary 14 *Consider the stochastic differential equation in (3.1) with* $a = 0$ *controlled*

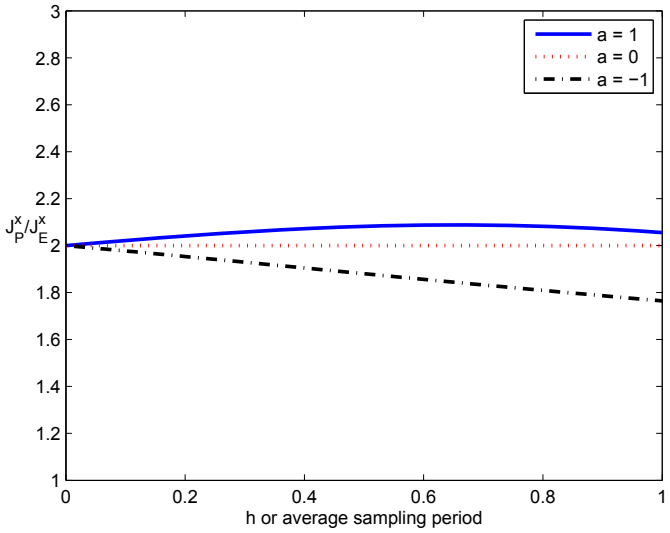

Figure 3.8: The ratio of the variances between periodic and event based impulse control for $a = -1, 0, 1$.

by impulses. The periodic control scheme with a sampling periodic h has the same average control rate with an event based control scheme with the bound $\Delta = \sqrt{2h}$, but the ratio of the state variances is

$$\frac{J_P^x}{J_E^x} = 2.$$

The proof can be easily done by equating $J_E^u = J_P^u$.

For fair comparison between periodic and event based impulse control it is natural to assume that the average control rate is the same. Therefore, it is sufficient to compare J^x only instead of J. Note that the distortion of periodic impulse control is twice higher than that of event based impulse control for $a = 0$. It turns out that the ratio is independent of the sampling period. Recall that for the first order integrator dynamics an event based impulse control gives a variance that is three times smaller than periodic impulse control [6].

Figure 3.8 shows the ratio J_P^x/J_E^x as a function of the average sampling period. It can be seen that all the curves are beyond 1, which shows that event based impulse control has better performance than periodic impulse control for the same average sampling rate. The advantage of event based control is more obvious for unstable systems in contrast with stable systems, for which the ratio decreases as the average sampling period increases.

The behaviors of the process for $a = 0$ with different sampling strategies are shown in Figure 3.9. The simulation was performed by choosing the same Wiener process and the boundary $\Delta = 2$. Notice that the process states are limited within the boundary all the

time for event based impulse control. However, the norm of the states with periodic impulse control is large around $t = 6, 15, 18$.

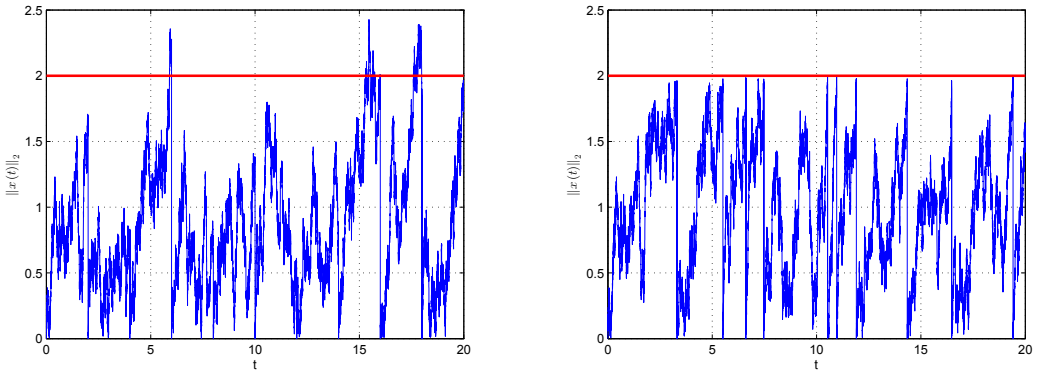

(a) Periodic impulse control

(b) Event based impulse control

Figure 3.9: Simulation with periodic and event based impulse control for $a = 0$.

3.6 Conclusion

In this chapter, the optimal sampling for periodic and event based impulse control was investigated for a class of second order stochastic systems. It provided an evidence that event based impulse control gave smaller variances than periodic impulse control with the same control rate for higher order systems. As an initial start, impulse control was used to reset the state of the system to the origin instantaneously. Another commonly used technique is pulse modulation, where event based control idea can be viewed as a combination of pulse width and frequency modulation. Our future research will focus on event based pulse modulation [112].

Chapter 4

Event Triggered Synchronization for Multi-Agent Networks

This chapter considers the synchronization problem for multi-agent systems with event based control updates, where all agents share the same dynamic model of any order, including single- and double-integrator dynamics as special cases.

4.1 Introduction

Multi-agent systems can be used to solve problems that are difficult or impossible for an individual agent or a monolithic system. Numerous contributions concerning distributed cooperative control strategies for continuous or periodic sampling have been given in the literature on multi-agent systems [101, 84]. Owing to their utility, developing tools for analysis and control of event triggered multi-agent systems is an active area of research. There are already some results on consensus control [17, 21, 68, 30, 25, 78, 118, 50], and tracking control [49, 119]. Note that existing results on distributed event triggered multi-agent systems focus on mostly single- or double-integrator dynamics [104]. Event triggered methods for linear multi-agent systems are presented in [18, 124, 69, 127]. In [18]: each agent predicts the future states of itself and its neighbors, and its state converges to a bounded region around some synchronous trajectory. A similar idea can be found in [69] as well, where a model based solution was applied to nonlinear agents.

Motivated by the existing work, we seek to further explore the problem of event triggered synchronization for multi-agent systems. In contrast to [18, 69, 127], the objective here is to attain asymptotic consensus which is distinguished from the related work of bounded consensus. All the agents in the network are assumed to have identical linear dynamics and a distributed event based control updating method is proposed to achieve synchronization be-

tween inter-connected agents under an undirected and connected network. An event detector is configured at each agent to determine when and which neighbor's state should be used to update the controller based on relative state differences. It is worth noting that the event conditions are required to be checked only at sampling instants. As pointed out in [6], it is more realistic to approximate continuous supervision by a high fast rate sampling. Here an explicit upper bound of the sampling period for event detection is given. In addition, to implement continuous event detectors requires delicate hardware to monitor local signals, and judge event conditions constantly; this may become a major source of energy consumption. The proposed framework is a generalization of applying event based control to synchronization of multi-agent systems in two ways: 1) the dynamics of each agent can be of any order, including single- and double-integrator dynamics as special cases; 2) a zero-order hold is used to solve dynamic synchronization problems instead of higher order holds. The main contributions of this chapter are highlighted as follows:

- A general problem is studied where the dynamics for each agent is described by a general linear model rather than single- or double-integrator dynamics.
- Continuous communication and control algorithms have been relaxed to periodic communication and event based control ones.
- A co-design of parameters of controllers and event detectors is realized.

4.2 Synchronization Problem

Consider a network $\mathcal{G}$ with N identical agents. The dynamics of the ith agent is described by the linear model

$$\dot{x}_i(t) = Ax_i(t) + Bu_i(t), \tag{4.1}$$

where $x_i(t) \in \mathbb{R}^n$ denotes the state, and $u_i(t) \in \mathbb{R}^p$ is the control input to be designed, A and B are constant real matrices with compatible dimensions. Assume that the matrix pair (A, B) is stabilizable. The edge state $z(t) = \begin{bmatrix} z_1^T(t) & z_2^T(t) & \cdots & z_m^T(t) \end{bmatrix}^T$ is defined by the transformation

$$z(t) = (\mathcal{D}^T \otimes I)x(t),$$

where $\mathcal{D}$ is the incidence matrix of $\mathcal{G}$, and

$$x(t) = \begin{bmatrix} x_1^T(t) & x_2^T(t) & \cdots & x_N^T(t) \end{bmatrix}^T.$$

The control law for agent i, adopting event triggered strategies, is designed as

$$u_i(t) = -K \sum_{j=1}^{m} d_{ij} \hat{z}_j(t), \tag{4.2}$$

where d_{ij} is the (i,j) entry of the incidence matrix $\mathcal{D} \in \mathbb{R}^{N\times m}$; note that the control law in 4.2 is distributed in the sense that each agent needs only the neighbors' information to perform control updates instead of all agents' information. The control gain K can be parameterized as

$$K = \frac{\alpha}{2} B^T S^{-1},$$

with the positive definite matrix S and the positive scalar α satisfying

$$SA^T + AS + \sigma\lambda_N S - \lambda_2 \rho \alpha B B^T < 0, \tag{4.3}$$

for any given $0 < \rho < 1$ and $\sigma > 0$ to be determined later; and $\hat{z}_j(t)$ is a piecewise constant signal

$$\hat{z}_j(t) = z_j\left(t_k^j\right), \text{ for } t \in \left[t_k^j, t_{k+1}^j\right),$$

where $\{t_0^j, t_1^j, \ldots\}$ forms the common event sequence of the two agents linked by the jth edge and it is a subsequence of $\{0, h, 2h, \ldots\}$. Here h is the sampling period for all agents synchronized physically by a clock. In other words, the triggering conditions are required to be checked only periodically not continuously as in the case for linear systems [43]. Note that the control law for agent i is updated at the union of event times of those edges that share vertex i. Therefore, an event detector will be configured on each agent to monitor the relative states between itself and each neighbor, and the number of event conditions is determined by the cardinality of its neighbor set.

Remark 15 *For each agent, the edge state of different communication links is related to a different event condition. A set of event conditions is provided that each event condition is used to decide when to trigger an event, thus updating the controller by using the edge state of the corresponding link. Two agents communicated via this link will update their controllers simultaneously since the event condition related to the same communication link is designed to be the same. The triggering of events is synchronized by a communication link, which can be regarded as an edge-based control updating law [117]. Let us discuss the pros and cons of the edge-based approach. For the edge-based approach, event detection is based on state differences of connected agents. For systems with any order, the differences converge to zero. Therefore, a zero-order hold of control signals can be used. For node-based approaches, event detection is based on state differences of an agent at different times.*

The differences converge to zero only when the dynamic is single integrator. For agents with double integrator dynamics, a first order hold for the position is incorporated to avoid the Zeno behavior [104]. For agents with general linear dynamics, a model based approach is incorporated to generate a control input for node-based event detection [18]. It is desirable to have holds that match the process. A drawback of edge-based event detection is that continuous or periodic communication is necessary to monitor state differences between two linked agents.

With the event based control protocol in (4.2), the synchronization is achieved by the team of agents under an undirected and connected communication topology if, for all $x_i(0)$, $i = 1, 2, \ldots, N$, $\|z_j(t)\| \longrightarrow 0$ for all $j = 1, 2, \ldots, m,$ as $t \longrightarrow \infty$.

4.3 Event Triggered Synchronization Algorithm for General Linear Dynamics

Define the state error for edge j as $e_j(kh) = \hat{z}_j(kh) - z_j(kh)$, and denote the stack vector $e(t) = \begin{bmatrix} e_1^T(t) & e_2^T(t) & \cdots & e_m^T(t) \end{bmatrix}^T$. The error defined reflects the relative difference of two agents between the state at the last event time and the currently sampled state. Then the closed-loop system with the event based control becomes

$$\begin{aligned} \dot{x}(t) &= (I \otimes A)\, x(t) - (\mathcal{D} \otimes BK)\, z(kh) - (\mathcal{D} \otimes BK)\, e(kh) \\ &= (I \otimes A)\, x(t) - (\mathcal{L} \otimes BK)\, x(kh) - (\mathcal{D} \otimes BK)\, e(kh) \end{aligned}$$

for $t \in [kh, kh + h)$.

Define the disagreement vector

$$\delta(t) = x(t) - \mathbf{1} \otimes \bar{x}(t),$$

where

$$\bar{x}(t) = \frac{1}{N} \sum\nolimits_{i=1}^{N} x_i(t)$$

denotes the average of the states for all agents. The disagreement vector has zero average by definition, that is,

$$\mathbf{1}^T \delta(t) = 0.$$

It can be acquired that

$$\begin{aligned} \dot{\bar{x}}(t) &= \frac{1}{N} \sum\nolimits_{i=1}^{N} \dot{x}_i(t) = \frac{1}{N} (\mathbf{1} \otimes I)^T \dot{x}(t) \\ &= \frac{1}{N} (\mathbf{1} \otimes I)^T (I \otimes A)\, x(t) = A\bar{x}(t) \end{aligned}$$

since

$$\mathbf{1}^T\mathcal{L}=0, \qquad \mathbf{1}^T\mathcal{D}=0.$$

Therefore, it can be obtained that

$$\bar{x}\left(t\right)=e^{At}\bar{x}\left(0\right)=\frac{1}{N}e^{At}\sum\nolimits_{i=1}^{N}x_i\left(0\right), \tag{4.4}$$

that is, the trajectories for all agents will converge to

$$\frac{1}{N}e^{At}\sum\nolimits_{i=1}^{N}x_i\left(0\right).$$

In fact,

$$\left\|z\left(t\right)\right\|=\left\|\left(\mathcal{D}^T\otimes I\right)x\left(t\right)\right\|\leq\left\|\mathcal{D}\right\|\left\|\delta\left(t\right)\right\|.$$

In lieu of the vertex-to-edge transformation induced by the incidence matrix of $\mathcal{G}$, it follows that agreement in the vertex states is equivalent to having $z\left(t\right)=0$ when $\mathcal{G}$ is connected.

The following theory ensures that the synchronization is reached asymptotically under certain conditions with the notations

$$\begin{aligned}\mu=&\lambda_{\min}(\lambda_2\alpha\rho S^{-1}BB^TS^{-1}-A^TS^{-1}-S^{-1}A-\sigma\lambda_NS^{-1})\\ \beta=&\lambda_{\max}\left\{\lambda_N^2\alpha^2S^{-1}BB^TS^{-1}\left(4ASA^T+4\lambda_NBB^T+\lambda_N^2\alpha^2BB^TS^{-1}BB^T\right)S^{-1}BB^TS^{-1}\right.\\ &\left.+16\left[2+\lambda_N\sigma\alpha\left(1-\rho\right)\right]S^{-1}\right\}.\end{aligned}$$

Theorem 16 *Consider the system in (4.1) over an undirected, connected graph $\mathcal{G}$. Choose the parameter $\sigma>0$ so that $(A+\frac{\sigma\lambda_N}{2}I,B)$ is stabilizable. Then the control law (4.2) and the periodic triggering conditions*

$$\alpha e_j^T\left(kh\right)S^{-1}BB^TS^{-1}e_j\left(kh\right)\leq4\sigma\left(1-\rho\right)z_j^T\left(kh\right)S^{-1}z_j\left(kh\right), \tag{4.5}$$

with any sampling period h less than $16\frac{\mu}{\beta}$ guarantee the states of all agents converge to

$$\frac{1}{N}e^{At}\sum\nolimits_{i=1}^{N}x_i\left(0\right),$$

for any initial condition $x_i\left(0\right)\in R^n$.

Proof. It is easy to see that

$$\left(\mathcal{L}\otimes I\right)x\left(t\right)=\left(\mathcal{L}\otimes I\right)\delta\left(t\right).$$

Then the closed-loop system can be rewritten in the form of time delayed differential equations

$$\begin{aligned}\dot{\delta}(t) &= \dot{x}(t) - \mathbf{1} \otimes \dot{\bar{x}}(t) \\ &= (I \otimes A)\,\delta(t) - (\mathcal{L} \otimes BK)\,\delta(t - r(t)) - (\mathcal{D} \otimes BK)\,e(t - r(t)), \end{aligned} \tag{4.6}$$

where $r(t) = t - kh$, for any $t \in [kh, kh + h)$ and $k \in \{0, 1, 2, \ldots\}$ is a sawtooth delay [27] used to model sample-and-hold circuits.

With the observation that

$$\begin{aligned}\delta(t - r(t)) &= \delta(t) - \int_{t-r(t)}^{t} \dot{\delta}(s)\,ds \\ &= \delta(t) + \int_{t-r(t)}^{t} (\mathcal{L} \otimes BK)\,\delta(s - r(s))\,ds \\ &\quad - \int_{t-r(t)}^{t} (I \otimes A)\,\delta(s)\,ds + \int_{t-r(t)}^{t} (\mathcal{D} \otimes BK)\,e(s - r(s))\,ds,\end{aligned}$$

the system in (4.6) can be transformed to

$$\begin{aligned}\dot{\delta}(t) = &(I \otimes A - \mathcal{L} \otimes BK)\,\delta(t) - r(t)\,(\mathcal{L} \otimes BK)^2\,\delta(t - r(t)) \\ &- r(t)\,(\mathcal{L} \otimes BK)\,(\mathcal{D} \otimes BK)\,e(t - r(t)) \\ &- (\mathcal{D} \otimes BK)\,e(t - r(t)) + (\mathcal{L} \otimes BK)\,(I \otimes A) \int_{t-r(t)}^{t} \delta(s)\,ds. \end{aligned} \tag{4.7}$$

The process of transforming the system represented by (4.6) to the one represented by (4.7) is known as a *model transformation*. The stability of the system represented by (4.7) implies the stability of the original system in (4.6). We can derive a stability condition for the transformed system in (4.7), which of course, is sufficient for the stability of the original system in (4.6).

Constructing the following Lyapunov function as

$$V(\delta(t)) = \delta^T(t)\,(I \otimes P)\,\delta(t),$$

where $P = S^{-1}$ is a positive definite matrix with appropriate dimensions, and S is a feasible solution of the LMI in (4.3). Since $\alpha > 0$ and the LMI condition in (4.3) is homogeneous in S and α, the product $\lambda_2 \rho \alpha$ can be taken as 1 without loss of generality, thus reducing the number of variables by one. We may as well absorb the product $\sigma\lambda_N$ into A. So an alternate equivalent condition can be derived:

$$S\left(A + \frac{\sigma\lambda_N}{2} I\right)^T + \left(A + \frac{\sigma\lambda_N}{2} I\right) S - BB^T < 0.$$

These LMI conditions are feasible if and only if $\left(A+\frac{\sigma\lambda_N}{2}I, B\right)$ is stabilizable [11]. We show here that by an appropriate choice of the parameter σ, the solutions to the LMI in (4.3) always exist. It is well known that the pair (A, B) is stabilizable if and only if $[A-\lambda I \quad B]$ has full row rank for all $\lambda \in \mathbb{C}$ with $\mathrm{Re}(\lambda) \geq 0$. If λ is an eigenvalue of A, then $\lambda+\frac{\sigma\lambda_N}{2}$ is an eigenvalue of the matrix $A+\frac{\sigma\lambda_N}{2}I$. For all $\lambda \in \mathbb{C}$ with $\mathrm{Re}(\lambda) \geq 0$, $\mathrm{rank}\left([A+\frac{\sigma\lambda_N}{2}I-\lambda I-\frac{\sigma\lambda_N}{2}I \quad B]\right) = \mathrm{rank}([A-\lambda I \quad B]) = n$. For all $\lambda \in \mathbb{C}$ with $\mathrm{Re}(\lambda) < 0$, if we choose $\sigma < \frac{2\min \mathrm{Re}(-\lambda)}{\lambda_N}$, then $\mathrm{Re}\left(\lambda+\frac{\sigma\lambda_N}{2}\right) < 0$ for all $\mathrm{Re}(\lambda) < 0$.

Since $P > 0$, we can conclude that

$$\lambda_{\min}(P)\|\delta(t)\|^2 \leq V(\delta(t)) \leq \lambda_{\max}(P)\|\delta(t)\|^2.$$

The next step is to show that $\dot{V}(\delta(t)) \leq -\varepsilon\|\delta(t)\|^2$ whenever

$$V(\delta(t-r(t))) \leq qV(\delta(t)),$$

for some $q > 1$.

Considering the derivative of $V(\delta(t))$, we have

$$\begin{aligned}\dot{V}(\delta(t)) &= \delta^T(t)\left[I\otimes\left(A^TP+PA\right)-2\mathcal{L}\otimes PBK\right]\delta(t)\\ &\quad -2\delta^T(t)(\mathcal{D}\otimes PBK)e(t-r(t))\\ &\quad -2r(t)\delta^T(t)\left(\mathcal{L}^2\otimes PBKBK\right)\delta(t-r(t))\\ &\quad -2r(t)\delta^T(t)(\mathcal{L}\mathcal{D}\otimes PBKBK)e(t-r(t))\\ &\quad +\int_{t-r(t)}^{t}2\delta^T(t)(\mathcal{L}\otimes PBKA)\delta(s)\,ds.\end{aligned}$$

Observe that

$$2a^Tb \leq a^T\Psi a + b^T\Psi^{-1}b \tag{4.8}$$

holds for any positive definite matrix Ψ. Thus, applying the inequality for the last term in $\dot{V}(\delta(t))$ with

$$a^T = \delta^T(t)(\mathcal{L}\otimes PBKA),\ b = \delta(s)$$

and

$$\Psi = (I\otimes P)^{-1},$$

we obtain

$$\begin{aligned}2\delta^T(t)(\mathcal{L}\otimes PBKA)\int_{t-r(t)}^{t}\delta(s)\,ds &\leq \int_{t-r(t)}^{t}V(s)\,ds\\ &\quad +\int_{t-r(t)}^{t}\delta^T(t)(\mathcal{L}\otimes PBKA)(I\otimes P)^{-1}(\mathcal{L}\otimes PBKA)^T\delta(t)\,ds.\end{aligned}$$

For the third term in $\dot{V}(\delta(t))$, using again the inequality in (4.8) with

$$a^T = \delta^T(t)\left(\mathcal{L}^2 \otimes PBKBK\right),\ b = -\delta(t - r(t)),$$

and

$$\Psi = (I \otimes P)^{-1},$$

we have

$$\begin{aligned}
&-2r(t)\,\delta^T(t)\left(\mathcal{L}^2 \otimes PBKBK\right)\delta(t - r(t)) \\
\leq\ & r(t)\,\delta^T(t)\left(\mathcal{L}^2 \otimes PBKBK\right)(I \otimes P)^{-1}\left(\mathcal{L}^2 \otimes PBKBK\right)^T\delta(t) \\
&+ r(t)\,\delta^T(t - r(t))(I \otimes P)\,\delta(t - r(t)) \\
\leq\ & h\delta^T(t)\left(\mathcal{L}^2 \otimes PBKBK\right)(I \otimes P)^{-1}\left(\mathcal{L}^2 \otimes PBKBK\right)^T\delta(t) + hV(t - r(t)), \quad (4.9)
\end{aligned}$$

where the last inequality is due to $0 \leq r(t) < h$. Similarly, for the other terms in $\dot{V}(\delta(t))$, we get

$$\begin{aligned}
& -2r(t)\,\delta^T(t)\left(\mathcal{L}\mathcal{D} \otimes PBKBK\right)e(t - r(t)) \\
=\ & -2r(t)\,\delta^T(t)\left(\mathcal{L}\mathcal{D} \otimes PBKB\right)(I \otimes K)\,e(t - r(t)) \\
\leq\ & r(t)\,\delta^T(t)\left(\mathcal{L}\mathcal{D} \otimes PBKB\right)\left(\mathcal{L}\mathcal{D} \otimes PBKB\right)^T\delta(t) \\
& + r(t)\,e^T(t - r(t))(I \otimes K)^T(I \otimes K)\,e(t - r(t)) \\
\leq\ & h\delta^T(t)\left(\mathcal{L}\mathcal{D}\mathcal{D}^T\mathcal{L} \otimes PBKBB^TK^TB^TP\right)\delta^T(t) \\
& + he^T(t - r(t))\left(I \otimes K^TK\right)e(t - r(t)), \quad (4.10)
\end{aligned}$$

$$\begin{aligned}
-2\delta^T(t)\left(\mathcal{D} \otimes PBK\right)e(t - r(t)) \leq\ & \alpha^{-1}(1 - \rho)^{-1}e^T(t - r(t))\left(I \otimes K^TK\right)e(t - r(t)) \\
& + \alpha(1 - \rho)\,\delta^T(t)\left(\mathcal{D}\mathcal{D}^T \otimes PBB^TP\right)\delta(t). \quad (4.11)
\end{aligned}$$

The event condition in (4.5) implies that

$$e_j^T(t - r(t))\,K^TKe_j(t - r(t)) \leq \sigma\alpha(1 - \rho)\,z_j^T(t - r(t))\,Pz_j(t - r(t)),$$

for $j = 1, 2, \ldots, m$. Since

$$z^T(t - r(t))(I \otimes P)\,z(t - r(t)) = \delta^T(t - r(t))(\mathcal{L} \otimes P)\,\delta(t - r(t)),$$

we have

$$\begin{aligned}
e^T(t - r(t))\left(I \otimes K^TK\right)e(t - r(t)) &\leq \sigma\alpha(1 - \rho)\,z^T(t - r(t))(I \otimes P)\,z(t - r(t)) \\
&= \sigma\alpha(1 - \rho)\,\delta^T(t - r(t))(\mathcal{L} \otimes P)\,\delta(t - r(t)).
\end{aligned}$$

We can conclude from the above inequalities that

$$\begin{aligned}\dot{V}\left(\delta(t)\right) \leq & \delta^T\left(t\right)\left[I\otimes\left(A^TP+PA\right)-\mathcal{L}\otimes\left(2PBK\right)\right]\delta\left(t\right)\\ &+\delta^T\left(t\right)\left[\mathcal{L}\otimes\left(\alpha PBB^TP-\alpha\rho PBB^TP\right)\right]\delta\left(t\right)\\ &+\sigma\delta^T\left(t-r\left(t\right)\right)\left(\mathcal{L}\otimes P\right)\delta\left(t-r\left(t\right)\right)\\ &+h\delta^T\left(t-r\left(t\right)\right)\left(I\otimes P\right)\delta\left(t-r\left(t\right)\right)\\ &+h\delta^T\left(t\right)\left(\mathcal{L}^4\otimes PBKBKP^{-1}K^TB^TK^TB^TP\right)\delta\left(t\right)\\ &+h\sigma\alpha\left(1-\rho\right)\delta^T\left(t-r\left(t\right)\right)\left(\mathcal{L}\otimes P\right)\delta\left(t-r\left(t\right)\right)\\ &+h\delta^T\left(t\right)\left(\mathcal{L}^3\otimes PBKBB^TK^TB^TP\right)\delta\left(t\right)\\ &+h\delta^T\left(t\right)\left(\mathcal{L}^2\otimes PBKAP^{-1}A^TK^TB^TP\right)\delta\left(t\right)\\ &+\int_{t-r(t)}^{t}V\left(\delta\left(s\right)\right)ds.\end{aligned}$$

Whenever

$$V\left(\delta(t-r\left(t\right))\right)\leq qV\left(\delta(t)\right),$$

for $q>1$, we have

$$\int_{t-r(t)}^{t}V\left(\delta\left(s\right)\right)ds=\int_{-r(t)}^{0}V\left(\delta\left(t+s\right)\right)ds\leq\int_{-r(t)}^{0}qV\left(\delta(t)\right)ds\leq qhV\left(\delta\left(t\right)\right).$$

Substituting

$$K=\frac{\alpha}{2}B^TP$$

yields

$$\begin{aligned}\dot{V}\left(\delta(t)\right)\leq & \delta^T\left(t\right)\left[I\otimes\left(A^TP+PA+q\lambda_N\sigma P\right)\right]\delta\left(t\right)\\ &-\delta^T\left(t\right)\left(I\otimes\lambda_2\alpha\rho PBB^TP\right)\delta\left(t\right)\\ &+h\delta^T\left(t\right)\left[I\otimes\left(2+\lambda_N\sigma\left(1-\rho\right)\right)16qP\right]\delta\left(t\right)/16\\ &+h\delta^T\left(t\right)\left[I\otimes\lambda_N^2\alpha^2PBB^TPAP^{-1}A^TPBB^TP\right]\delta\left(t\right)/4\\ &+h\delta^T\left(t\right)\left[I\otimes\left(\alpha^2\lambda_N^3PBB^TPBB^TPBB^TP\right)\right]\delta\left(t\right)/4\\ &+h\delta^T\left(t\right)\left[I\otimes\alpha^4\lambda_N^4PBB^TPBB^TPBB^TPBB^TP\right]\delta\left(t\right)/16.\end{aligned}$$

Multiplying the inequality in (4.3) by P on the left and right, we have that

$$Q=\lambda_2\alpha\rho PBB^TP-A^TP-PA-\sigma\lambda_NP$$

is positive definite, which implies that for some sufficiently small θ, $q=1+\theta$,

$$\dot{V}\left(\delta(t)\right)\leq-\mu\delta^T\left(t\right)\delta\left(t\right)+h\beta\delta^T\left(t\right)\delta\left(t\right)/16.$$

Choosing the upper bound of the sampling period to satisfy

$$h = 16\eta\frac{\mu}{\beta}$$

with $0 < \eta < 1$, we get

$$\dot{V}\left(\delta\left(t\right)\right) \leq -\varepsilon \left\|\delta\left(t\right)\right\|^2.$$

According to the Razumikhin theorem, $\delta\left(t\right) = 0$ is asymptotically stable. ■

Remark 17 *There are a few parameters involved in the LMI condition. To clarify, the role of different parameters are explained as follows. The parameter σ can be predetermined by users, which is indirectly related to the event frequency: A larger σ leads to a lower frequency of control updates, while a smaller σ leads to a faster convergence rate. Therefore, there is a trade-off between the control updating frequency and the synchronization speed. The parameter α is used to parameterize the controller, which is decided by the solution to the LMI condition. It can be taken as 1 without loss of generality.*

Remark 18 *The design is finally cast in the form of an LMI feasibility problem. In the LMI condition in (4.3), the smallest positive and largest eigenvalues have to be known to all agents. Since these parameters depend on the global network topology, the problem cannot be solved locally. However, an upper bound on the largest eigenvalue λ_N and a lower bound on the smallest positive eigenvalue of λ_2 can be found by*

$$\lambda_N \leq 2\left(N-1\right), \quad \lambda_2 \geq \frac{4}{N\left(N-1\right)}$$

based on the results in [36] and [86], and the fact that the maximum number of neighbors is no more than $N-1$. Therefore, the LMI condition in (4.3) can be relaxed to

$$N\left(N-1\right)SA^T + N\left(N-1\right)AS + 2\sigma N\left(N-1\right)^2 S - 4\rho\alpha BB^T < 0,$$

if the total number of agents N is known.

Example 19 *Consider a network with 4 harmonic oscillators shown in Figure 4.1.*

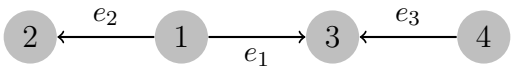

Figure 4.1: An undirected graph with 4 vertices that is arbitrarily oriented

The dynamics of the ith agent satisfies

$$\dot{x}_i\left(t\right) = Ax_i\left(t\right) + Bu_i\left(t\right), \qquad x_i\left(t\right) \in \mathbb{R}^2,\ i = 1,2,3,4$$

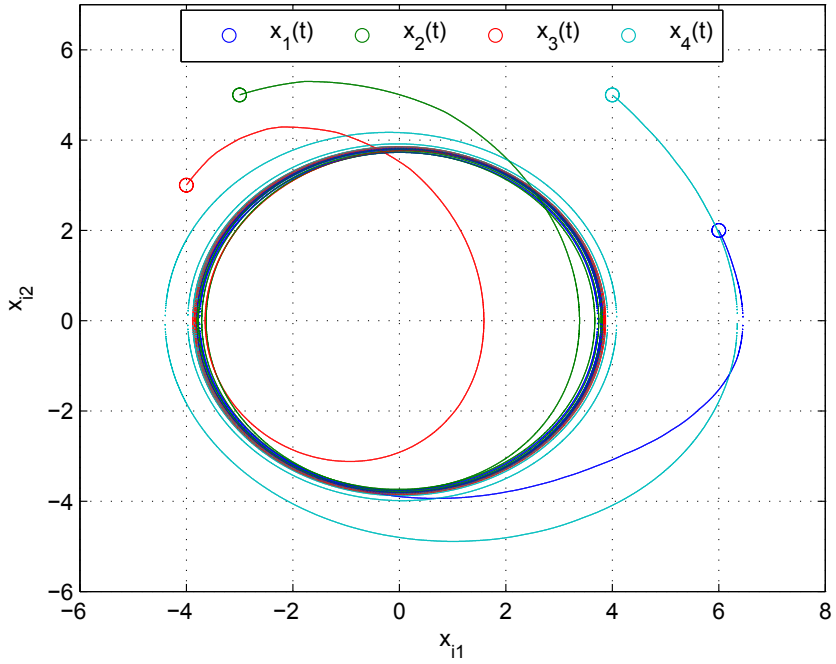

Figure 4.2: Trajectory of each agent

where

$$A = \begin{bmatrix} 0 & 1 \\ -1 & 0 \end{bmatrix}, \qquad B = \begin{bmatrix} 0 \\ 1 \end{bmatrix}.$$

Obviously, the communication topology is connected, and the smallest and largest nonzero eigenvalues are $\lambda_2 = 0.5858$ *and* $\lambda_N = 3.4142$*, respectively.*

First, letting

$$\rho = 0.2, \qquad \sigma = 0.01$$

and solving the LMI condition in (4.3), we have

$$S = \begin{bmatrix} 1.3185 & -0.0467 \\ -0.0467 & 1.3201 \end{bmatrix}.$$

Thus, the feedback controller gain is

$$K = \begin{bmatrix} 0.0150 & 0.4236 \end{bmatrix},$$

and the sampling period satisfies

$$h < 0.0026.$$

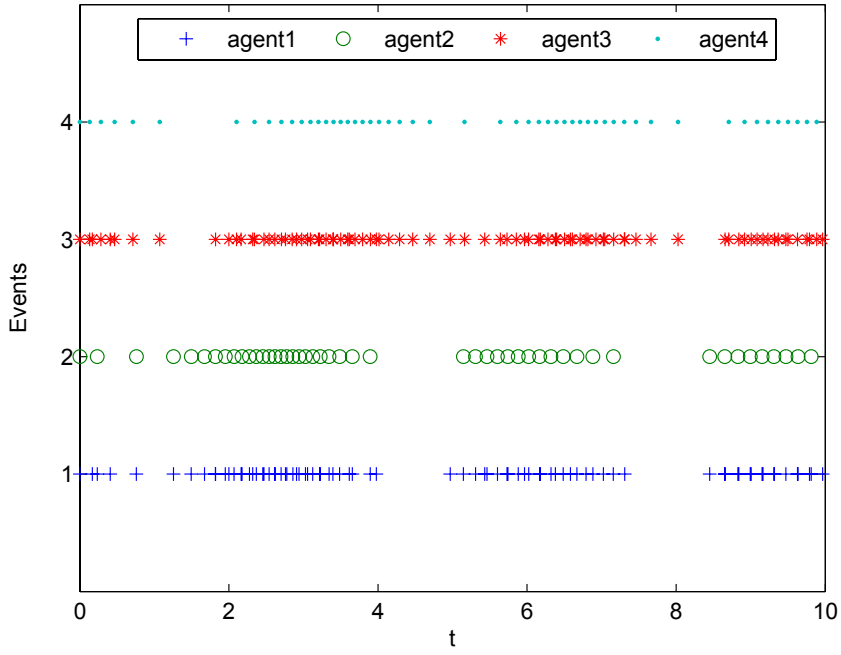

Figure 4.3: Event times for each agent

In simulation, choose $h = 0.001$ *and initial values as*

$$x_1(0) = \begin{bmatrix} 6 \\ 2 \end{bmatrix}; \qquad x_2(0) = \begin{bmatrix} -3 \\ 5 \end{bmatrix};$$
$$x_3(0) = \begin{bmatrix} -4 \\ 3 \end{bmatrix}; \qquad x_4(0) = \begin{bmatrix} 4 \\ 5 \end{bmatrix}.$$

Since each agent is of the second order, it is straightforward to show the trajectories in Figure 4.2. It can be observed that the states exhibit an oscillation behavior after a short transient time. The trajectories of all the four agents converge to a common circle centered at the origin with radius 3.8243. The time instants when each agent updates its controller are shown in Figure 4.3 for the first 10 seconds, and the aggregate numbers of events are 238, 127, 244, 134, respectively, for agents 1-4, during a simulation of 30 seconds. Figure 4.4 shows the evolution of the event condition which triggers the control updates for both agent 1 and agent 2. In the figure, an event is generated when the left-hand side value of the event condition in equation (4.5) shown in solid lines reaches the threshold given by the right-hand side value of the event condition in equation (4.5) shown in dashed lines, and then the left-hand signal is reset to zero immediately. The actual minimum inter-event time of the events on edge e_2 *is the sampling period. Therefore, the Zeno behavior is excluded*

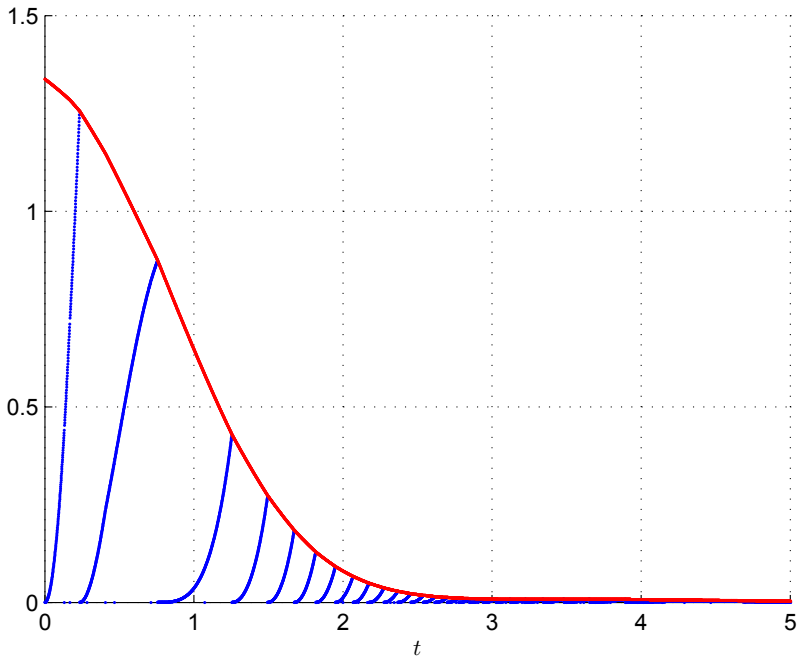

Figure 4.4: Evolution of the event condition shared by agent 1 and agent 2

both theoretically and numerically. The theoretical analysis is validated very well by the simulation results.

4.4 Event Triggered Synchronization Algorithm for Double Integrator Dynamics

Consider agents with double-integrator dynamics given by

$$\dot{\xi}_i(t) = \zeta_i(t), \qquad \dot{\zeta}_i(t) = u_i(t), \qquad i = 1, \ldots, N, \tag{4.12}$$

where $\xi_i(t) \in \mathbb{R}^n$, $\zeta_i(t) \in \mathbb{R}^n$ and $u_i(t) \in \mathbb{R}^n$ are, respectively, the position, velocity and acceleration associated with the ith agent.

Define

$$z^{\xi}(t) = \left(\mathcal{D}^T \otimes I\right) \xi(t), \qquad z^{\zeta}(t) = \left(\mathcal{D}^T \otimes I\right) \zeta(t).$$

Then an event based consensus algorithm is proposed as

$$u_i(t) = -\sum_{j=1}^{m} d_{ij} \left[\hat{z}_j^{\xi}(t) + \gamma \hat{z}_j^{\zeta}(t)\right], \; i = 1, \ldots, N, \tag{4.13}$$

where γ is a positive scalar to be determined later. With (4.13), consensus is achieved by the team of agents under an undirected and connected communication topology if, for all $\xi_i(0)$ and $\zeta_i(0)$, $i = 1, \ldots, N$, $\|z_j^{\xi}(t)\| \to 0$ and $\|z_j^{\zeta}(t)\| \to 0$, as $t \to \infty$ for all $j = 1, \ldots, m$.

Let

$$x_i(t) \triangleq \left[\begin{array}{cc} \xi_i(t)^T & \zeta_i(t)^T \end{array} \right]^T,$$

and

$$z_j(t) \triangleq \left[\begin{array}{cc} z_j^{\xi}(t)^T & z_j^{\zeta}(t)^T \end{array} \right]^T.$$

By applying the algorithm in (4.13), the equation in (4.12) can be written as

$$\dot{x}(t) = (I \otimes A)\, x(t) - (\mathcal{D} \otimes BK)\, z(kh) - (\mathcal{D} \otimes BK)\, e(kh),$$

for $t \in [kh, kh + h)$, where

$$A = \left[\begin{array}{cc} 0 & 1 \\ 0 & 0 \end{array} \right], \qquad B = \left[\begin{array}{c} 0 \\ 1 \end{array} \right], \qquad K = \left[\begin{array}{cc} 1 & \gamma \end{array} \right].$$

According to (4.4) and

$$e^{At} = \left[\begin{array}{cc} 1 & t \\ 0 & 1 \end{array} \right],$$

the average position and velocity of all agents are

$$\bar{\xi}(t) = \frac{1}{N} \sum\nolimits_{i=1}^{N} \xi_i(t) = \frac{1}{N} \sum\nolimits_{i=1}^{N} \xi_i(0) + \frac{t}{N} \sum\nolimits_{i=1}^{N} \zeta_i(0)$$

and

$$\bar{\zeta}(t) = \frac{1}{N} \sum\nolimits_{i=1}^{N} \zeta_i(t) = \frac{1}{N} \sum\nolimits_{i=1}^{N} \zeta_i(0),$$

respectively. Therefore, the average velocity remains constant as their initial average over time, and the average position is their initial average plus the average velocity multiplied by t.

Thus, the disagreement vector can be defined as

$$\delta_i(t) = x_i(t) - \bar{x}(t)$$

with

$$\bar{x}(t) = \frac{1}{N} \sum\nolimits_{i=1}^{N} \left[\begin{array}{c} \xi_i(0) + t\zeta_i(0) \\ \zeta_i(0) \end{array} \right],$$

and the disagreement dynamics can be written in a compact form:

$$\dot{\delta}(t) = (I \otimes A)\, \delta(t) - (\mathcal{L} \otimes BK)\, \delta(kh) - (\mathcal{D} \otimes BK)\, e(kh).$$

Defining

$$\begin{aligned}\mu =&\lambda_{\min}\left(2\lambda_2\rho PBB^TP - A^TP - PA - \sigma\lambda_N P\right)\\ \beta =&\lambda_{\max}\left\{\lambda_N^2 PBB^TP\left(ASA^T + \lambda_N^2 BB^TPBB^T\right.\right.\\ &\left.\left.+\lambda_N BB^T\right)PBB^TP + 2\left[1+\lambda_N\sigma\left(1-\rho\right)\right]P\right\},\end{aligned}$$

we can thus summarize the result as follows.

Theorem 20 *Consider the system in (4.12) over an undirected, connected graph $\mathcal{G}$. Choose the parameters $0<\rho<1,\ \gamma,\ p$ and σ satisfying (4.14) or (4.15). Then for the control law in (4.13) and the event condition*

$$\begin{bmatrix} e_j^{\xi}(kh)\\ e_j^{\zeta}(kh)\end{bmatrix}^T\begin{bmatrix}1 & \gamma\\ \gamma & \gamma^2\end{bmatrix}\begin{bmatrix} e_j^{\xi}(kh)\\ e_j^{\zeta}(kh)\end{bmatrix}\le 2\sigma\left(1-\rho\right)\begin{bmatrix} z_j^{\xi}(kh)\\ z_j^{\zeta}(kh)\end{bmatrix}^T P\begin{bmatrix} z_j^{\xi}(kh)\\ z_j^{\zeta}(kh)\end{bmatrix},$$

$j=1,\dots m$, *with any sampling period h less than $\frac{\mu}{\beta}$, the position and velocity states of all agents converge to*

$$\frac{1}{N}\sum\nolimits_{i=1}^{N}\xi_i(0)+t\zeta_i(0)$$

and

$$\frac{1}{N}\sum\nolimits_{i=1}^{N}\zeta_i(0),$$

respectively, for any initial condition $\xi_i(0)\in\mathbb{R}^n$ and $\zeta_i(0)\in\mathbb{R}^n$, $i=1,\dots N$.

Proof. Take a candidate Lyapunov function

$$V(t)=\delta^T(t)\left(I\otimes P\right)\delta(t),$$

with a symmetric positive definite matrix

$$P=\begin{bmatrix}p & 1\\ 1 & \gamma\end{bmatrix},$$

with

$$p\gamma>1.$$

According to Theorem 16, the corresponding LMI condition in (4.3) becomes

$$\begin{bmatrix}2-\sigma\lambda_N\gamma & -p+\sigma\lambda_N\\ -p+\sigma\lambda_N & 2\lambda_2\rho\left(p\gamma-1\right)-\sigma\lambda_N p\end{bmatrix}>0.$$

Then the condition is held if and only if

$$\sigma<\frac{2}{\lambda_N\gamma}$$

and

$$(\lambda_N\sigma)^2 - 2\gamma\lambda_2\rho\,(\lambda_N\sigma) + 4\lambda_2\rho - \frac{p^2}{p\gamma - 1} > 0.$$

Consider the left-hand side of the second inequality as a quadratic function

$$f(\chi) = \chi^2 - b\gamma\chi + 2b - \frac{p^2}{p\gamma - 1}$$

where

$$\chi = \lambda_N\sigma, \qquad b = 2\lambda_2\rho.$$

The quadratic function has two real roots

$$\frac{b\gamma \pm \sqrt{\Delta}}{2},$$

since the discriminant

$$\Delta = (b\gamma)^2 - 8b + \frac{4p^2}{p\gamma - 1} = \left(\gamma b - \frac{4}{\gamma}\right)^2 + \frac{4\,(p\gamma - 2)^2}{\gamma^2\,(p\gamma - 1)} \geq 0.$$

From

$$\Delta \geq \left(\gamma b - \frac{4}{\gamma}\right)^2,$$

it follows that

$$\frac{b\gamma - \sqrt{\Delta}}{2} \leq \frac{2}{\gamma} \leq \frac{b\gamma + \sqrt{\Delta}}{2}.$$

Therefore, the feasible χ exists if and only if $2b - \frac{p^2}{p\gamma - 1} > 0$, and two different cases depending on the choices of γ and p exist:

Case 1 Assume $\Delta = 0$, that is,

$$\gamma b - \frac{4}{\gamma} = 0, \qquad p\gamma - 2 = 0.$$

Then, it follows that

$$\frac{2}{\gamma} = \frac{\gamma b}{2}.$$

The feasible range of the parameter χ is given by

$$0 < \chi < \frac{2}{\gamma}.$$

That is,

$$\gamma = \sqrt{\frac{2}{\lambda_2\rho}}, \qquad p = \sqrt{2\lambda_2\rho}, \qquad 0 < \sigma < \frac{\sqrt{2\lambda_2\rho}}{\lambda_N}. \tag{4.14}$$

Case 2 Assume $\Delta > 0$ and $2b\left(p\gamma - 1\right) - p^2 > 0$. The second inequality can be written as

$$\left(p - b\gamma\right)^2 < b^2\gamma^2 - 2b.$$

Thus, it can be seen that

$$\gamma > \sqrt{\frac{2}{b}}, \qquad b\gamma - \sqrt{b^2\gamma^2 - 2b} < p < b\gamma + \sqrt{b^2\gamma^2 - 2b}$$

are necessary and sufficient conditions for the existence of feasible solutions. This leads to

$$0 < \chi < \frac{\gamma b - \sqrt{b^2\gamma^2 - 8b + 4p^2/\left(p\gamma - 1\right)}}{2}.$$

That is,

$$\begin{aligned} &\gamma > \sqrt{\frac{1}{\lambda_2\rho}},\ b\gamma b - \sqrt{b^2\gamma^2 - 2b} < p < b\gamma + \sqrt{b^2\gamma^2 - 2b}, \\ &0 < \sigma < \frac{\gamma b - \sqrt{b^2\gamma^2 - 8b + 4p^2/\left(p\gamma - 1\right)}}{2\lambda_N}. \end{aligned} \tag{4.15}$$

The proof is completed. ■

Remark 21 *The upper bound on the maximum sampling period for all agents may be conservative, as shown in the following numerical example. However, it is more realistic to approximate the continuous event detection by a fast rate sampled-data event detection. The performance of continuous event detection can be expected to be recovered by sampled-data event detection with a relatively small sampling period* h.

Example 22 *Consider the multi-agent system with double-integrator dynamics under the interaction topology shown in Figure 4.1 which is undirected and connected. The initial conditions on* ξ *and* ζ *are randomly generated from uniform distributions on the interval* $[0, 2]$ *and* $[-0.4, 0.4]$*, respectively. The constant is set to* $\rho = 0.6$*, and the parameters are chosen as* $\gamma = 2.3854, p = 0.8384, \sigma = 0.2$*, which leads to the upper bound:* $h < 3.8836 \times 10^{-6}$*. The sampling period is taken to be* $h = 10^{-6}$*. Figure 4.5 and Figure 4.6 show the evolution of the position states and the velocity states, respectively, using the event based consensus algorithm in (4.13) under the interaction topology given by Figure 4.1. Consensus can be achieved asymptotically for the team of agents. The control signals for the agents are demonstrated in Figure 4.7, which shows that the zero-order hold strategy is used for both position and velocity states. Then, the evolution of the event condition which triggers control updates for both agent 3 and agent 4 is obtained as shown in Figure 4.8,*

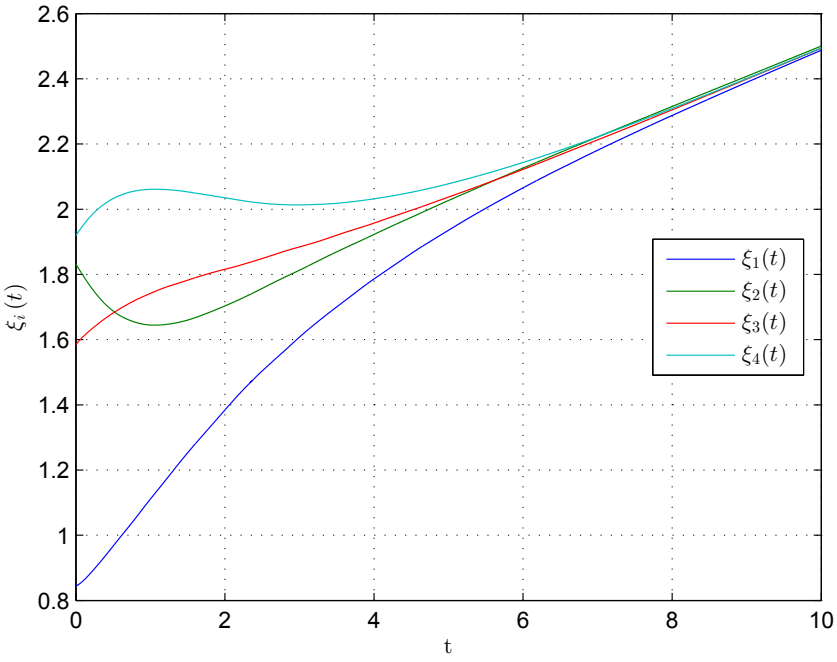

Figure 4.5: Evolution of position states for the agents

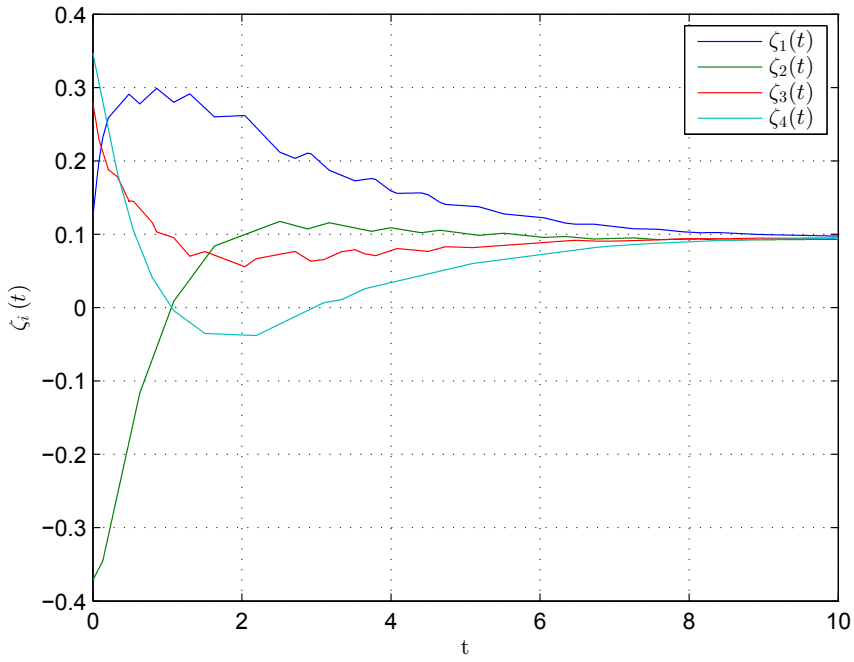

Figure 4.6: Evolution of velocity states for the agents

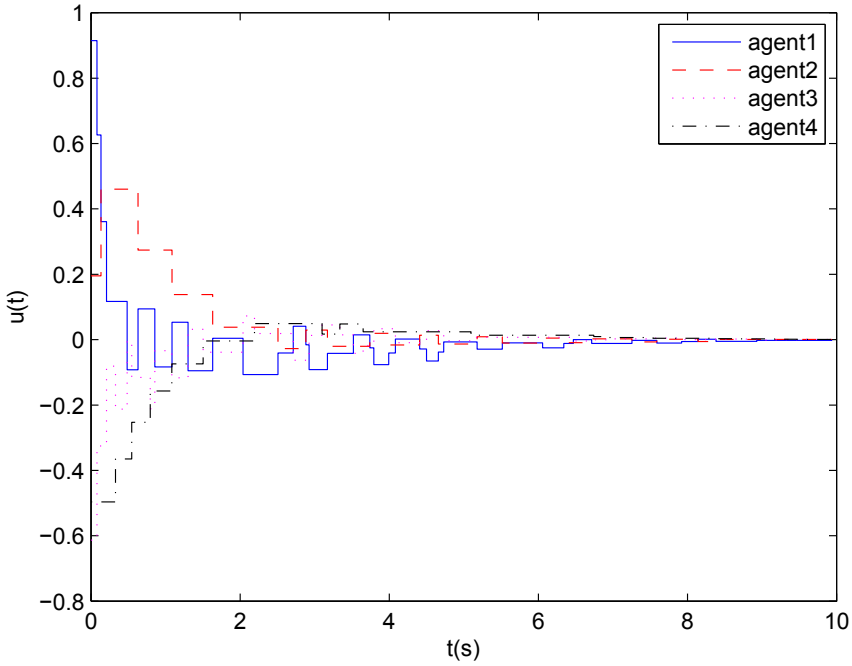

Figure 4.7: Control inputs for the agents

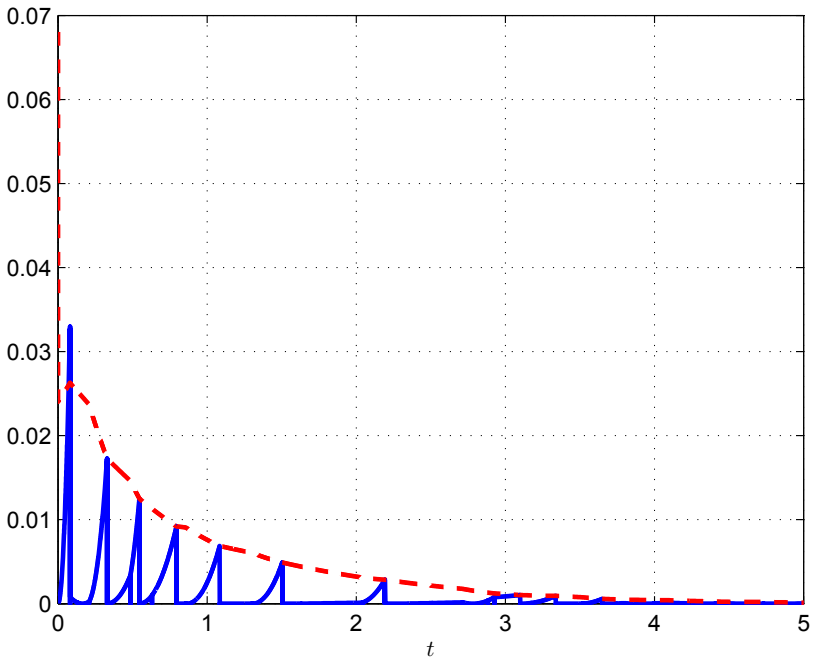

Figure 4.8: Evolution of the event condition shared by agent 3 and agent 4

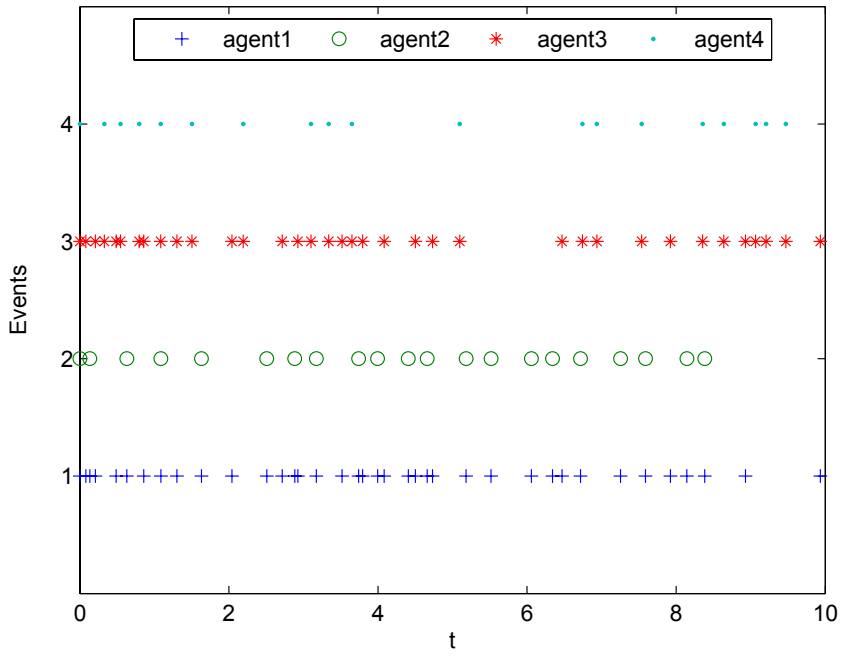

Figure 4.9: Event times for the agents

and the time instants when each agent updates its control law are shown in Figure 4.9. By comparing, it can be seen that more control updates are involved in agent 1 and agent 3. Evaluation of the event triggered control strategy shows that the average control updating period over $t \in [0, 10]$ *and for all agents is* 0.3509*. According to [102], the maximum control updating period which guarantees asymptotic consensus of double-integrator multi-agent systems under sampled-data control is*

$$\min\left\{2\gamma, \frac{2}{\gamma\lambda_N}\right\},$$

which is 0.2456*. Thus, the event triggered control requires less control updates on the average.*

4.5 Conclusions

A unified sampled-data control and event detection framework is developed to solve consensus problems for linear multi-agent systems under an undirected, connected network, which includes agents with single- and double-integrator dynamics as special cases. Along the way, the relative state differences between any two adjacent agents provide measurements of the

synchronization. The work described here is in contrast with earlier work in that it does not require continuous communication between neighboring agents and continuous event detection. Furthermore, the connection between the controller gain and parameters of the event detector has been captured as an LMI-based condition, which can be efficiently checked by existing tools. Simulation case studies are performed to verify the results obtained from the theoretic analysis. The existence of a global synchronized sampling period to evaluate event conditions may be restrictive in practice. An interesting future work would be to design one sampling period per edge instead of a global sampling period.

Chapter 5

Event Triggered State Estimation via Wireless Sensor Networks

This chapter presents distributed state estimation methods through wireless sensor networks with event triggered communication protocols among the sensors.

5.1 Introduction

In recent years, wireless sensor networks have come into prominence with a range of applications [39, 125]. One of the most important applications is trajectory tracking. The Kalman filter and its various extensions are effective algorithms for tracking the state of known dynamic processes [2, 13]; while $\mathcal{H}_\infty$ filter is specifically designed for robustness [22]. Typically, sensor networks are often deployed in environments with limited computational and communication resources. Communication over radio is the most energy-consuming function performed by these devices, so that the communication frequency needs to be minimized. These constraints dictate that sensor network problems are best approached in a holistic manner, by jointly maintaining estimation performance while reducing the number of transmissions.

As pointed out in [4], event triggered state estimation is not a standard problem due to the non-standard information pattern. Information is obtained precisely only when an event occurs; if no event takes place, the information can only be inferred from the event condition. Currently, most research on event based state estimation focuses on centralized algorithms, either in stochastic [107, 63, 105] or deterministic [123, 109, 81] settings. However, some problems are difficult or impossible for a monolithic system to solve. This necessitates the use of wireless sensor networks. Unfortunately, the current existing filter designs for wireless sensor networks, most of which are based on time triggered sampling, result in

high power consumption and network congestion.

Based on the above observations, event triggered distributed state estimation approaches having a low transmission frequency are proposed which significantly reduce the overall bandwidth consumption, and increase the lifetime of the network. These approaches are an extension of [90] to the event triggered transmission case. Event triggered transmissions pose new challenges to existing design methodologies as novel requirements, like adaptivity, uncertainty, and nonlinearity, arise. Specifically, the sensor node will not receive any information from the neighbors if the events at neighboring sensor nodes are not triggered. In this case, the behavior of neighboring sensors has to be estimated with the aid of the system model and information obtained from neighbors at event instants. After an event has occurred, the sensor broadcasts its predictive state to its neighbors and the state of the internal system models will be re-initialized for both itself and its neighbors. Then, a modified consensus filter is proposed to accommodate the generic uniform and asynchronous information exchange scenario. In this chapter, a formal stability analysis of the consensus filter is provided, and a specific event triggered transmission mechanism is constructed. Additionally, the event conditions can be checked without the knowledge of neighbors' information.

5.2 Problem Formulation

Consider a system whose state at time k is $x(k) \in \mathbb{R}^n$. The time index k of the state evolution will be discrete and identified with $\mathbb{N} = \{0, 1, 2, \ldots\}$.

Let $(\Omega, \mathcal{F}, P)$ be a probability space upon which $\{w(k), k \in \mathbb{N}\}$ is an independent sequence of Gaussian random variables, having zero mean and covariance matrices $\{Q(k)\}$. That is,

$$\mathbb{E}\left[w(k)\, w^T(l)\right] = Q(k)\, \delta(k, l), \tag{5.1}$$

where $\delta(k, l) = 1$ if $k = l$, and $\delta(k, l) = 0$, otherwise. The state at the initial time $x(0)$ is a Gaussian random variable with mean x_0 and covariance matrix P_0.

The state of the system satisfies linear dynamics

$$x(k+1) = A(k)\, x(k) + B(k)\, w(k), \tag{5.2}$$

where $A(k)$ and $B(k)$ are matrices of appropriate dimensions. The state can be observed only indirectly through a sensor network whose communication topology can be modeled by an undirected graph $\mathcal{G} = (\mathcal{V}, \mathcal{E})$. Here $\mathcal{V} = \{1, 2, \ldots, N\}$ is the set of sensor nodes. The edge set $\mathcal{E} \subseteq \mathcal{V} \times \mathcal{V}$ consists of the communication links between sensors. Each sensor

$i \in \mathcal{V}$ has a linear sensing model

$$z_i(k) = H_i(k)\, x(k) + v_i(k), \qquad z_i(k) \in \mathbb{R}^m, \tag{5.3}$$

where $H_i(k)$ and $v_i(k)$ are observation matrix and measurement noise of sensor i at time k, respectively. Each pair $(A(k), H_i(k))$ is assumed to be completely detectable. The measurement noise processes $\{v_i(k)\}$ and $\{v_j(k)\}$ for $i \neq j$ are independent Gaussian processes with zero mean and known covariances $\{R_i(k)\}$ and $\{R_j(k)\}$, respectively. Note also that $\{w(k)\}$ and $\{v_i(k)\}$ for all $i \in \mathcal{V}$ are independent processes. Sensor i can only communicate with other sensors within its sensing radius r. All the other sensors that sensor i can communicate with are referred to as the neighbors of sensor i, which can be mathematically defined as $\mathcal{N}_i = \{j \in \mathcal{V} | d_{ij} \leq r\}$ with d_{ij} being the Euclidean distance between sensor i and sensor j. Note that the underlying graph $\mathcal{G}$ of the wireless sensor network is required to be connected, and could be a switching graph.

The local consensus filter is described for $k \geq 0$ by the equations

$$\hat{x}_i(k) = \bar{x}_i(k) + K_i(k)\left[z_i(k) - H_i(k)\,\bar{x}_i(k)\right] + C_i(k)\sum\nolimits_{j\in\mathcal{N}_i}\left[\tilde{x}_j(k) - \tilde{x}_i(k)\right], i \in \mathcal{V}, \tag{5.4}$$

where $K_i(k) \in \mathbb{R}^{n\times m}$ and $C_i(k) \in \mathbb{R}^{n\times n}$ are the filter gain and consensus gain, respectively. Here $\hat{x}_i(k)$[1] is sensor i's estimation of the process state $x(k)$; $\bar{x}_i(k)$ is the estimate prior to assimilating the measurements at time k, and it is obtained by projecting the estimate $\hat{x}_i(k-1)$ via the transition matrix

$$\bar{x}_i(k) = A(k-1)\,\hat{x}_i(k-1). \tag{5.5}$$

The estimates $\tilde{x}_j(k)$ for $j \in \mathcal{N}_i$ are constructed for sensor i to estimate the neighboring sensors' state using only the measurements received from the neighbors, while $\tilde{x}_i(k)$ is constructed for sensor i to know what neighboring sensors assume its state estimate by using only predictive state estimates broadcasted to the neighbors. Hence, these estimates are the same for all sensors, which can be simply constructed by the following equations

$$\tilde{x}_j(k) = \gamma_j(k)\,\bar{x}_j(k) + \left[1 - \gamma_j(k)\right] A(k-1)\tilde{x}_j(k-1), \tag{5.6}$$

where $\gamma_j(k) = 1$ or 0 indicates the sensor node j does or not broadcast the data to its neighbors at the time instant k, respectively. The structure in (5.6) is chosen because the information exchange usually happens at the beginning of each discrete time instant. At that time, only the predicted state is available instead of the estimated state.

[1]To avoid confusion, it should be emphasized that the subscript does not indicate an element of a vector.

Remark 23 *When $\tilde{x}_j(k)$ is replaced by $\bar{x}_j(k)$ for all $j \in \mathcal{J}_i = \mathcal{N}_i \cup \{i\}$, the consensus filter in (5.4) reduces to the distributed Kalman consensus filter proposed in [90]. It reflects that time triggered transmission is a special case of event triggered transmission when events happen at each time instant. Also different from the distributed event triggered consensus filter in [64], the local consensus filter in (5.4) for sensor i can have access to the common estimate $\tilde{x}_i$. Keeping a copy of this global estimate ensures consistency in the sensor network. This is crucial for event detector design to decide broadcasting instants if the deviation between the true predictive state of sensor i and what the neighboring sensors assume its predictive state goes beyond some tolerance limit.*

The problem now is to find the particular blending factor $K_i(k)$ and consensus gain $C_i(k)$ for all $i \in \mathcal{V}$ that yields a consensus state estimate for the sensor network under event triggered transmission.

5.3 Stability of Event Triggered Consensus Filters

The following notation is defined to distinguish the different errors for sensor i at time k:

$$\begin{aligned}
\eta_i(k) &= \hat{x}_i(k) - x(k) \text{ estimation error,} \\
\bar{\eta}_i(k) &= \bar{x}_i(k) - x(k) \text{ prediction error,} \\
\tilde{\eta}_i(k) &= \tilde{x}_i(k) - x(k) \text{ common error.}
\end{aligned}$$

The filter for sensor i is given in the following form:

$$\hat{x}_i(k) = \bar{x}_i(k) + K_i(k)\left(z_i(k) - H_i(k)\bar{x}_i(k)\right) + C_i(k)\sum\nolimits_{j\in\mathcal{N}_i}\left[\tilde{x}_j(k) - \tilde{x}_i(k)\right],$$

where

$$\begin{aligned}
&F_i(k) = I - K_i(k)H_i(k), \\
&K_i(k) = \bar{P}_i(k)H_i^T(k)\left(R_i(k) + H_i(k)\bar{P}_i(k)H_i^T(k)\right)^{-1}, \\
&P_i(k) = F_i(k)\bar{P}_i(k)F_i^T(k) + K_i(k)R_i(k)K_i^T(k), \\
&\bar{P}_i(k+1) = A(k)P_i(k)A^T(k) + B(k)Q(k)B^T(k), \\
&\tilde{x}_j(k+1) = \gamma_j(k+1)\bar{x}_j(k+1) + \left(1 - \gamma_j(k+1)\right)A(k)\tilde{x}_j(k), \\
&\bar{x}_i(k+1) = A(k)\hat{x}_i(k).
\end{aligned}$$

Now the main result on stability of the consensus filter will be presented in the following theorem.

Theorem 24 *Consider the consensus filter with the choice of consensus gain*

$$C_i(k) = \frac{2F_i(k)\Gamma_i^{-1}(k)}{\lambda_{\max}(\mathcal{L})\lambda_{\max}(\Gamma^{-1}(k))},$$

where $\mathcal{L}$ is the Laplacian matrix associated with the graph $\mathcal{G}$ and

$$\Gamma(k) = \operatorname{diag}\{\Gamma_1(k), \ldots, \Gamma_N(k)\}$$

with $\Gamma_i(k) = F_i^T(k) A^T(k) \bar{P}_i^{-1}(k+1) A(k) F_i(k)$. Suppose $A(k)$ and $R_i(k)$ are invertible for all $i \in \mathcal{V}$ and $k \geq 0$. Then, the noise free error dynamics of the consensus filter is globally asymptotically stable under the event condition

$$[\tilde{x}_i(k) - \bar{x}_i(k)]^T \sum\nolimits_{j\in\mathcal{N}_i} [\tilde{x}_i(k) - \tilde{x}_j(k)] \leq 0. \tag{5.7}$$

Furthermore, all estimators asymptotically reach a consensus on state estimates.

Proof. Given the consensus estimator of sensor node i,

$$\begin{aligned}\bar{x}_i(k+1) =& A(k)\{\bar{x}_i(k) + K_i(k)[z_i(k) - H_i(k)\bar{x}_i(k)]\} \\ &+ A(k) C_i(k) \sum\nolimits_{j\in\mathcal{N}_i} [\tilde{x}_j(k) - \tilde{x}_i(k)],\end{aligned}$$

the noise free error dynamics of the consensus filter can be written as

$$\bar{\eta}_i(k+1) = A(k) F_i(k) \bar{\eta}_i(k) + A(k) C_i(k) u_i(k). \tag{5.8}$$

The stability result for (5.8) will be proved through the use of a Lyapunov function

$$V(k) = \sum\nolimits_{i=1}^{N} \bar{\eta}_i^T(k) \bar{P}_i^{-1}(k) \bar{\eta}_i(k).$$

Calculating the change $\Delta V(k) = V(k+1) - V(k)$ in the Lyapunov function, it can be shown that

$$\Delta V(k) = \sum\nolimits_{i=1}^{N} \bar{\eta}_i^T(k+1) \bar{P}_i^{-1}(k+1) \bar{\eta}_i(k+1) - \sum\nolimits_{i=1}^{N} \bar{\eta}_i^T(k) \bar{P}_i^{-1}(k) \bar{\eta}_i(k). \tag{5.9}$$

Substituting (5.8) into (5.9), we have

$$\begin{aligned}\Delta V(k) =& \sum\nolimits_{i=1}^{N} \bar{\eta}_i^T(k)(\Gamma_i(k) - \bar{P}_i^{-1}(k))\bar{\eta}_i(k) \\ &+ 2\sum_{i=1}^{N} \bar{\eta}_i^T(k) \Lambda_i(k) u_i(k) + \sum_{i=1}^{N} u_i^T(k) \Pi_i(k) u_i(k),\end{aligned} \tag{5.10}$$

where

$$\Lambda_i(k) = F_i^T(k) A^T(k) \bar{P}_i^{-1}(k+1) A(k) C_i(k),$$
$$\Pi_i(k) = C_i^T(k) A^T(k) \bar{P}_i^{-1}(k+1) A(k) C_i(k).$$

Using the error covariance matrix update rules, we get

$$\bar{P}_i(k+1) = A(k) F_i(k) \bar{P}_i(k) F_i^T(k) A^T(k) + W_i(k),$$

where

$$W_i(k) = A(k) K_i(k) R_i(k) K_i^T(k) A^T(k) + B(k) Q(k) B^T(k).$$

Multiplying $\bar{P}_i(k)$ on both sides of $\bar{P}_i^{-1}(k) - \Gamma_i(k)$ and using the matrix inversion lemma gives

$$\bar{P}_i(k) \left[\bar{P}_i^{-1}(k) - \Gamma_i(k)\right] \bar{P}_i(k) = \left[\bar{P}_i^{-1}(k) + M_i(k)\right]^{-1},$$

where

$$M_i(k) = F_i^T(k) A^T(k) W_i^{-1}(k) A(k) F_i(k).$$

Now multiplying the above equation from left and right by $\bar{P}_i^{-1}(k)$ results in

$$\bar{P}_i^{-1}(k) - \Gamma_i(k) = \bar{P}_i^{-1}(k) \left[\bar{P}_i^{-1}(k) + M_i(k)\right]^{-1} \bar{P}_i^{-1}(k),$$

which is a symmetric and positive definite matrix.

The first term in (5.10) is clearly negative semi-definite. Let $C_i(k)$ satisfy $\Lambda_i(k) = \sigma(k) I > 0$ for all $i \in \mathcal{V}$. This can be achieved by setting the consensus gain to

$$C_i(k) = \sigma(k) \left[F_i^T(k) A^T(k) \bar{P}_i^{-1}(k+1) A(k)\right]^{-1}.$$

Using this choice of $C_i(k)$, the second term in (5.10) becomes

$$2\sum_{i=1}^{N} \bar{\eta}_i^T(k) \Lambda_i(k) u_i(k) = 2\sigma(k) \bar{\eta}^T(k) u(k).$$

Defining

$$\Psi = \operatorname{diag}\left\{\bar{P}_1^{-1}(k) - \Gamma_1(k), \ldots, \bar{P}_N^{-1}(k) - \Gamma_N(k)\right\}$$

and noting that $\Pi_i(k) = \sigma^2(k) \Gamma_i^{-1}(k)$, $\Delta V(k)$ can be rewritten as

$$\Delta V(k) = -\bar{\eta}^T(k) \Psi \bar{\eta}(k) + 2\sigma(k) \bar{\eta}^T(k) u(k) + \sigma^2(k) \sum_{i=1}^{N} u_i^T(k) \Gamma_i^{-1}(k) u_i(k).$$

Noting that $u(k) = -(\mathcal{L} \otimes I)\,\tilde{\eta}(k)$, we have

$$\begin{aligned}\Delta V(k) \leq & -\bar{\eta}^T(k)\,\Psi\bar{\eta}(k) + 2\sigma(k)\,\bar{\eta}^T(k)\,u(k) \\ & -\sigma^2(k)\,\lambda_{\max}\left(\Gamma^{-1}(k)\right)\lambda_{\max}(\mathcal{L})\,\tilde{\eta}^T(k)\,u(k).\end{aligned}$$

Choosing

$$\sigma(k) = \frac{2}{\lambda_{\max}\left(\Gamma^{-1}(k)\right)\lambda_{\max}(\mathcal{L})},$$

$\Delta V(k)$ becomes

$$\Delta V(k) \leq -\bar{\eta}^T(k)\,\Psi\bar{\eta}(k) + 2\sigma\sum_{i=1}^{N}\left(\bar{x}_i(k) - \tilde{x}_i(k)\right)^T u_i(k).$$

Choose the event condition for sensor i as,

$$\left[\tilde{x}_i(k) - \bar{x}_i(k)\right]^T \sum_{j\in\mathcal{N}_i}\left[\tilde{x}_i(k) - \tilde{x}_j(k)\right] \leq 0,$$

so that the last term of $\Delta V(k)$ is negative semi-definite. One can conclude that $\Delta V(k) < 0$ for all $\bar{\eta}_i(k) \neq 0$, $i \in \mathcal{V}$. Therefore, $\bar{\eta} = 0$ is asymptotically stable for the error dynamics of the consensus filter without noise, which follows that $\bar{x}_i(k+1)$ for all $i \in \mathcal{V}$ is converging to $x(k+1)$ for $k \to \infty$. From the fact that

$$\bar{x}_i(k+1) = A(k)\hat{x}_i(k),\ x(k+1) = A(k)x(k),$$

the implication that $\hat{x}(k)$ is converging to $x(k)$ as $k \to \infty$ holds. Furthermore, since $\hat{\eta}_i = \hat{\eta}_j = 0$ for all $j \neq i$, all estimators asymptotically reach a consensus on state estimates, i.e., $\hat{x}_1 = \cdots = \hat{x}_N$. ■

Remark 25 *To calculate the consensus gain for each sensor, the largest eigenvalue of* $\Gamma^{-1}(k)$ *has to be known to all sensors at every time instant, which might be restrictive in a distributed environment. However, this could be amended by bounding it above by a constant. The particular choice of* C_i *in Theorem 24 is chosen to derive an event condition for each sensor. In order to reduce the frequency of communication, each sensor node predicts the behavior of itself and its neighbors one step ahead. An event is generated by a sensor if the condition in (5.7) is violated; at the same time, the event condition is satisfied again by broadcasting its information to the neighbors.*

Remark 26 *According to the proof of Theorem 24, the result is also valid for linear time-varying deterministic systems. To the best of the authors' knowledge, either control or estimation problems with event triggered sampling for linear time-varying systems have not*

been investigated despite of their importance. The algorithm above can be viewed as an event triggered estimation strategy for linear time-varying systems. The time-varying consensus filter is also a generalization of the steady-state filter for linear time-invariant systems with non-stationary noise covariance.

5.4 Time-Invariant Filters

In this section, we consider the time-invariant system

$$x(k+1) = Ax(k) + Bw(k)$$

with associated measurement process

$$z_i(k) = H_i x(k) + v_i(k).$$

We shall assume that $v_i(k)$ and $w(k)$ are independent, zero mean, stationary, white Gaussian processes, with covariances given by

$$E\left[w\left(k\right)w^T\left(l\right)\right] = Q\delta\left(kl\right), \qquad E\left[v_i\left(k\right)v_i^T\left(l\right)\right] = R_i\delta\left(kl\right).$$

The following time-invariant filter is concerned in this section

$$\hat{x}_i\left(k\right) = \bar{x}_i\left(k\right) + K_i\left(z_i\left(k\right) - H_i\bar{x}_i\left(k\right)\right) + C_i\sum\nolimits_{j\in\mathcal{N}_i}\left[\tilde{x}_j\left(k\right) - \tilde{x}_i\left(k\right)\right],$$

for $i \in \mathcal{V}$, where

$$\begin{aligned}
&F_i = I - K_iH_i,\\
&K_i = \bar{P}_iH_i^T\left(R_i + H_i\bar{P}_iH_i^T\right)^{-1},\\
&P_i = F_i\bar{P}_iF_i^T + K_iR_iK_i^T,\\
&\bar{P}_i = AP_iA^T + BQB^T,\\
&\tilde{x}_j\left(k+1\right) = \gamma_j\left(k+1\right)\bar{x}_j\left(k+1\right) + \left(1-\gamma_j\left(k+1\right)\right)\tilde{x}_j\left(k\right),\\
&\bar{x}_i\left(k+1\right) = A\hat{x}_i\left(k\right).
\end{aligned}$$

The event condition for sensor i has the following form

$$\gamma_j\left(k+1\right) = \begin{cases} 0, & \text{if } \left(\tilde{x}_i - \bar{x}_i\right)^T\sum_{j\in\mathcal{N}_i}\left(\tilde{x}_i - \tilde{x}_j\right) \le 0,\\ 1, & \text{otherwise.}\end{cases} \tag{5.11}$$

Now the result on stability of the time-invariant consensus filter will be presented in the following corollary.

Corollary 27 *Consider the time-invariant consensus filter with the choice of consensus gain*

$$C_i = \frac{2F_i\Gamma_i^{-1}}{\lambda_{\max}(\mathcal{L})\,\lambda_{\max}(\Gamma)}$$

where $\mathcal{L}$ is the Laplacian matrix associated with the graph $\mathcal{G}$ and

$$\Gamma_i = F_i^T A^T \bar{P}_i^{-1} A F_i, \qquad \Gamma = \operatorname{diag}\{\Gamma_1, \ldots, \Gamma_N\}.$$

Suppose A and R are invertible for all $i \in V$. Then, the noise free error dynamics of the consensus filter is globally asymptotically stable under the event condition in (5.11). Furthermore, all estimators asymptotically reach a consensus on state estimates.

The results can be obtained by following similar lines as in the proof of Theorem 24.

One can express the consensus filter in the information form with filter gain

$$K_i(k) = P_i(k) H_i^T R^{-1}$$

and information matrix

$$P_i(k) = \left(\bar{P}_i^{-1} + H_i^T R_i^{-1} H_i\right)^{-1}.$$

A further application to the identities above yields

$$\bar{P}_i(k+1) = A\left[\bar{P}_i(k) - \bar{P}_i(k) H_i \left(H_i^T \bar{P}_i(k) H_i + R_i\right)^{-1} H_i^T \bar{P}_i(k)\right] A^T + BQB^T. \tag{5.12}$$

Time invariance, or asymptotic time invariance, arises when there is a constant, or asymptotically constant solution to the variance equation in (5.12). The main conclusions are summarized as follows:

If the signal model is time invariant and not necessarily asymptotically stable, but the pair (A, H_i) is detectable and the pair (A, BD) is stabilizable for any D with $DD' = Q$, then [2]

a) For any nonnegative symmetric initial condition $\bar{P}_i(0)$, one has

$$\lim_{k\to\infty} \bar{P}_i(k) = \bar{P}_i$$

with $\bar{P}_i$ independent of $\bar{P}_i(0)$ and satisfying a steady-state version of (5.12):

$$\bar{P}_i = A\left[\bar{P}_i - \bar{P}_i H_i \left(H_i^T \bar{P}_i H_i + R_i\right)^{-1} H_i^T \bar{P}_i\right] A^T + BQB^T.$$

b)

$$|\lambda_i(A(I - K_i H_i))| < 1$$

with

$$K_i = \bar{P}_i H_i \left(H_i^T \bar{P}_i H_i + R_i\right)^{-1}.$$

5.5 Simulation Results

Suppose the discrete time model is

$$x(k+1) = Ax(k) + Bw(k)$$

with

$$A = \begin{bmatrix} 0.9996 & -0.03 \\ 0.03 & 0.9996 \end{bmatrix}, \qquad B = \begin{bmatrix} 0.375 & 0 \\ 0 & 0.375 \end{bmatrix},$$

and $Q = I$. Note that the state is moving on noisy divergent circular trajectories due to a pair of complex-conjugate eigenvalues with magnitude greater than 1. The initial state vector and the covariance matrix are set to be $x_0 = [15 \ -10]^T$, $P_0 = 10I$, respectively.

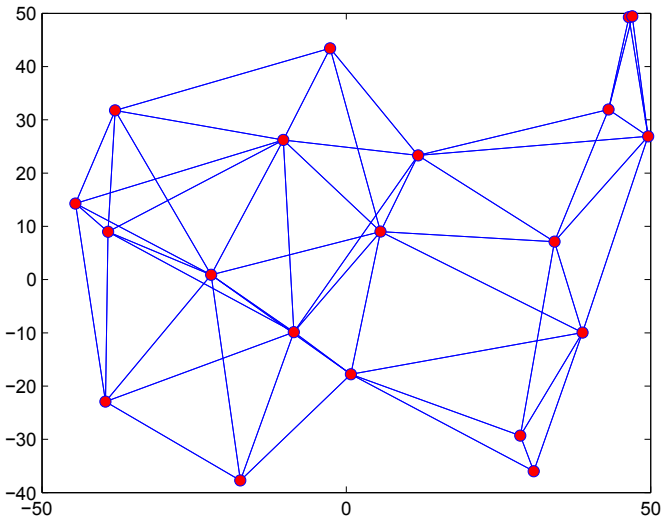

Figure 5.1: The sensor network topology

A sensor network is generated by randomly deploying 20 sensors in the monitoring area, where two sensors can communicate if they are within a distance less than 40 as shown in Figure 5.1. Label the 20 sensors with 1 through 20. The sensors take noisy measurements of the position of the target. The odd and even numbered sensors can observe along the x-axis and y-axis, respectively, where

$$\begin{aligned} z_{2i+1}(k) &= H_{2i+1}x(k) + v_{2i+1}(k), \\ z_{2i+2}(k) &= H_{2i+2}x(k) + v_{2i+2}(k), \end{aligned}$$

with $H_{2i+1} = [1 \quad 0]$, and $H_{2i+2} = [0 \quad 1]$ for $i = 0, \ldots, 9$. Moreover, the covariance matrices of v_i are $R_i = 900\sqrt{i}$ for $i = 1, 2, \ldots, 20$. Note that the noises have large variances,

and are different for different sensors. First assume that the dynamical system is noise-free, that is, $w\left(k\right) \equiv 0$, and $v_i\left(k\right) \equiv 0$. The initial state of each sensor is generated randomly from the normal distribution with the mean x_0 and variance P_0. Figure 5.2 depicts the evolution of the Lyapunov function $V(k)$ using the consensus filters based on the event condition in (5.7). It can be seen that all sensors reach consensus at the true trajectory of the target for the noise free case.

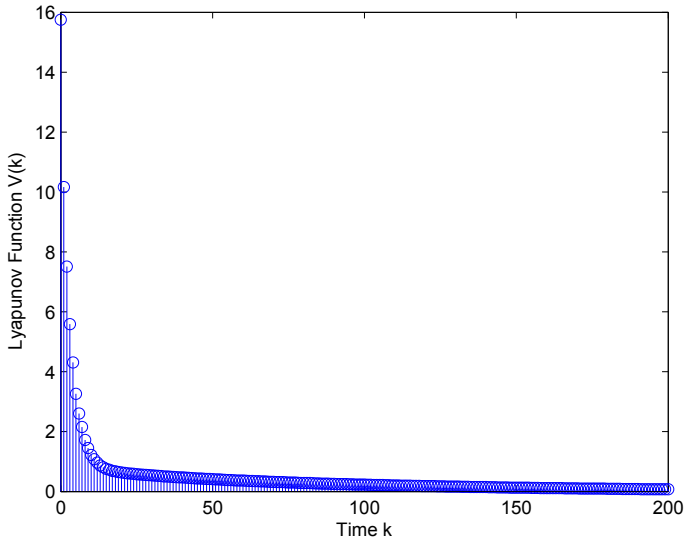

Figure 5.2: The Lyapunov function

Now return to the noise case, where the process noise $w(k)$ and measurement noises $v_i(k)$ for each sensor are generated according to their statistic properties, respectively. The consensus filters are run through 201 steps beginning at $k = 0$ and ending at $k = 200$. The result is shown in Figure 5.3, where the estimate trajectory is obtained by taking the average of the estimates of all sensor nodes. From the figure, it can be seen the event triggered consensus filtering algorithm can effectively track the target even though the system model is unstable and the measurement noise covariance matrices R_i for all $i \in \mathcal{V}$ are relatively large. The total number of broadcasting for the entire sensor network is 3034, which is 75.85% of the complete transmission scheme. The number of events for each sensor node under the event condition defined in (5.7) is shown in Figure 5.4.

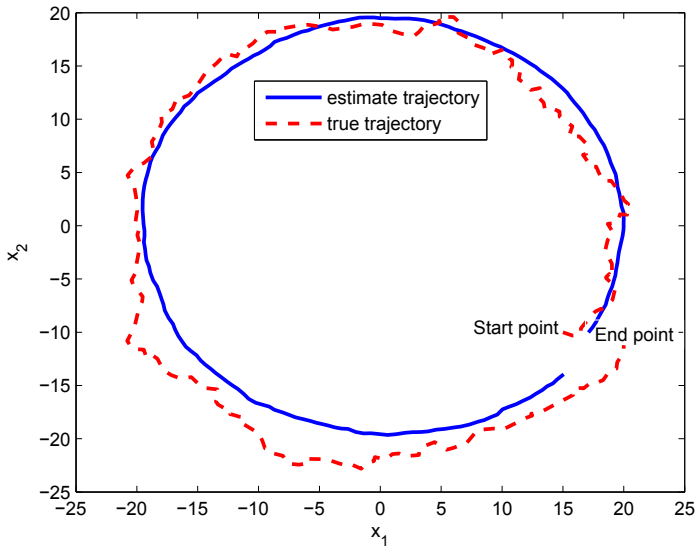

Figure 5.3: Tracking result

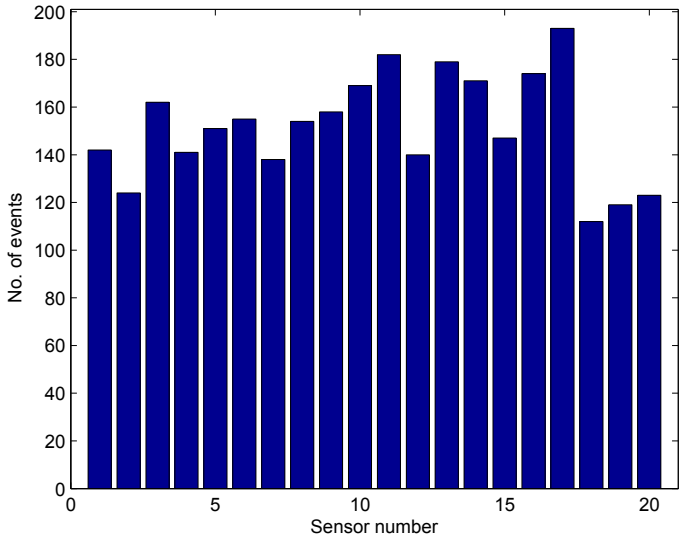

Figure 5.4: Number of events for all 20 sensors

5.6 Conclusions

Distributed state estimation algorithms were established for linear time-varying discrete-time systems with event triggered transmission using wireless sensor networks. Initially, the optimal event triggered consensus filter was constructed, and then it was approximated by a suboptimal filter. An event condition was presented for the suboptimal filter to reduce the number of transmissions for the wireless sensor network. The effectiveness of the proposed method was illustrated through a simulation example. Future work will address triggering rules for the optimal consensus filter to guarantee stability. The focus here is the interaction reduction among estimator sensors. Employing event detection rules between measurement sensor and estimator sensors would be an interesting extension.

Chapter 6

Event Triggered Optimization for Network Utility Maximization Problems

This chapter is concerned with event triggered distributed optimization for network utility maximization (NUM) problems.

6.1 Introduction

Interest in distributed optimization problems has seen rapidly growing in recent years. Many important practical problems require a distributed approach. One example is the network utility maximization problem, where each source generates a flow over shared links with limited capacity to achieve the maximization of total sources' utility. Moreover, large spatially distributed automated systems, such as the power grid, can make complete communication infeasible. Various techniques have been used in order to solve NUM problems distributively, such as dual decomposition approaches [91], and Newton methods [115]. An alternative decomposition approach to NUM problems can be found in [92]. In the design of distributed algorithms for NUM problems, one important factor to control is communication traffic in the network. A significant requirement in a large-scale network is the need for the computation of the optimal solution to be distributed, relying on local measurements and limited battery life, as opposed to requiring a central computation system.

As a consequence of these issues, event triggered communication could be used in distributed optimization algorithms for which the above issues can be mitigated and the resulting optimization problems become tractable [62]. In [62], barrier and augmented Lagrangian methods have been proposed to solve NUM problems based on a continuous flow updating rule and a continuous event detection scheme. In contrast to [62], a discrete time flow updating rule and a discrete time event detection scheme have been presented in this chapter to

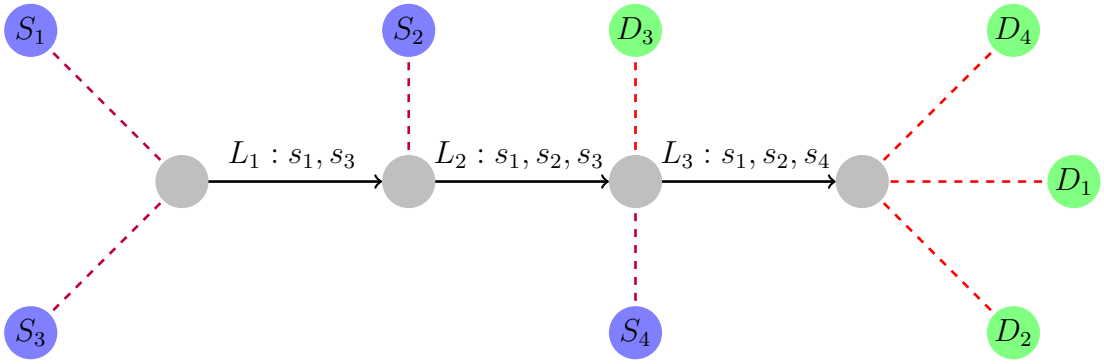

Figure 6.1: A sample network with four sources and three links

solve the same problem.

The main contributions of this chapter are briefly summarized as follows:

- propose a discrete time distributed interior point method for optimization problems with constraints;
- develop a triggering rule to mediate the communication between sources and links;
- solve the network utility maximization problem with guaranteed accuracy.

6.2 Problem Formulation

Consider a network in which two special nodes, called the *source* and the *destination*, are distinguished. The nodes of a network are usually numbered, say, $1, 2, 3, \ldots, S$. A network is typically represented as shown in Figure 6.1. The nodes are designated by circles, with a symbol inside each circle denoting the type and index of that node. Denote $\mathcal{S} = \{1, \ldots S\}$ as the index set of sources in the network. Corresponding to each source node $i \in \mathcal{S}$, there is a nonnegative number s_i representing a flow along a predetermined route to a destination. Use $\mathcal{L} = \{1, \ldots, L\}$ to denote the index set of directed links. Associated with each link is a finite number $c_l > 0$ for $l \in \mathcal{L}$, representing the maximum allowable flow. The network utility maximization (NUM) problem is that of determining the maximal aggregate sources' utilities subject to links' capacity constraints. When written out, it takes the form

$$\begin{array}{ll} \text{maximize} & \sum_{i=1}^{S} U_i\left(s_i\right) \\ \text{subject to} & Rs \leq c,\, s \geq 0. \end{array} \tag{6.1}$$

Here $U_i : \mathbb{R}_+ \to \mathbb{R}$ is the utility of source i as a function of the source rate s_i. It is assumed to be twice differentiable, strictly concave in s_i, and strictly monotonically increasing on

$(0, \infty)$. The vectors $s = [s_1, \cdots, s_S]^T$ and $c = [c_1, \cdots, c_L]^T$ are compact forms of the source data rates and link capacities, respectively. The matrix R is the routing matrix of dimension $L \times S$, i.e.,

$$r_{ij} = \begin{cases} 1, & \text{if link } i \text{ is on the route of source } j, \\ 0, & \text{otherwise.} \end{cases}$$

For each link l, let $\mathcal{S}_l$ denote the set of sources that use link l; for each source i, let $\mathcal{L}_i$ denote the set of links that source i uses. Also assume that the problem is strictly feasible, i.e. the constraint set $\mathcal{F}$ taking the form

$$\mathcal{F} = \{s : Rs - c \leq 0, s \geq 0\}$$

has a nonempty interior that is arbitrarily close to any point in $\mathcal{F}$. Intuitively, this means that the set has an interior and it is possible to get to any boundary point by approaching it from the interior. Such a set is referred to as *robust* [70].

The barrier method is used to approximately formulate the inequality constrained problem in (6.1) as a sequence of unconstrained problems. The approximation is accomplished by adding terms to the objective function that favors points interior to the feasible region over those near the boundary. The first step is to rewrite the problem in (6.1), making the inequality constraints implicit in the objective function:

$$\text{minimize} \qquad -\sum\nolimits_{i\in\mathcal{S}} U_i(s_i) - \sum\nolimits_{j\in\mathcal{L}} \frac{1}{\lambda_j} \log\left(c_j - r_j^T s\right) - \sum\nolimits_{i\in\mathcal{S}} \frac{1}{\mu_i} \log s_i, \qquad (6.2)$$

where $r_1^T, \ldots, r_L^T$ are the rows of R. Here $\lambda = [\lambda_1, \cdots, \lambda_L]^T$ and $\mu = [\mu_1, \cdots, \mu_S]^T$ are constant vectors with positive entries that set the accuracy of the approximation.

Remark 28 *The objective function in (6.2) is convex. This can be shown via the definition of convex function and operations that preserve convexity of functions.*

The functions

$$\phi_{\mathcal{L}}(s) = -\sum\nolimits_{j\in\mathcal{L}} \log\left(c_j - r_j^T s\right), \text{ and } \phi_{\mathcal{S}}(s) = -\sum\nolimits_{i\in\mathcal{S}} \log s_i,$$

with $\mathbf{dom}\phi_{\mathcal{L}} \cap \mathbf{dom}\phi_{\mathcal{S}} = \left\{s \in \mathbb{R}^S \,\middle|\, s_i > 0,\ r_j^T s < c_j,\ i = 1, \ldots, S,\ j = 1, \ldots, L\right\}$, are called the *logarithmic barriers* or *log barriers* for the problem in (6.1).

Remark 29 *The above domain is the set of points that satisfy the inequality constraints in (6.1) strictly. No matter what values the positive parameters λ_j, $j = 1, \ldots, L$ and μ_i,*

$i = 1, \ldots, S$ *have, the logarithmic barriers grow without bound if* $c_j - r_j^T s \to 0$ *or* $s_i \to 0$, *for any* i *and* j. *Of course, the problem in (6.2) is only an approximation of the original problem in (6.1). The quality of the approximation improves as the parameters* λ_j *and* μ_i *grow. It can be soon shown that the original problem can be circumvented by solving a* sequence *of problems of the form in (6.2), increasing the parameters* λ_j *and* μ_i, *and starting each minimization at the solution to the problem with the previous values of* λ_j *and* μ_i.

For $\lambda \succeq 0$ and $\mu \succeq 0$, define $s^*(\lambda, \mu)$ as the optimal solution to (6.2). The *central path* associated with the problem in (6.1) is defined as the set of points $s^*(\lambda, \mu)$, $\lambda \succeq 0$ and $\mu \succeq 0$, which are called the *central points*. Points on the central path are characterized by the following necessary and sufficient conditions: $s^*(\lambda, \mu)$ is strictly feasible, i.e., it satisfies

$$r_j^T s < c_j,\ j = 1, \ldots, L, \qquad s_i > 0,\ i = 1, \ldots, N,$$

and

$$0 = -\sum\nolimits_{i \in \mathcal{S}} \nabla U_i(s_i) - \sum\nolimits_{i \in \mathcal{S}} \frac{1}{\mu_i}\frac{1}{s_i} + \sum\nolimits_{j \in \mathcal{L}} \frac{1}{\lambda_j}\frac{1}{c_j - r_j^T s} \tag{6.3}$$

holds.

Every central point yields a dual feasible point, and hence a lower bound on the optimal value p^*. More specifically, define

$$\begin{aligned} \nu_i^*(\mu_i) &= \frac{1}{\mu_i}\frac{1}{s_i},\ i = 1, \ldots, S, \\ \upsilon_i^*(\lambda_j) &= \frac{1}{\lambda_j}\frac{1}{c_j - r_j^T s},\ j = 1, \ldots, L. \end{aligned}$$

The pair $\nu^*(\mu), \upsilon^*(\lambda)$ is dual feasible.

First, it is clear that $\nu^*(\mu) \succ 0$ and $\upsilon^*(\lambda) \succ 0$ because $s_i > 0$, $i = 1, \ldots, S$, and $r_j^T s < c_j$, $j = 1, \ldots, L$. By expressing the optimality condition in (6.3) as

$$-\sum\nolimits_{i \in \mathcal{S}} \nabla U_i(s_i^*(\mu, \lambda)) - \sum\nolimits_{i \in \mathcal{S}} \nu_i^*(\mu_i) + \sum\nolimits_{j \in \mathcal{L}} \upsilon_i^*(\lambda_j) = 0,$$

it can be seen that $s^*(\mu, \lambda)$ minimizes the Lagrangian

$$f(s; \lambda, \mu) = -\sum\nolimits_{i \in \mathcal{S}} U_i(s_i) - \sum\nolimits_{j \in \mathcal{L}} \frac{1}{\lambda_j} \log\left(c_j - r_j^T s\right) - \sum\nolimits_{i \in \mathcal{S}} \frac{1}{\mu_i} \log s_i,$$

for $\nu = \nu^*(\mu)$ and $\upsilon = \upsilon^*(\lambda)$, which means that $\nu^*(\mu)$, $\upsilon^*(\lambda)$ is a dual feasible pair. Therefore, the dual function $g(\nu^*(\mu), \upsilon^*(\lambda))$ is finite, and

$$\begin{aligned} g(\nu^*(\mu), \upsilon^*(\lambda)) &= -\sum\nolimits_{i \in \mathcal{S}} U_i(s_i^*) - \sum\nolimits_{i \in \mathcal{S}} \nu_i^*(\mu) s_i + \sum\nolimits_{j \in \mathcal{L}} \upsilon_j^*(\lambda)\left(r_j^T s - c_j\right) \\ &= -\sum\nolimits_{i \in \mathcal{S}} U_i(s_i^*) - \sum\nolimits_{i \in \mathcal{S}} \frac{1}{\mu_i} - \sum\nolimits_{j \in \mathcal{L}} \frac{1}{\lambda_j}. \end{aligned}$$

In particular, the duality gap associated with $s^*(\mu,\lambda)$ and the dual feasible pair $\nu^*(\mu)$, $v^*(\lambda)$ is simply $-\sum_{i\in\mathcal{S}}\mu_i^{-1}-\sum_{j\in\mathcal{L}}\lambda_j^{-1}$. As an important consequence, it follows that

$$-\sum\nolimits_{i\in\mathcal{S}}U_i\left(s_i^*\right)-p^*\leq\sum\nolimits_{i\in\mathcal{S}}\frac{1}{\mu_i}+\sum\nolimits_{j\in\mathcal{L}}\frac{1}{\lambda_j},$$

i.e., $s^*(\lambda,\mu)$ is no more than $\sum_{i\in\mathcal{S}}\mu_i^{-1}+\sum_{j\in\mathcal{L}}\lambda_j^{-1}$-suboptimal. This confirms the intuitive idea that $s^*(\lambda,\mu)$ converges to an optimal point as $\lambda_i\to\infty$ and $\mu_j\to\infty$.

Remark 30 *Barrier methods are also referred to as interior point methods. They work by establishing a barrier on the boundary of the feasible region that prevents a search procedure from leaving the region. This suggests that the link capacity constraints can always be guaranteed. Therefore, this method is reliable enough to be embedded in real-time control applications with little or no human oversight.*

Define the jth link's local state as

$$\alpha_j(k)=\frac{1}{\lambda_j}\frac{1}{c_j-a_j^Ts(k)}.$$

Link j is able to measure the total flow that goes through it and calculate its link state. The benefit of introducing event triggered techniques lies in reduced computation cost and communication cost at each link. Links do not need to calculate the state information and send it to sources at each time instant.

The sampling strategy is push type, which means that sources do not request information from links; links send their information to sources when it is necessary. The same strategy applies for sources.

6.3 Convergence Analysis for Event Triggered Barrier Algorithms

Let $T_n^{L_j}$, $n=1,2,\ldots$, denote the time when link j samples its link state α_j and broadcasts it to sources $i\in\mathcal{S}_j$. Therefore, the sampled link state is a piecewise constant function in which

$$\hat{\alpha}_j(k)=\alpha_j(T_n^{L_j})$$

for any $k\in[T_n^{L_j},T_{n+1}^{L_j})$. Define

$$z_i(k)=\nabla U_i\left(s_i(k)\right)+\frac{1}{\mu_i}\frac{1}{s_i(k)}-\sum\nolimits_{j\in\mathcal{L}_i}\hat{\alpha}_j(k)$$

as the ith source state for all $i \in \mathcal{S}$. Let $T_n^{S_i}$, $n = 1, 2, \ldots$, denote the time when source i samples its source state $z_i(k)$ and broadcasts it to links $j \in \mathcal{L}_i$. Therefore, the sampled source state is also a piecewise constant function in which

$$\hat{z}_i(k) = z_i\left(T_n^{S_i}\right)$$

for any $k \in [T_n^{S_i}, T_{n+1}^{S_i})$. Let $\mathcal{E}_{L_j}$ and $\mathcal{E}_{S_i}$ be the set of indices in $\{T_n^{L_j}\}$ and $\{T_n^{S_i}\}$ corresponding to events at link j and source i, respectively. The communication event instants at source i and link j are determined by

$$z_i^2(k) \geq \rho_i \hat{z}_i^2(k), \tag{6.4}$$

and

$$\left(\alpha_j(k) - \hat{\alpha}_j(k)\right)^2 \leq \frac{\sum_{i \in S_j} \frac{\rho_i \gamma_i}{|\mathcal{L}_i|}\left(1 - \frac{\varepsilon_i}{2} - \frac{M}{2}\gamma_i\right)\hat{z}_i^2}{\sum_{i \in S_j} \frac{\gamma_i |\mathcal{L}_i|}{2\varepsilon_i}}, \tag{6.5}$$

respectively.

The minimizer of the Lagrangian $L(s; \lambda, \mu)$ for fixed λ and μ can be searched using the basic descent methods. Given an initial feasible vector $s(0)$, the iteration of event triggered optimization algorithms for source i is given by

$$s_i(k+1) = s_i(k) + \gamma_i z_i(k), \tag{6.6}$$

where the positive scalar γ_i is called the *step length*. In other words, communication is invoked only when the event conditions are not satisfied. When a communication event is triggered, $\hat{z}_i$ or $\hat{\alpha}_j$ is set to z_i or α_j. Therefore, the event conditions are satisfied instantaneously.

Theorem 31 *Under the communication logic in (6.4) and (6.5), and the flow update scheme in (6.6), if the step length is set by*

$$0 < \gamma_i < \frac{2 - \varepsilon_i}{M},$$

then the source rates $s(k)$ asymptotically converge to the unique minimizer of $f(s; \lambda, \mu)$.

Proof. Given a suitable starting point $s^0 \in \mathbf{dom}\ f$, the sublevel set

$$A = \left\{s \in \mathbf{dom}\ f | f(s) \leq f\left(s^0\right)\right\}$$

is closed since the function f is closed. Since the objective function is strongly convex on A, which means that there exists an $m > 0$ such that

$$\nabla^2 f(s) \geq mI \tag{6.7}$$

for all $s \in A$, the inequality

$$f(y) \geq f(x) + \nabla f(x)^T (y - x) + \frac{m}{2} \|y - x\|_2^2 \tag{6.8}$$

is held for all x and y in A. The inequality in (6.8) implies that the sublevel set contained in A is bounded, so in particular, A is bounded. Therefore the maximum eigenvalue of $\nabla^2 f(s)$, which is a continuous function of s on A, is bounded above on A, *i.e.*, there exists a constant such that

$$\nabla^2 f(x) \leq MI$$

for all $s \in A$. This upper bound on the Hessian implies for $s(k+1) \in A$ and $s(k) \in A$,

$$f(s(k+1)) \leq f(s(k)) + \nabla f(s(k))^T (\gamma \cdot z(k)) + \frac{M}{2} \|\gamma \cdot z(k)\|_2^2,$$

where $\cdot$ denotes the element-wise multiplication of two vectors.

From the definition of $z_i(k)$, $\alpha_j(k)$, and $\hat{\alpha}_j(k)$, we have

$$\nabla_i f(s(k); \lambda, \mu) = -z_i(k) + \sum\nolimits_{j \in \mathcal{L}_i} [\alpha_j(k) - \hat{\alpha}_j(k)].$$

For convenience, parameter dependence is omitted temporarily to save writing.

Define $V(s(k)) = f(s(k); \lambda, \mu) - f(s^*; \lambda, \mu)$ as a Lyapunov function candidate for the system in (6.6), where $s^*(\lambda, \mu)$ is the minimizer for any fixed λ and μ, and the corresponding Lagrangian function is $f(s^*; \lambda, \mu)$. By using the properties of $U_i(s_i)$, it is easy to show that such a minimizer is unique. It is trivial to see that $\Delta V(s) = \Delta f(s; \lambda, \mu)$.

For all $k \geq 0$, we have

$$\Delta V \leq \sum\nolimits_{i=1}^{S} \left\{ \gamma_i z_i \left[\sum\nolimits_{j \in L_i} (\alpha_j - \hat{\alpha}_j) - z_i \right] + \frac{M}{2} \gamma_i^2 z_i^2 \right\}.$$

Using the Young's inequality

$$xy \leq \frac{x^2}{2\varepsilon} + \frac{\varepsilon y^2}{2},$$

we get

$$\Delta V \leq \sum\nolimits_{i=1}^{S} \left\{ -\gamma_i \left(1 - \frac{\varepsilon_i}{2} - \frac{M}{2} \gamma_i \right) z_i^2 + \frac{\gamma_i}{2\varepsilon_i} \left[\sum\nolimits_{j \in L_i} (\alpha_j - \hat{\alpha}_j) \right]^2 \right\}.$$

Remember there are $|\mathcal{L}_i|$ terms in the sum $\sum_{j \in \mathcal{L}_i} (\alpha_j - \hat{\alpha}_j)$, and then by using the sum of squares inequality

$$\left[\sum\nolimits_{j \in \mathcal{L}_i} (\alpha_j - \hat{\alpha}_j) \right]^2 \leq |\mathcal{L}_i| \sum\nolimits_{j \in \mathcal{L}_i} (\alpha_j - \hat{\alpha}_j)^2,$$

we have

$$\Delta V \leq \sum_{i=1}^{S} \left[-\gamma_i \left(1 - \frac{\varepsilon_i}{2} - \frac{M}{2} r_i \right) z_i^2 + \frac{\gamma_i \left| \mathcal{L}_i \right|}{2\varepsilon_i} \sum\nolimits_{j \in L_i} \left(\alpha_j - \hat{\alpha}_j \right)^2 \right].$$

We can write the last term as

$$\sum_{i=1}^{S} \frac{\gamma_i \left| \mathcal{L}_i \right|}{2\varepsilon_i} \sum\nolimits_{j \in L_i} \left(\alpha_j - \hat{\alpha}_j \right)^2 = \sum_{j=1}^{L} \left(\alpha_j - \hat{\alpha}_j \right)^2 \sum_{i \in S_j} \frac{\gamma_i \left| \mathcal{L}_i \right|}{2\varepsilon_i}.$$

This means

$$\Delta V \leq \sum_{i=1}^{S} -\gamma_i \left(1 - \frac{\varepsilon_i}{2} - \frac{M}{2} r_i \right) z_i^2 + \sum_{j=1}^{L} \left(\alpha_j - \hat{\alpha}_j \right)^2 \sum_{i \in S_j} \frac{\gamma_i \left| \mathcal{L}_i \right|}{2\varepsilon_i}.$$

Considering the term $\sum_{i=1}^{S} \rho_i \gamma_i \left(1 - \frac{\varepsilon_i}{2} - \frac{M}{2} r_i \right) \hat{z}_i^2$, we have

$$\sum_{i=1}^{S} \rho_i \gamma_i \left(1 - \frac{\varepsilon_i}{2} - \frac{M}{2} \gamma_i \right) \hat{z}_i^2 = \sum\nolimits_{j=1}^{L} \sum\nolimits_{i \in S_j} \frac{\rho_i \gamma_i}{\left| \mathcal{L}_i \right|} \left(1 - \frac{\varepsilon_i}{2} - \frac{M}{2} \gamma_i \right) \hat{z}_i^2.$$

Adding and subtracting the term $\sum_{i=1}^{S} \rho_i \gamma_i \left(1 - \frac{\varepsilon_i}{2} - \frac{M}{2} \gamma_i \right) \hat{z}_i^2$, we obtain

$$\begin{aligned} \Delta V \quad \leq \quad & -\sum\nolimits_{i=1}^{S} \gamma_i \left(1 - \frac{M}{2} r_i - \frac{\varepsilon_i}{2} \right) \left(z_i^2 - \rho_i \hat{z}_i^2 \right) \\ & + \sum\nolimits_{j=1}^{L} \left[\left(\alpha_j - \hat{\alpha}_j \right)^2 \sum_{i \in S_j} \frac{\gamma_i \left| \mathcal{L}_i \right|}{2\varepsilon_i} - \sum\nolimits_{i \in S_j} \frac{\rho_i \gamma_i}{\left| \mathcal{L}_i \right|} \left(1 - \frac{\varepsilon_i}{2} - \frac{M}{2} \gamma_i \right) \hat{z}_i^2 \right]. \end{aligned}$$

This immediately suggests that $\Delta V \left(s \right) \leq 0$ is guaranteed for all k because the inequalities in (6.4) and (6.5) hold for any $i \in \mathcal{S}$ and $j \in \mathcal{L}$.

The only scenario that $\Delta V = 0$ can happen is

$$z_i = \hat{z}_i = 0, \qquad \forall i \in \mathcal{S}, \qquad \alpha_j = \hat{\alpha}_j = 0, \qquad \forall j \in \mathcal{L},$$

which corresponds to $s^* \left(\mu, \lambda \right)$. As a result, the equilibrium $s^* \left(\mu, \lambda \right)$ is asymptotically stable.

■

6.4 Event Triggered NUM Algorithm Implementation

The initial condition can be chosen distributively. Assume that each link knows the number of sources that use the link, that is, $|\mathcal{S}_j|$, and then it sends the information

$$\frac{c_j}{|\mathcal{S}_j|}$$

to each source. Each source receives $|\mathcal{L}_i|$ such information. Then the source can choose the initial flow rate

$$s_i^0 = \theta_i \min\left\{\frac{c_j}{|\mathcal{S}_j|}, \qquad j \in \mathcal{L}_i\right\}, \tag{6.9}$$

with $0 < \theta_i < 1$.

Suppose that $k_i \in \mathcal{L}_i$, and $\frac{c_{k_i}}{|\mathcal{S}_{k_i}|} = \min\left\{\frac{c_j}{|\mathcal{S}_j|}, j \in \mathcal{L}_i\right\}$. It is easy to show that the link constraints are satisfied automatically

$$\sum_{i\in\mathcal{S}_j} s_i^0 = \sum_{i\in\mathcal{S}_j} \theta_i \frac{c_{k_i}}{|\mathcal{S}_{k_i}|} < \sum_{i\in\mathcal{S}_j} \frac{c_j}{|\mathcal{S}_j|} = c_j.$$

Algorithm 32 *Source i's Update Algorithm*

1. *Source i's initialization*

   Initialize local tolerance $\epsilon_i > 0$, penalty factor $\mu_i \triangleq \mu_i^0 > 0$. Choose parameters $\sigma_i > 1$, $0 < \varepsilon_i < 2$, $0 < \gamma_i < \frac{2-\varepsilon_i}{M}$, and $0 < \rho_i < 1$. Receive information from links and derive initial source rates s_i^0. Send the information $\rho_i, \varepsilon_i, \gamma_i$ and $|\mathcal{L}_i|$ to links $j \in \mathcal{L}_i$.

2. *Local schedule update*

   a) *State initialization: wait for all links $j \in \mathcal{L}_i$ to send their link states $\hat{\alpha}_j$ and set $\hat{\alpha}_j = \alpha_j$.*

   b) *Update source rate:*

   $$\begin{aligned} z_i &\triangleq \nabla U_i(s_i) + \frac{\gamma_i}{\mu_i}\frac{1}{s_i} - \gamma_i \sum\nolimits_{j\in\mathcal{L}_i} \hat{\alpha}_j, \\ s_i &\triangleq s_i + \gamma_i z_i. \end{aligned}$$

   c) *Communication protocol: Transmit z_i to all links $j \in \mathcal{L}_i$ when the following condition is true*

   $$z_i^2 < \rho_i \hat{z}_i^2,$$

   and set $\hat{z}_i = z_i$.

3. *Increase μ_i. $\mu_i \triangleq \sigma_i \mu_i$ if*

   $$|z_i| \le \epsilon_i,$$

   until $\mu_i \delta_i > 2S$. Inform the links $j \in \mathcal{L}_i$ that source i performed a barrier update.

4. *Repeat Step 2.*

Algorithm 33 *Link j's Update Algorithm*

1. *State initialization: Initialize $\lambda_j \triangleq \lambda_j^0$, and choose parameter $\eta_j > 1$. Wait for users to return z_i, and $I_i = 0$ for all $i \in S_j$ and set $\hat{z}_i = z_i$.*

2. *Link update: Monitor the link state*

$$\alpha_j = \frac{1}{\lambda_j} \frac{1}{c_j - r_j^T s}.$$

3. *Communication protocol: Transmit α_j to all users in $i \in S_j$ when the following condition is true*

$$\left(\alpha_j(k) - \hat{\alpha}_j(k)\right)^2 > \frac{\sum_{i \in \mathcal{S}_j} \frac{\rho_i \gamma_i}{|\mathcal{L}_i|} \left(1 - \frac{\varepsilon_i}{2} - \frac{M}{2}\gamma_i\right) \hat{z}_i^2}{\sum_{i \in \mathcal{S}_j} \frac{\gamma_i |L_i|}{2\varepsilon_i}},$$

   and set $\hat{\alpha}_i = \alpha_i$.

4. *Barrier update notification: If link j receives a notice that source i performed a barrier update, set $I_i = 1$. If $I_i = 1$ for all $i \in \mathcal{S}_j$, then set $\lambda_j \triangleq \eta_j \lambda_j$, reset $I_i = 0$, and broadcast λ_j to all $i \in \mathcal{S}_j$ until $\lambda_j \delta_i > 2L$.*

5. *Go to Step 2.*

Remark 34 *Some comments are made on the accuracy of the solution to centering problems. Computing $s_i(k)$ exactly is not necessary since the central path has no significance beyond the fact that it leads to a solution to the original problem; inexact centering will still yield a sequence of points that converges to the optimal point. On the other hand, the cost of computing an extremely accurate minimizer as compared to the cost of computing a good minimizer is only marginally more. For this reason it is not unreasonable to assume exact centering.*

Remark 35 *There are a few parameters involved here. To clarify, the role of each parameter is explained as follows. The stopping criterion for inter iteration of source i is determined by ϵ_i, which is related to the decrement of the objective function involved in source i. The choice of the parameters σ_i and η_j involves a trade-off in the number of inner and outer iterations required. If σ_i and η_j are small then at each outer iteration μ_i and λ_j increase by a small factor. Values from around 10 to 20 or so seem to work well. The parameter ε_i is used for the Yong's inequality; ρ_i is the parameter of source i's event detector. Let $\delta = \max\{\delta_i\}$, then δ is a certificate for $f(s^*) - p \leq \delta$.*

We will prove that the point $s^*(k)$ is δ-suboptimal, where δ is the desired accuracy of the difference between the objective function value at the approximate solution and the true optimal value.

Theorem 36 *Under the assumptions of U_i, R and ρ in Theorem 1, the flow rates $s_i(k)$ generated by algorithms 32 and 33 converge asymptotically to the δ-suboptimal solution to the NUM problem.*

Proof. The proof is straightforward. By algorithms 32 and 33, all the parameters satisfy $\mu_i \geq \frac{2S}{\delta_i}$ for all $i \in \mathcal{S}$, and $\lambda_j \geq \frac{2L}{\delta_i}$, for all $j \in \mathcal{L}$. They are fixed after the conditions are satisfied. ■

6.5 Numerical Examples

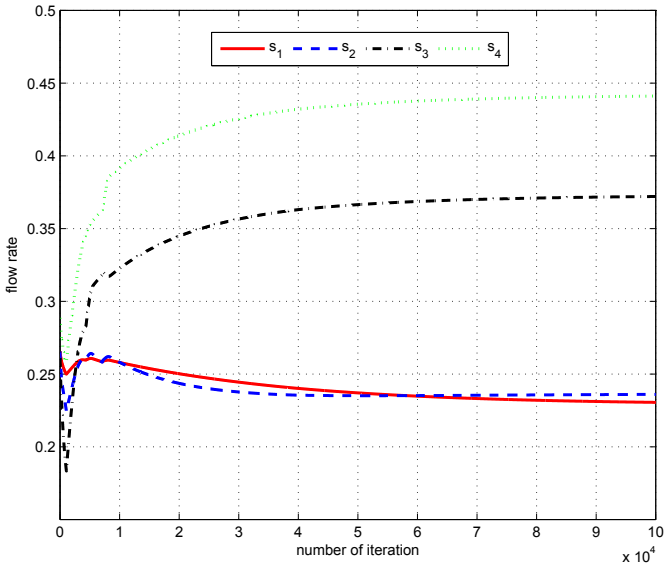

Figure 6.2: Flow rate for each source

To verify the proposed method, a simulation is demonstrated as follows. The utility functions are chosen as

$$U_i(s_i) = w_i \log s_i,$$

where w_i are random variables uniformly distributed on $[0.8, 1.2]$ to distinguish different sources. Functions $U_i(s_i)$ obey the assumptions of utility functions obviously. A network

Table 6.1: The transmission rates of sources and links

	Links			Sources			
	L_1	L_2	L_3	S_1	S_2	S_3	S_4
No. Events	3	525	66	13	30	52	2
Transmission Rate %	0.0366	6.4017	0.8048	0.1585	0.3658	0.6341	0.0244

of 4 sources and 3 links is set up and shown in Figure 6.1. Link j is assigned a capacity c_j uniformly distributed on $[0.8, 1.2]$.

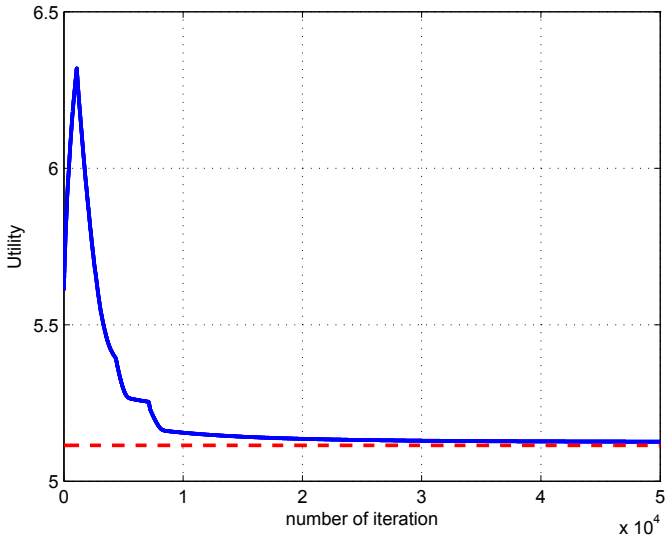

Figure 6.3: Evolution of the opposite of the objective function

The settings for simulation are illustrated as follows. The initial condition is generated distributively according to (6.9) with $\theta_i = 0.95$, for all $i \in \mathcal{S}$, which is kept in the feasible set. The initial values for multipliers λ_j and μ_i are 1, which are increased by $\sigma_i = \eta_j = 10$ during each outer interaction. Parameters ρ_i of the triggering logic for all sources are chosen randomly from a uniform distribution on $[0, 1]$. Figure 6.2 plots the flow rate for each source over time. After a period of transit time, all flow rates tend to be a steady value. Figure 6.3 shows the opposite of the aggregate utility over time, that is, $-\sum_{i\in\mathcal{S}} U_i(s_i)$. In the figure, the red dashed line means the opposite of the maximum utility, where the optimal rate s^* and its corresponding utility U^* are calculated using a global optimization technique. The objective function does not show a monotonic behavior at the beginning. This is due to the Lagrangian parameters update. The objective function is monotonically decreasing only

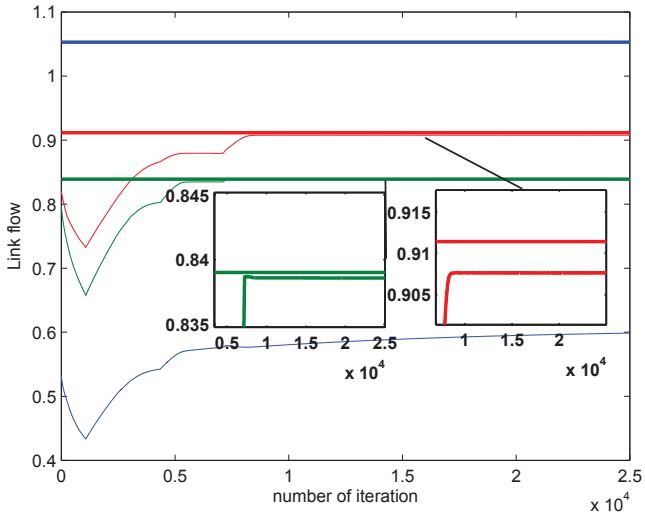

Figure 6.4: Evolution of flow in each link

during each inner iteration, that is, when the Lagrangian parameters are fixed. The derived sub-optimal result is very close to the optimal utility value. For real-time implementation, it is very important to guarantee that the constraints are satisfied all the time. That is, the problem of overflow does not happen. Figure 6.4 shows the aggregate flow for each link over time. When flow rates are approaching the optimal values, the total flow through each link is close to the link capacity limit. There is still plenty of room in Link 1's capacity. However, since other links are already near their capacity limits, the flow in link 1 cannot be increased. This happens because the link capacity in the simulation is generated randomly. Actually, the link capacity should be well designed before installation.

Define the relative error as $e(k) = \left|\frac{U(s_i(k))-U^*}{U^*}\right|$, where $s(k)$ is the rate at time k, and $e(k)$ is the normalized derivation from the optimal point at the kth iteration. The number of iteration K is counted for $e(k)$ to decrease to and stay in the neighborhood $\{e(k)\,|e(k) \leq e_r\}$. For 1% relative error, the algorithm stops after 8201 iterations. Table 6.1 shows the number of information exchange and the corresponding transmission rate. It is easy to see that the communication cost is reduced significantly.

To see the effect of e_r on the algorithm, the error e_r is varied from 0.1% to 10%, while keeping all other parameters unchanged. The resulting Figure 6.5 plots the iteration number K as a function of e_r for the broadcasting event triggered algorithm. As e_r increases from 0.1% to 10%, the iteration number K decreases from 225977 to 1705. There is an underlying result that the number of iterations based on event triggered barrier methods increases

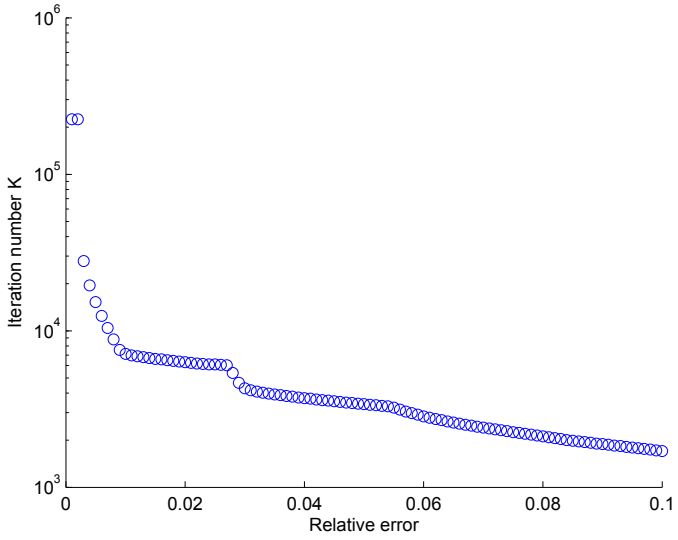

Figure 6.5: Number of iterations with respect to relative errors

dramatically for high precision solutions [62].

6.6 Conclusion

We presented a barrier method for distributed optimization with event triggered communication. The proposed method is applicable to problems with convex objective functions constrained by a convex set. We showed convergence for the algorithm and gave accuracy estimate. Moreover, numerical results show that the application to the network utility maximization problem with local event triggered communication can significantly reduce information exchange between sources and links without loosing accuracy.

Chapter 7

Summary and Conclusions

In this last chapter, we will summarize the contributions of this thesis, discuss some challenging open problems, and present directions for future work.

7.1 Original Contributions

The summary is organized according to the earlier chapters.

Sensing and Actuation Strategies for Event Triggered Optimal Control

Chapter 2 discusses the problem of event triggered sampling and control co-design for first order stochastic systems. A quadratic performance index is considered as the criterion for designing event detectors and controllers in a finite time horizon. The controller co-locates with the actuator but resides on a separate node with the sensor in the network topology. The sensor is connected to the controller through a digital communication network medium. It is assumed that the sensor monitors the state signal continuously with perfect measurements. Nevertheless a strict upper bound is imposed on the number of data transmissions from the sensor over a finite time horizon, and the transmission is mediated by the event detector. There is a plethora of event detectors on the menu, but only three are presented here: deterministic sampling, level-crossing sampling and optimal sampling. Two types of hold circuits are studied: zero order hold and generalized order hold. Their selection is based on their widespread use in practice as well as throughout the literature. For zero order hold, these measurements are directly used for feedback; whereas for generalized hold, these measurements permit us to perform a mean square estimation of the state, and the estimated state is subsequently used for feedback. The feedback gain and the parameter of the event detector are optimized based on a quadratic performance index. The impulse hold in which

the control signal is an impulse, an extreme case of generalized hold, becomes optimal when the control weight of the quadratic performance index is zero. By comparing the different event triggered sensing and actuation schemes, it is demonstrated that level-crossing sampling improves the performance significantly, and generalized hold is desirable for event based control.

Optimal Sampling and Performance Comparison of Periodic and Event Based Impulse Control

In Chapter 3, periodic impulse and event based impulse controls are investigated for a class of second order stochastic systems; the contributions of this work include: (a) providing an optimal sampling period for periodic impulse control; (b) determining an optimal threshold for event based impulse control; (c) obtaining a performance ratio between periodic control and event based control. For event based impulse control, the states are reset to zero whenever the magnitude reaches a given level. As mentioned earlier, the partial differential equations with boundary conditions for the mean first passage time and stationary variance are not simple to solve in two dimensions. To make the problem tractable, second order stochastic systems in the Cartesian coordinates are first converted to first order stochastic systems in the polar coordinates at the cost of losing linearity. Next, the Kolmogorov backward equation is constructed based on the derived first order nonlinear stochastic differential equation. It is shown that the average sampling period can be expressed as an absolutely convergent series. Furthermore, the stationary distribution of the state is obtained by solving the Kolmogorov forward equation. Finally, it is shown that for the same average control rate, event based impulse control outperforms periodic impulse control. It is worth noting that all the calculations are performed analytically.

Event Triggered Synchronization for Multi-agent Networks

In Chapter 4, we further explore the problem of event triggered synchronization for multi-agent systems. In contrast to [18, 69, 127], the objective here is to attain asymptotic consensus which is distinguished from the related work of bounded consensus. All agents in the network are assumed to have identical linear dynamics and a distributed event based control updating method is proposed to achieve synchronization between inter-connected agents under an undirected and connected network. An event detector is configured at each agent to determine when and which neighbor's state should be used to update the controller based on relative state differences. It is worth noting that the event conditions are required to be

checked only at sampling instants. As pointed out in [4], it is more realistic to approximate continuous supervision by a high fast rate sampling. Here an explicit upper bound of the sampling period for event detection is given. In addition, to implement continuous event detectors also requires delicate hardware to monitor local signals, and judge event conditions constantly; this may become a major source of energy consumption. The proposed framework is a generalization of event based control to synchronization of multi-agent systems in two ways: 1) the dynamics of each agent can be of any order, including single- and double-integrator dynamics as special cases; 2) a zero-order hold is used to solve dynamic synchronization problems instead of higher order holds. The main contributions are highlighted as follows:

- A comprehensive case is studied where the dynamics for each agent is described by a general linear system rather than single- or double-integrator dynamics.
- Continuous communication and control algorithms have been relaxed to periodic communication and event based control ones.
- A co-design of control and event detection is realized.

Event Triggered State Estimation via Wireless Sensor Networks

In Chapter 5, event triggered distributed state estimation approaches having a low transmission frequency are proposed which significantly reduce the overall bandwidth consumption, and increase the lifetime of the network. These approaches are an extension of [90] to the event triggered transmission case. Event triggered transmissions pose new challenges to existing design methodologies as novel requirements, like adaptivity, uncertainty, and nonlinearity, arise. Specifically, the sensor node will not receive any information from the neighbors if the events at neighboring sensor nodes are not triggered. In this case, the behavior of neighboring sensors has to be estimated with the aid of the system model and information obtained from neighbors at event instants. After an event has occurred, the sensor broadcasts its predictive state to its neighbors and the state of the internal system models will be re-initialized for both itself and its neighbors. Then, a modified consensus filter is proposed to accommodate the asynchronous information exchange scenario. Formal stability analysis of the proposed filter is provided, and a specific event triggered transmission mechanism is constructed. Additionally, the event conditions can be checked without the knowledge of neighbors' information.

Event Triggered Optimization for Network Utility Maximization Problems

Chapter 6 considers a system viewed as a network of sources and destination nodes. The system goal is to maximize an aggregate of the objective functions of different sources, which is not known by others. Each source updates its own flow rate to achieve the overall optimality. A key difficulty is that each source in fact does not fully know others flow rates. Thus, information exchange through links is necessary to provide the knowledge. This is extremely costly in terms of communication in a large network. The concern here is to determine instants when a source node should broadcast its state to the links that it traverses. Note that such communication events occur at different times for each source node. Also note that a distributed optimization framework is necessitated by the fact that nodes operate in a dynamic and uncertain environment and each node generally has local information which is not available to others. An error based triggering scheme is proposed through which a node calculates the difference between its current state and its state at the last event instant. A node transmits its current state only if the error exceeds a given threshold. In other words, a node does not incur any communication cost unless it detects the derivation of the difference. The analysis is based on a distributed interior-point optimization algorithm for a network utility maximization problem that uses event triggered communication protocols. It is proved that the proposed algorithm converges to the global optimal solution of the network utility maximization problem. Simulation results suggest that the resulting algorithm has a potential to reduce the message exchange.

7.2 Recommendations for Industrial Application

Event triggered communication occurs naturally in many situations from simple servo systems to large factory complexes, computer networks, and biological systems. Many industry processes are triggered by events, not times. Event triggered control techniques and their combination with wireless sensor networks have already been tested in green house climate control [93]. Event Triggered control reduced the number of changes by more than 80% in comparison with a traditional time triggered controller. It allows reduction of the electricity costs and increases the actuator lifetime. Five different event-based sampling strategies have been compared to control of a tank system via wireless sensor networks [103]. The conclusion is made that event triggered approaches are convenient control strategies when the key design constraint is the reduction of exchange of information among control agents or the reduction of the computational load. There are many reasons to use event triggered

communication:

- It is a substitute for human behavior. Event detection is closer to human intelligence. Event detectors have the ability to perform logic operations.
- Event triggered communication can reduce information exchange between sensors, controllers, and actuators. This is equivalent to reduce network bandwidth usages, and save computational sources.
- Sampled-data event detection techniques have an additional advantage of extending the lifetime of battery-powered wireless sensors.
- This type of sampling strategies is more flexible for scheduling between different sensors and subsystems.

Because of these advantages, event triggered communication has been used in industry for some time. Moreover, it is easy to implement. Event detectors may be implemented using application-specific integrated circuits or field-programmable gate array processors. To conduct research on event triggered communication would provide tools for control engineers in better analyzing and designing complex control systems; this would in turn help to improve product quality, safety, and increase economic efficiency in many industrial sectors.

7.3 Open Problems and Future Work

First, we list some unsolved problems in event triggered sampling.

Comparison of Event and Time Triggered Control for Stochastic Higher-order Systems

So far, only first and second order systems are considered for event based impulse control. However, there are several possible extensions that may be worth pursuing but have some difficulties.

Higher order systems: Consider a nonlinear stochastic differential equation

$$dx(t) = f\left(x,t\right)dt + \sigma\left(x,t\right)dw(t), \tag{7.1}$$

where $x(t) \in \mathbb{R}^n$, and $w(t) \in \mathbb{R}^n$ is a Wiener process with incremental covariance Idt. Now introduce the Kolmogorov forward operator

$$\mathscr{L}\phi = -\sum_{i=1}^{n} \frac{\partial}{\partial x_i}\left(\phi f_i\right) + \frac{1}{2}\sum_{i,j,k=1}^{n} \frac{\partial^2}{\partial x_i \partial x_j}\left(\phi \sigma_{ik}\sigma_{jk}\right) \tag{7.2}$$

and the Kolmogorov backward operator

$$\mathscr{L}^* = \sum_{i=1}^{n} f_i \frac{\partial}{\partial x_i} + \frac{1}{2} \sum_{i,j,k=1}^{n} \sigma_{ik}\sigma_{jk} \frac{\partial^2}{\partial x_i \partial x_j}.$$

It can be shown that any unnormalized probability density $p(x,t)$ of the state $x(t)$ satisfies the Fokker-Planck equation [3]

$$\frac{\partial p\,(x,t)}{\partial t} = \mathscr{L} p\,(x,t)$$

and the mean exit time $h_E(x)$ from Ω, starting in x, is given by the Dynkin's equation

$$\mathscr{L}^* h_E = -1 \qquad \text{in } \Omega$$

with $h_E(x) = 0$ on $\partial\Omega$. However, the probability densities and exit times are not easily computable in higher dimensions.

Systems with output feedback: Suppose that the state $x(t)$ is partially observed and obeys the stochastic differential equation in (7.1). The output equation is

$$dy(t) = g\,(x,t)\,dt + dv(t),$$

where $y(t) \in \mathbb{R}^m$, and $v(t) \in \mathbb{R}^m$ is a standard Wiener process independent of $w(t)$. Under suitable regularity conditions, the conditional probability density $\rho(x,t)$ of the state given the observations satisfies the following Duncan-Mortensen-Zakai equation

$$d\rho\,(x,t) = \mathscr{L}\rho\,(x,t)\,dt + \sum_{i=1}^{m} g_i\,(x,t)\,\rho\,(x,t)\,dy_i\,(t)$$

where $\mathscr{L}$ is the Kolmogorov forward operator given in (7.2). However, the existence and uniqueness of solutions for Duncan-Mortensen-Zakai equations are still not well understood.

Event Triggered Output Feedback Control

In general, the goal addressed by event triggered control strategies for deterministic systems is two fold: (1) stabilize the closed-loop system; and (2) derive a strictly positive lower bound for inter-event intervals. The stability for event triggered control systems can be solved by various approaches (see Chapter 1), which is relatively straightforward. The difficulty lies in the way of finding a strictly positive lower bound for inter-event intervals. In the

event triggered state feedback case, the lower bound is derived by differentiating the function $\frac{\|e(t)\|}{\|x(t)\|}$, and with the aid of the comparison principle. Such analysis cannot be extended to the output feedback case analogously by

$$\frac{d}{dt}\frac{\|e\left(t\right)\|}{\|y\left(t\right)\|}=\frac{d}{dt}\frac{e^{T}\left(t\right)e\left(t\right)}{y^{T}\left(t\right)y\left(t\right)}.$$

Suppose $y\left(t\right)=Cx\left(t\right)$. There does not exist such a ρ, which makes

$$\|y\left(t\right)\|_{2}^{2}\geq\rho\left\|x\left(t\right)\right\|_{2}^{2}$$

hold for an arbitrary C. Therefore, the comparison principle is inapplicable.

Event Triggered Control for Multi-agent Systems

The same difficulty exists for event triggered control for multi-agent systems, while the reason of failing to find a strictly positive lower bound of inter-event intervals is not the same. For multi-agent systems, it may happen that all agents in a neighborhood reach consensus locally instead of globally. In this case, events might be triggered frequently due to the local consensus. Moreover, the ultimate trajectory for all agents are not static for higher-order systems. Thus, for node-based approaches, the Zeno behavior cannot be excluded although the consensus can be guaranteed.

Next we summarize some future work below.

Event Triggered Control for Multi-agent Systems

We aim to further explore the consensus problem for multi-agent systems from the pulse modulation point of view. A sampled-data triggering logic was proposed in [78] to overcome the difficulties of obtaining a strictly positive lower bound of inter-event intervals. However, the triggering logic requires periodic communication between neighboring agents. The first task would be to relax this communication pattern from periodic to event triggered transmission. The event detector would use only the local sampled data and the event data received from its neighbors to make the transmission decision. In this sense, the data exchange with neighbors would be greatly reduced, which would ease the local data processing burden of exhaustive utilization of local sensing devices. Moreover, the utilization of a common sampling period for all agents might be restrictive in distributed networks. Employing different sampling periods for different agents would be an interesting extension. Asynchronous sampling is possible for the PWM scheme. The PWM is to modulate the portion of the time that

the signal switches on versus the time that the signal switches off in a fixed interval. After obtaining neighbors' information, each agent would convert the information into the width of a rectangular pulse wave with unit amplitude. Then the pulse wave would be applied to the local agent as an input signal. Future work will also address the generalization to directed topology networks with communication delays as well as disturbances.

Event Triggered Optimization with Applications to Smart Grids

Advanced monitoring, communication, and control capabilities of smart meters and other sensing devices will be essential for the successful management of smart grids [8]. While many of these technologies are well established in their particular areas, the interactions when combining them into a fully functioning cyber-physical system can result in much unexpected behavior. Therefore, rigorous studies will become necessary to evaluate the performance of these systems in order to reveal unintended and potentially harmful interactions between subsystems before deploying such technologies in the field. We propose to investigate the optimal power flow and demand response problems with the aid of modern communication technology extensively to maximize operational efficiency of energy production, transmission, and delivery. The traditional power system infrastructure for communication is power line communication. However, the communication network is the first thing to go down during power disruptions. One way around this problem is to utilize wireless communication networks that operate independently of the main power grid. Sensor nodes in wireless sensor networks are usually powered by batteries, running untethered. They have limited computational and communication resources. These constraints dictate that the amount of information transmits across the network should be limited. One way of doing this is to adopt an event triggered approach to information transmission.

Event Triggered Resilience for Cyber-Physical Systems under Attacks

Cyber security is one of the most important problems in cyber-physical systems. The overall goal of cyber security is to create a safe, secure, and resilient cyber environment. In the context of CPSs, resilience is the ability of a system to continue operating satisfactorily when stressed by unexpected inputs, subsystem failures, environmental conditions, or inputs that are outside the specified operating range. All networked computing systems face risk of malicious attacks. As CPS networks become more open, they are in a more vulnerable situation. There are risks due to illegal access to information, attacks causing physical disruptions in service availability in suppliers, and the possibility of accidental introduction of

malicious codes. System resources can be rendered unavailable through denial of service attacks by congesting the network or system with unnecessary data [96]. Therefore, the sporadic nature of event triggered feedback would be appropriate to determine when to update the control signal.

Appendix A

Stability

There are a number of different types of stability for different formulations of an event triggered control system.

Input-to-State Stability [55]

Consider the system

$$\dot{x} = f(t, x, u) \tag{A.1}$$

where $f : [0, \infty) \times \mathbb{R}^n \times \mathbb{R}^m \to \mathbb{R}^n$ is piecewise continuous in t and locally Lipschitz in x and u. The input $u(t)$ is a piecewise continuous, bounded function of t for all $t \geq 0$. Suppose the unforced system

$$\dot{x} = f(t, x, 0)$$

has a globally uniformly asymptotically stable equilibrium point at the origin $x = 0$.

Definition 37 *A continuous function $\alpha : [0, a) \to [0, \infty)$ is said to belong to class $\mathcal{K}$ if it is strictly increasing and $\alpha(0) = 0$. It is said to belong to class $\mathcal{K}_\infty$ if $a = \infty$ and $\alpha(r) \to \infty$ as $r \to \infty$.*

Definition 38 *A continuous function $\beta : [0, a) \times [0, \infty) \to [0, \infty)$ is said to belong to class $\mathcal{KL}$ if, for each fixed s, the mapping $\beta(r, s)$ belongs to class $\mathcal{K}$ with respect to r and, for each fixed r, the mapping $\beta(r, s)$ is decreasing with respect to s and $\beta(r, s) \to 0$ as $s \to \infty$.*

Definition 39 *The system in (A.1) is said to be input-to-state stable if there exist a class $\mathcal{KL}$ function β and a class $\mathcal{K}$ function γ such that for any initial state $x(t_0)$ and any bounded input $u(t)$, the solution $x(t)$ exists for all $t \geq t_0$ and satisfies*

$$\|x(t)\| \leq \beta(\|x(t_0)\|, t - t_0) + \gamma\left(\sup_{t_0 \leq \tau \leq t} \|u(\tau)\|\right).$$

The Lyapunov-like theorem that follows gives a sufficient condition for input-to-state stability.

Theorem 40 *Let $V : [0,\infty) \times \mathbb{R}^n \to \mathbb{R}$ be a continuously differentiable function such that*

$$\alpha_1(\|x\|) \le V(t,x) \le \alpha_2(\|x\|),$$
$$\frac{\partial V}{\partial t} + \frac{\partial V}{\partial x} f(t,x,u) \le -W_3(x), \qquad \forall \|x\| \ge \rho(\|u\|) > 0$$

$\forall (t,x,u) \in [0,\infty) \times \mathbb{R}^n \times \mathbb{R}^m$, where α_1, α_2 are class $\mathcal{K}_\infty$ functions, ρ is a class $\mathcal{K}$ function, and $W_3(x)$ is a continuous positive definite function on $\mathbb{R}^n$. Then, the system in (A.1) is input-to-state stable with $\gamma = \alpha_1^{-1} \circ \alpha_2 \circ \rho$.

Stability of Time-delay Systems [38]

Let $\mathcal{C} = \mathcal{C}([-r,0],\mathbb{R}^n)$ be the set of continuous functions mapping the interval $[-r,0]$ to $\mathbb{R}^n$, and let $\psi_t \in \mathcal{C}$ be the function ψ defined as $\psi_t(\theta) = \psi(t+\theta)$, $-r \le \theta \le 0$. The general form of a retarded functional differential equation is

$$\dot{x}(t) = f(t, x_t), \tag{A.2}$$

where $x(t) \in \mathbb{R}^n$ and $f : \mathbb{R} \times \mathcal{C} \to \mathbb{R}^n$. Specify the initial state variables $x(t)$ in a time interval of length r, say, from $t_0 - r$ to t_0, i.e.,

$$x_{t_0} = \phi,$$

where $\phi \in \mathcal{C}$ is given. In other words, $x(t_0+\theta) = \phi(\theta)$, $-r \le \theta \le 0$.

For a function $\phi \in \mathcal{C}([-r,0],\mathbb{R}^n)$, define the continuous norm $\|\cdot\|_c$ by

$$\|\phi\|_c = \max_{-r\le\theta\le 0} \|\phi(\theta)\|.$$

Definition 41 *For the system described by (A.2), the trivial solution $x(t) = 0$ is said to be stable if for any $t_0 \in \mathbb{R}$ and any $\epsilon > 0$, there exists a $\delta = \delta(t_0,\epsilon) > 0$ such that $\|x_{t_0}\|_c < \delta$ implies $\|x(t)\| < \epsilon$ for $t \ge t_0$. It is said to be asymptotically stable if it is stable, and for any $t_0 \in \mathbb{R}$ and any $\epsilon > 0$, there exists a $\delta_a = \delta(t_0,\epsilon) > 0$ such that $\|x_{t_0}\|_c < \delta_a$ implies $\lim_{t\to\infty} x(t) = 0$. It is said to be uniformly stable if it is stable and $\delta(t_0,\epsilon)$ can be chosen independently of t_0. It is uniformly asymptotically stable if it is uniformly stable and there exists a $\delta_a > 0$ such that for any $\eta > 0$, there exists a $T = T(\delta_a,\eta)$, such that $\|x_{t_0}\|_c < \delta$ implies $\|x(t)\| < \eta$ for $t \ge t_0 + T$ and $t_0 \in \mathbb{R}$. It is globally (uniformly) asymptotically stable if it is (uniformly) asymptotically stable and δ_a can be an arbitrarily large, finite number.*

The Lyapunov-Krasovskii theorem and Razumikhin theorem will be stated in the following:

Theorem 42 *(Lyapunov-Krasovskii Stability Theorem) Suppose* $f : \mathbb{R} \times \mathcal{C} \to \mathbb{R}^n$ *in (A.2) maps* $\mathbb{R}\times$*(bounded sets in* $\mathcal{C}$*) into a bounded sets in* $\mathbb{R}^n$*, and that* $u, v, w : \bar{R}_+ \to \bar{R}_+$ *are continuous nondecreasing functions, where additionally* $u(s)$ *and* $v(s)$ *are positive for* $s > 0$*, and* $u(0) = v(0) = 0$*. If there exists a continuous differentiable functional* $V : \mathbb{R} \times \mathcal{C} \to \mathbb{R}$ *such that*

$$u(\|\phi(0)\|) \leq V(t, \phi) \leq v(\|\phi\|_c)$$

and

$$\dot{V}(t, \phi) \leq -w(\|\phi(0)\|),$$

then the trivial solution of (A.2) is uniformly stable. If $w(s) > 0$ *for* $s > 0$*, then it is uniformly asymptotically stable. If, in addition,* $\lim_{s\to\infty} u(s) = \infty$*, then it is globally uniformly asymptotically stable.*

Theorem 43 *[41] (Razumikhin Theorem) Suppose* $f : \mathbb{R} \times \mathcal{C} \to \mathbb{R}^n$ *in (A.2) takes* $\mathbb{R}\times$ *(bounded sets of* $\mathcal{C}$*) into bounded sets of* $\mathbb{R}^n$*, and* $u, v, w : \bar{\mathbb{R}}_+ \to \bar{\mathbb{R}}_+$ *are continuous nondecreasing functions,* $u(s)$ *and* $v(s)$ *are positive for* $s > 0$*, and* $u(0) = v(0) = 0$*,* v *strictly increasing. If there exists a continuous differentiable functional* $V : \mathbb{R} \times \mathbb{R}^n \to \mathbb{R}$ *such that*

$$u(\|x\|) \leq V(t, x) \leq v(\|x\|), \text{ for } t \in \mathbb{R} \text{ and } x \in \mathbb{R}^n$$

and the derivative of V *along the solution* $x(t)$ *of (A.2) satisfies*

$$\dot{V}(t, x(t)) \leq -w(\|x(t)\|) \text{ whenever } V(t + \theta, x(t + \theta)) \leq V(t, x(t)) \tag{A.3}$$

for $\theta \in [-r, 0]$*, then system in (A.2) is uniformly stable.*

If, in addition, $w(s) > 0$ *for* $s > 0$*, and there exist a continuous nondecreasing function* $p(s) > s$ *for* $s > 0$ *such that condition in (A.3) is strengthened to*

$$\dot{V}(t, x(t)) \leq -w(\|x(t)\|) \text{ if } V(t + \theta, x(t + \theta)) \leq p(V(t, x(t)))$$

for $\theta \in [-r, 0]$*, then system in (A.2) is uniformly asymptotically stable.*

If in addition $\lim_{s\to\infty} u(s) = \infty$*, then system in (A.2) is globally uniformly asymptotically stable.*

Stability of Impulsive Dynamical Systems [40]

The state-dependent impulsive dynamical system can be written in the form of

$$\dot{x}(t) = f_c(x(t)),\ x(0) = x_0,\ x(t) \notin \mathcal{Z}, \tag{A.4}$$

$$\triangle x(t) = f_d(x(t)),\ x(t) \in \mathcal{Z}. \tag{A.5}$$

Definition 44 **i)** *The zero solution $x(t) \equiv 0$ to (A.4) and (A.5) is Lyapunov stable if, for all $\varepsilon > 0$, there exists $\delta = \delta(\varepsilon) > 0$ such that if $\|x(0)\| < \delta$, then $\|x(t)\| < \varepsilon$, $t \geq 0$.*

ii) *The zero solution $x(t) \equiv 0$ to (A.4) and (A.5) is asymptotically stable if it is Lyapunov stable and there exists $\delta > 0$ such that if $\|x(0)\| < \delta$, then $\lim_{t\to\infty} x(t) = 0$.*

iii) *The zero solution $x(t) \equiv 0$ to (A.4) and (A.5) is exponentially stable if there exist positive constants α, β, and δ such that if $\|x(0)\| < \delta$, then $\|x(t)\| < \alpha \|x(0)\| e^{-\beta t}$, $t \geq 0$.*

iv) *The zero solution $x(t) \equiv 0$ to (A.4) and (A.5) is globally asymptotically stable if it is Lyapunov stable and for all $x(0) \in \mathbb{R}^n$, $\lim_{t\to\infty} x(t) = 0$.*

v) *The zero solution $x(t) \equiv 0$ to (A.4) and (A.5) is globally exponentially stable if there exist positive constants α and β such that $\|x(t)\| < \alpha \|x(0)\| e^{-\beta t}$, $t \geq 0$, for all $x(0) \in \mathbb{R}^n$.*

vi) *Finally, the zero solution $x(t) \equiv 0$ to (A.4) and (A.5) is unstable if it is not Lyapunov stable.*

Theorem 45 *Consider the nonlinear impulsive dynamical system $\mathcal{G}$ given by (A.4) and (A.5). Suppose there exists a continuously differentiable function $V : \mathcal{D} \to [0, \infty)$ satisfying $V(0) = 0$, $V(x) > 0$, $x \in \mathcal{D}$, $x \neq 0$, and*

$$\frac{\partial V(x)}{\partial x} f_c(x) \leq 0,\ x \notin \mathcal{Z}, \tag{A.6}$$

$$V(x + f_d(x)) \leq V(x),\ x \in \mathcal{Z}. \tag{A.7}$$

Then the zero solution $x(t) \equiv 0$ to (A.4) and (A.5) is Lyapunov stable. Furthermore, if the inequality (A.6) is strict for all $x \neq 0$, then the zero solution $x(t) \equiv 0$ to (A.4) and (A.5) is asymptotically stable. Alternatively, if there exist scalars α, β, $\varepsilon > 0$, and $p \geq 1$ such that

$$\alpha \|x\|^p \leq V(x) \leq \beta \|x\|^p,\ x \in \mathcal{D},$$

$$\frac{\partial V(x)}{\partial x} f_c(x) \leq -\varepsilon V(x),\ x \notin \mathcal{Z},$$

and (A.7) holds, then the zero solution $x(t) \equiv 0$ to (A.4) and (A.5) is exponentially stable. Finally, if, in addition, $\mathcal{D} = \mathbb{R}^n$ and

$$V(x) \to \infty \text{ as } \|x\| \to \infty,$$

then the above asymptotic and exponential stability results are global.

Stability of Hybrid Dynamical Systems [34]

The model of a hybrid system can be represented in the following form:

$$\begin{cases} x \in C & \dot{x} \in F(x), \\ x \in D & x^+ \in G(x), \end{cases}$$

where C is the *flow set*, F is the *flow map*, D is the *jump set*, and G is the *jump map*.

Definition 46 *(Uniform global pre-asymptotic stability (UGpAS)) Consider a hybrid system $\mathcal{H}$ on $\mathbb{R}^n$. Let $\mathcal{A} \subset \mathbb{R}^n$ be closed. The set $\mathcal{A}$ is said to be*

- *uniformly globally stable for $\mathcal{H}$ if there exists a class-$\mathcal{K}_\infty$ function α such that any solution ϕ to $\mathcal{H}$ satisfies $|\phi(t,j)|_{\mathcal{A}} \leq \alpha(|\phi(0,0)|_{\mathcal{A}})$ for all $(t,j) \in \operatorname{dom}\phi$;*
- *uniformly globally pre-attractive for $\mathcal{H}$ if for each $\varepsilon > 0$ and $r > 0$ there exists $T > 0$ such that, for any solution ϕ with $|\phi(0,0)|_{\mathcal{A}} \leq r$, $(t,j) \in \operatorname{dom}\phi$ and $t + j \geq T$ imply $|\phi(t,j)|_{\mathcal{A}} \leq \varepsilon$;*
- *uniformly globally pre-asymptotically stable for $\mathcal{H}$ if it is both uniformly globally stable and uniformly globally pre-attractive.*

Theorem 47 *(Sufficient Lyapunov conditions) Let $\mathcal{H} = (C, F, D, G)$ be a hybrid system and let $\mathcal{A} \subset \mathbb{R}^n$ be closed. If V is a Lyapunov function candidate for $\mathcal{H}$ and there exist α_1, $\alpha_2 \in \mathcal{K}_\infty$, and a continuous $\rho \in \mathcal{PD}$ such that*

$$\begin{aligned} \alpha_1(|x|_{\mathcal{A}}) &\leq V(x) \leq \alpha_2(|x|_{\mathcal{A}}) \quad \forall x \in C \cup D \cup G(D), \\ \langle \nabla V(x), f \rangle &\leq -\rho(|x|_{\mathcal{A}}) \quad \forall x \in C,\ f \in F(x), \\ V(g) - V(x) &\leq -\rho(|x|_{\mathcal{A}}) \quad \forall x \in D,\ g \in G(x), \end{aligned}$$

then $\mathcal{A}$ is uniformly globally pre-asymptotically stable for $\mathcal{H}$.

Appendix B

Stochastic Control Theory

We now present some basic concepts and important results in stochastic control theory used in deriving the results in Chapter 2, Chapter 3, and Chapter 5.

Probability Space [89]

Definition 48 *If Ω is a given set, then a σ-algebra $\mathcal{F}$ on Ω is a family $\mathcal{F}$ of subsets of Ω with the following properties:*

(i) $\emptyset \in \mathcal{F}$

(ii) $F \in \mathcal{F} \Rightarrow F^C \in \mathcal{F}$, *where* $F^C = \Omega \backslash F$ *is the complement of* F *in* Ω

(iii) $A_1, A_2, \ldots \in \mathcal{F} \Rightarrow A := \cup_{i=1}^{\infty} A_i \in \mathcal{F}$.

The pair $(\Omega, \mathcal{F})$ *is called a* measurable space. *A* probability measure P *on a measurable space* $(\Omega, \mathcal{F})$ *is a function* $P : \mathcal{F} \longrightarrow [0, 1]$ *such that*

(a) $P(\emptyset) = 0, \qquad P(\Omega) = 1$

(b) *if* $A_1, A_2, \ldots \in \mathcal{F}$ *and* $\{A_i\}_{i=1}^{\infty}$ *is* disjoint *then*

$$P\left(\cup_{i=1}^{\infty} A_i\right) = \sum_{i=1}^{\infty} P(A_i).$$

The triple $(\Omega, \mathcal{F}, P)$ *is called a* probability space.

If $(\Omega, \mathcal{F}, P)$ is a given probability space, then a function $Y : \Omega \to \mathbb{R}$ is called $\mathcal{F}$-*measurable* if

$$Y^{-1}(U) := \{\omega \in \Omega; Y(\omega) \in U\} \in \mathcal{F}$$

for all open sets $U \in \mathbb{R}^n$.

Suppose $0 \leq S \leq T$ and $f(t,\omega)$ is given. Define the Itô integral

$$\int_S^T f(t,\omega)\, dB_t(\omega),$$

where B_t is 1-dimensional Brownian motion. An important property of the Itô integral is that [89]

$$E\left[\int_S^T f(t,\omega)\, dB_t(\omega)\right] = 0.$$

Solutions of Linear Stochastic Differential Equations [3]

Consider

$$dx = A(t)\, x dt + dB, \tag{B.1}$$

where x is an n-dimensional vector, $\{B(t), t \in T\}$ an n-dimensional Wiener process with incremental covariance $R_1 dt$. It is assumed that the initial value $x(t_0)$ is a normal random variable with mean m_0 and covariance R_0.

The solution of (B.1) can be written as

$$x(t) = \Phi(t;t_0)\, x(t_0) + \int_{t_0}^t \Phi(t;s)\, dB(s), \tag{B.2}$$

where Φ satisfies the differential equation

$$\frac{d\Phi(t;t_0)}{dt} = A(t)\, \Phi(t;t_0)$$

with the initial condition

$$\Phi(t_0;t_0) = I.$$

The properties of the solution of (B.2) is summarized as follows.

Theorem 49 *The solution of the stochastic differential equation is a normal process with mean value $m_x(t)$ and covariance $R(s,t)$ where*

$$\begin{aligned}
\frac{dm_x}{dt} &= A(t)\, m_x, \\
m_x(t) &= m_0, \\
R(s,t) &= \begin{cases} \Phi(s;t)\, P(t) & s \geq t, \\ P(s)\, \Phi^T(t;s) & s \leq t, \end{cases} \\
\frac{dP}{dt} &= AP + PA^T + R_1, \\
P(t_0) &= R_0.
\end{aligned}$$

The Cost over A Fixed Finite Time Interval [57]

Here the process is of interest over the finite interval $[0, T]$ only, and the process stops on hitting the boundary of the region G. Let $g(\cdot)$ be a continuous and bounded function on $R^k \times [0, T]$. The process will stop if it hits the boundary of G before time T. If this occurs at time $s < T$ and the exit point is x, then the penalty will be $g(x, s)$. If the process does not exit G before time T, then the cost will be $g(x(T), T)$. It is, therefore, natural to set the problem up with a terminal value imposed at time $t = T$. The problem may be rewritten as an initial value problem if desired. Then the cost, starting at point $x \in G^0$ at time $t < T$, is

$$W(x, T) = \mathbb{E}_{x,t}\left[\int_t^{T\wedge\tau} k(x(s))\, ds + g(x(T \wedge \tau), T \wedge \tau)\right].$$

From a formal point of view, it can be shown that $W(\cdot)$ satisfies the PDE

$$\frac{\partial W(x,t)}{\partial t} + \mathscr{L}W(x,t) + k(x) = 0$$

for $x \in G^0$, $t < T$, together with $W(x, T) = g(x, T)$. We also have $W(y, t) \to g(x, t)$ as $y \to x \in \partial G$ for regular points x and

$$\mathbb{E}_{x,t}W(x(\tau \wedge T), \tau \wedge T) = \mathbb{E}_{x,t}g(x(\tau \wedge T), \tau \wedge T).$$

Martingales [24]

Definition 50 *A* filtration *is a family $\mathcal{M} = \{\mathcal{M}_t\}_{t\geq 0}$ of σ-algebras $\mathcal{M}_t \subset \mathcal{F}$ such that*

$$0 \leq s < t \Rightarrow \mathcal{M}_s \subset \mathcal{M}_t.$$

An n-dimensional stochastic process $\{M_t\}_{t\geq 0}$ on $(\Omega, \mathcal{F}, P)$ is called a martingale with respect to a filtration $\{\mathcal{M}_t\}_{t\geq 0}$ if

(i) *M_t is $\mathcal{M}_t$-measurable for all t,*

(ii) *$\mathbb{E}[|M_t|] < \infty$ for all t and*

(iii) *$\mathbb{E}[M_s|\mathcal{M}_t] = M_t$ for all $s \geq t$.*

Theorem 51 *[24] If $u(t, x)$ is a polynomial in t and x with*

$$\frac{\partial u}{\partial t} + \frac{1}{2}\frac{\partial^2 u}{\partial x^2} = 0, \tag{B.3}$$

then $u(t, B_t)$ is a martingale.

Examples of functions that satisfy (B.3) are $\exp(\theta x - \theta^2 t/2)$, x, $x^2 - t$, $x^3 - 3tx$, $x^4 - 6x^2t + 3t^2 \cdots$

Appendix C

Algebraic Graph Theory

Some facts from algebraic graph theory are reviewed [33, 20, 84]. A *graph* is a pair $\mathcal{G} = (\mathcal{V}, \mathcal{E})$ of sets such that $\mathcal{E} \subseteq \mathcal{V} \times \mathcal{V}$. The elements of $\mathcal{V}$ are the *vertices* of the graph $\mathcal{G}$; the elements of $\mathcal{E}$, 2-element subsets of $\mathcal{V}$, are its *edges*. A vertex v is incident with an edge e if $v \in e$; then e is an edge at v. Two vertices x, y of $\mathcal{G}$ are *adjacent*, or *neighbors*, if xy is an edge of $\mathcal{G}$. A *path* is a non-empty subgraph $\mathcal{P} = (\mathcal{V}', \mathcal{E}')$ of $\mathcal{G}$ of the form

$$\mathcal{V}' = \{i_0, i_1, \ldots i_k\} \qquad \mathcal{E}' = \{i_0 i_1, i_1 i_2, \ldots, i_{k-1} i_k\},$$

where the i_j are all distinct. A non-empty graph $\mathcal{G}$ is called *connected* if any two of its vertices are linked by a path in $\mathcal{G}$.

Assigning an arbitrary direction to each edge, then the $N \times m$ *incidence matrix* $\mathcal{D}$ is thus defined as

$$\mathcal{D} = [d_{ij}],$$

where

$$d_{ij} = \begin{cases} -1, & \text{if } v_i \text{ is the tail of } e_j, \\ 1, & \text{if } v_i \text{ is the head of } e_j, \\ 0, & \text{otherwise.} \end{cases}$$

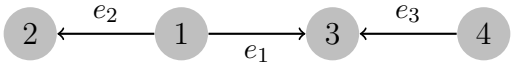

Figure C.1: An undirected graph with 4 vertices that is arbitrarily oriented

For example, the incidence matrix associated with the graph $\mathcal{G}$ that has been oriented in Figure C.1 is

$$\mathcal{D} = \begin{bmatrix} -1 & -1 & 0 \\ 0 & 1 & 0 \\ 1 & 0 & 1 \\ 0 & 0 & -1 \end{bmatrix}.$$

All incidence matrices have a column sum equal to zero, since every edge has to have exactly one tail and one head as can be seen from this example.

The *Laplacian* and *edge Laplacian* for an arbitrary oriented graph $\mathcal{G}$ is defined as

$$\mathcal{L} = \mathcal{D}\mathcal{D}^T, \quad \text{and} \quad \mathcal{L}_e = \mathcal{D}^T\mathcal{D},$$

respectively. The definitions directly reveal that the Laplacian and edge Laplacian are both symmetric and positive semi-definite matrices; and it follows that they have the same nonzero eigenvalues with the same multiplicities from the fact that

$$\det\left(I - \mathcal{D}\mathcal{D}^T\right) = \det\left(I - \mathcal{D}^T\mathcal{D}\right).$$

For a connected graph, the Laplacian matrix has exactly a single zero eigenvalue and the corresponding eigenvector is the vector of ones, that is,

$$\mathcal{L}\mathbf{1} = \mathbf{0}.$$

For a connected graph with Laplacian matrix $\mathcal{L}$, let λ_2 be the smallest positive eigenvalue and λ_N the maximum eigenvalue of $\mathcal{L}$; two important variational characterizations of them are given below:

$$\lambda_2 = \min_{x \perp \mathbf{1}, \|x\|_2 = 1} x^T\mathcal{L}x, \qquad \lambda_N = \max_{\|x\|_2 = 1} x^T\mathcal{L}x.$$

Appendix D

Matrix Theory

We now present some results from matrix theory used in deriving the results in Chapter 4 and Chapter 5 [47, 48].

Kronecker Products [58]

The kronecker product is an operation on two matrices $A = [a_{ij}]$ and B of arbitrary size, resulting in a block matrix, which is defined as $A \otimes B = [a_{ij}B]$. Some properties of the Kronecker product are given as follows:

1. $\|A \otimes I\|_2 = \|A\|_2$.
2. $(A \otimes B)^T = A^T \otimes B^T$.
3. $A \otimes (B + C) = A \otimes B + A \otimes C$ (distributivity).
4. For scalar k, $(kA) \otimes B = A \otimes (kB) = k(A \otimes B)$.
5. For compatible matrices, $(A \otimes B)(C \otimes D) = AC \otimes BD$.
6. For square nonsingular matrices A and B: $(A \otimes B)^{-1} = A^{-1} \otimes B^{-1}$.
7. For a square matrix A, $A \otimes I$ and A have the same eigenvalues without considering their multiplicity.

Matrix Inversion Lemma

Matrix inversion lemma, also known as Woodbury matrix identity, is

$$(A + UCV)^{-1} = A^{-1} - A^{-1}U\left(C^{-1} + VA^{-1}U\right)^{-1}VA^{-1}$$

where A, U, C and V all denote matrices of the correct size.

Appendix E

Convex Optimization

We now present some concepts and results on convex functions used in deriving the results in Chapter 6 [12].

Definition 52 *A function* $f : \mathbb{R}^n \to \mathbb{R}$ *is convex if* $\mathbf{dom}\ f$ *is convex set and if for all* $x, y \in \mathbf{dom}\ f$, *and* θ *with* $0 \leq \theta \leq 1$, *it holds*

$$f\left(\theta x + (1-\theta)\, y\right) \leq \theta f\left(x\right) + (1-\theta)\, f\left(y\right). \tag{E.1}$$

A function f *is strictly convex if strict inequality holds in (E.1) whenever* $x \neq y$ *and* $0 \leq \theta \leq 1$. *The function* f *is concave if* $-f$ *is convex, and strictly concave if* $-f$ *is strictly convex.*

For example, $\log x$ is concave on $\mathbb{R}_{++}$.
Now introduce two operations that preserve convexity or concavity of functions.

1. A nonnegative weighted sum of convex functions,

$$f = w_1 f_1 + \cdots + w_m f_m,$$

is convex. Similarly, a nonnegative weighted sum of concave functions is concave. A nonnegative, nonzero weighted sum of strictly convex (concave) functions is strictly convex (concave).

2. Suppose $f : \mathbb{R}^n \to \mathbb{R}$, $A \in \mathbb{R}^{n \times m}$, and $b \in \mathbb{R}^n$. Define $g : \mathbb{R}^m \to \mathbb{R}$ by

$$g\left(x\right) = f\left(Ax + b\right),$$

with $\mathbf{dom}\ g = \{x \,|Ax + b \in \mathbf{dom}\ f\}$. Then if f is convex, so is g; if f is concave, so is g.

Definition 53 *A function $f : \mathbb{R}^n \to \mathbb{R}$ is said to be closed if, for each $\alpha \in \mathbb{R}$, the sublevel set*

$$\{x \in \mathbf{dom}\ f \,|\, f(x) \leq \alpha\}$$

is closed.

For example, the functions $f(x) = -\log x$ with $\mathbf{dom}\ f = \mathbb{R}_{++}$ and

$$f(x) = -\sum_{i=1}^{m} \log\left(b_i - a_i^T x\right)$$

with $\mathbf{dom}\ f = \left\{x \,\middle|\, a_i^T x < b_i,\ i = 1, \ldots, m\right\}$ are closed.

Assume f is strongly convex on a sublevel set S, so there are positive constants m and M such that

$$mI \leq \nabla^2 f(x) \leq MI$$

for all $x \in S$. The lower and upper bounds on the Hessian imply for any $x, y \in S$,

$$\nabla f(x)^T (y - x) + \frac{m}{2} \|y - x\|_2^2 \leq f(y) - f(x) \leq \nabla f(x)^T (y - x) + \frac{M}{2} \|y - x\|_2^2 .$$

Bibliography

[1] M. Aigner and G. Ziegler. *Proofs from the Book*. Springer, fourth edition, 2010.

[2] B. Anderson and J. Moore. *Optimal Filtering*. Dover Publications, 2005.

[3] K. Åström. *Introduction to Stochastic Control Theory*. New York: Dover Publications, 2006.

[4] K. Åström. Event based control. In A. Astolfi and L. Marconi, editors, *Analysis and Design of Nonlinear Control Systems: In Honor of Alberto Isidori*, pages 127–147. Berlin/Heidelberg: Springer, 2008.

[5] K. Åström and B. Wittenmark. *Computer-Controlled Systems: Theory and Design*. Dover Publications, 3rd, reprint edition, 2011.

[6] K. J. Åström and B. M. Bernhardsson. Comparison of Riemann and Lebesgue sampling for first order stochastic systems. In *Proc. of the 41st IEEE Conf. on Decision and Control*, pages 2011–2016, December 2002.

[7] G. Battistelli, A. Benavoli, and L. Chisci. Data-driven communication for state estimation with sensor networks. *Automatica*, 48(5):926–935, 2012.

[8] A. Bergen and V. Vittal. *Power Systems Analysis*. Prentice Hall, 2nd edition, 2000.

[9] D. P. Bertsekas. *Dynamic Programming and Optimal Control*, volume I. Athena Scientific, 3 edition, 2005.

[10] D. P. Bertsekas. *Dynamic Programming and Optimal Control*, volume II. Athena Scientific, 4 edition, 2012.

[11] S. Boyd, L. El Ghaoui, E. Feron, and V. Balakrishnan. *Linear Matrix Inequalities in System and Control Theory*, volume 15 of *SIAM Studies in Applied Mathematics*. Society for Industrial Mathematics, 1994.

[12] S. Boyd and L. Vandenberghe. *Convex Optimization*. Cambridge, U.K.: Cambridge University Press, 2004.

[13] R. Brown and P. Hwang. *Introduction to Random Signals and Applied Kalman Filtering with Matlab Exercises*. John Wiley & Sons, 4 edition, 2012.

[14] E. F. Camacho and C. B. Alba. *Model Predictive Control*. Springer, 2004.

[15] C. Cassandras. Event-driven control, communication, and optimization. In *Proc. of 32nd Chinese Control Conference (CCC)*, pages 1–5, 2013.

[16] M. G. Cea and G. C. Goodwin. Event based sampling in non-linear filtering. *Control Engineering Practice*, 20(10):963–971, 2012.

[17] X. Chen and F. Hao. Event-triggered average consensus control for discrete-time multi-agent systems. *IET Control Theory Appl.*, 6(16):2493–2498, 2012.

[18] O. Demir and J. Lunze. Event-based synchronisation of multi-agent systems. In *Proc. 4th IFAC Conf. on Analysis and Design of Hybrid Systems*, pages 1–6, 2012.

[19] O. Demir and J. Lunze. Optimal and event-based networked control of physically interconnected systems and multi-agent systems. *Int. J. Control*, 87(1):169–185, 2014.

[20] R. Diestel. *Graph Theory*. Springer, 4th edition, 2010.

[21] D. V. Dimarogonas, E. Frazzoli, and K. H. Johansson. Distributed event-triggered control for multi-agent systems. *IEEE Trans. Autom. Control*, 57(5):1291 –1297, 2012.

[22] H. Dong, Z. Wang, D. Ho, and H. Gao. Robust $\mathcal{H}_\infty$ filtering for Markovian jump systems with randomly occurring nonlinearities and sensor saturation: the finite-horizon case. *IEEE Transactions on Signal Processing*, 59(7):3048–3057, 2011.

[23] M. Donkers and W. Heemels. Output-based event-triggered control with guaranteed $\mathcal{L}_\infty$-gain and improved and decentralized event-triggering. *IEEE Trans. Autom. Control*, 57(6):1362 –1376, 2012.

[24] R. Durrett. *Probability: Theory and Examples*. Cambridge University Press, 4 edition, 2010.

[25] Y. Fan, G. Feng, Y. Wang, and C. Song. Distributed event-triggered control of multi-agent systems with combinational measurements. *Automatica*, 49(2):671–675, 2013.

[26] F. Forni, S. Galeani, D. Nešić, and L. Zaccarian. Event-triggered transmission for linear control over communication channels. *Automatica*, 50(2):490–498, 2014.

[27] E. Fridman, A. Seuret, and J. Richard. Robust sampled-data stabilization of linear systems: an input delay approach. *Automatica*, 40(8):1441–1446, 2004.

[28] E. Garcia and P. Antsaklis. Parameter estimation in time-triggered and event-triggered model-based control of uncertain systems. *Int. J. Control*, 85(9):1327–1342, 2012.

[29] E. Garcia and P. J. Antsaklis. Model-based event-triggered control for systems with quantization and time-varying network delays. *IEEE Trans. Autom. Control*, 58(2):422–434, 2013.

[30] E. Garcia, Y. Cao, H. Yu, P. Antsaklis, and D. Casbeer. Decentralised event-triggered cooperative control with limited communication. *Int. J. Control*, 86(9):1479–1488, 2013.

[31] C. W. Gardiner. *Handbook of Stochastic Methods: for Physics, Chemistry and the Natural Sciences*. New York: Springer, 3rd edition, 2004.

[32] P. Gawthrop and L. Wang. Event-driven intermittent control. *Int. J. Control*, 82(12):2235–2248, 2009.

[33] C. Godsil and G. Royle. *Algebraic Graph Theory*. Springer, 2001.

[34] R. Goebel, R. G. Sanfelice, and A. R. Teel. *Hybrid Dynamical Systems: Modeling, Stability, and Robustness*. Princeton University Press, 2012.

[35] N. Gordon, B. Ristic, and S. Arulampalam. *Beyond the Kalman filter: Particle Filters for Tracking Applications*. Artech House, 2004.

[36] R. Grone and R. Merris. The Laplacian spectrum of a graph II. *SIAM Journal on Discrete Mathematics*, 7:221, 1994.

[37] L. Grüne and J. Pannek. *Nonlinear Model Predictive Control*. Springer, 2011.

[38] K. Gu, J. Chen, and V. L. Kharitonov. *Stability of Time-Delay Systems*. Birkhäuser Boston, 2003.

[39] A. Hać. *Wireless Sensor Network Designs*. John Wiley & Sons, 2003.

[40] W. M. Haddad, V. Chellaboina, and S. G. Nersesov. *Impulsive and Hybrid Dynamical Systems: Stability, Dissipativity, and Control*. Princeton University Press, 2006.

[41] J. Hale and S. Lunel. *Introduction to Functional Differential Equations*. Springer, 1993.

[42] W. Heemels and M. Donkers. Model-based periodic event-triggered control for linear systems. *Automatica*, 49(3):698–711, 2013.

[43] W. Heemels, M. Donkers, and A. Teel. Periodic event-triggered control for linear systems. *IEEE Trans. Autom. Control*, 58(4):847–861, 2013.

[44] W. Heemels, K. Johansson, and P. Tabuada. An introduction to event-triggered and self-triggered control. In *Proc. of 51st IEEE Conf. on Decision and Control*, pages 3270–3285, December 2012.

[45] W. Heemels, J. Sandee, and P. Van Den Bosch. Analysis of event-driven controllers for linear systems. *Int. J. Control*, 81(4):571–590, 2008.

[46] T. Henningsson, E. Johannesson, and A. Cervin. Sporadic event-based control of first-order linear stochastic systems. *Automatica*, 44(11):2890–2895, 2008.

[47] R. A. Horn and C. R. Johnson. *Matrix Analysis*. Cambridge university press, 2012.

[48] A. S. Householder. *The Theory of Matrices in Numerical Analysis*. Courier Dover Publications, 2013.

[49] J. Hu, G. Chen, and H. Li. Distributed event-triggered tracking control of leader-follower multi-agent systems with communication delays. *Kybernetika*, 47(4):630–643, 2011.

[50] J. Hu, Y. Zhou, and Y. Lin. Second-order multiagent systems with event-driven consensus control. *Abstract and Applied Analysis*, 2013, 2013.

[51] S. Hu and D. Yue. Event-triggered control design of linear networked systems with quantizations. *ISA transactions*, 51:153–162, 2011.

[52] S. Hu and D. Yue. Event-based $\mathcal{H}_\infty$ filtering for networked system with communication delay. *Signal Processing*, 92(9):2029–2039, 2012.

[53] L. Jetto and V. Orsini. Supervised stabilisation of linear discrete-time systems with bounded variation rate. *IET Control Theory Appl.*, 2(10):917–929, 2008.

[54] I. Karatzas and S. Shreve. *Brownian Motion and Stochastic Calculus*. Springer, second edition, 1991.

[55] H. K. Khalil. *Nonlinear Systems*. Prentice Hall, third edition, 2002.

[56] E. Kofman and J. H. Braslavsky. Level crossing sampling in feedback stabilization under data-rate constraints. In *Proc. of the 45th IEEE Conf. on Decision and Control*, pages 4423–4428, December 2006.

[57] H. J. Kushner and P. G. Dupuis. *Numerical Methods for Stochastic Control Problems in Continuous Time*. Springer, 2 edition, 2001.

[58] A. J. Laub. *Matrix Analysis for Scientists and Engineers*. SIAM: Society for Industrial and Applied Mathematics, 2005.

[59] E. A. Lee and S. A. Seshia. *Introduction to Embedded Systems - A Cyber-Physical Systems Approach*. LeeSeshia.org, 2011.

[60] D. Lehmann and J. Lunze. Extension and experimental evaluation of an event-based state-feedback approach. *Control Engineering Practice*, 19(2):101–112, 2011.

[61] D. Lehmann and J. Lunze. Event-based control with communication delays and packet losses. *Int. J. Control*, 85(5):563–577, 2012.

[62] M. Lemmon. *Networked Control Systems*, volume 406 of *Lecture Notes in Control and Information Sciences*, chapter Event-triggered feedback in control, estimation, and optimization, pages 293–358. Berlin/Heidelberg: Springer, 2011.

[63] S. Li, D. Sauter, and B. Xu. Fault isolation filter for networked control system with event-triggered sampling scheme. *Sensors*, 11(1):557–572, 2011.

[64] W. Li, S. Zhu, C. Chen, and X. Guan. Distributed consensus filtering based on event-driven transmission for wireless sensor networks. In *Proc. of the 31st Chinese Control Conference*, pages 6588–6593, 2012.

[65] G. Lipsa and N. Martins. Remote state estimation with communication costs for first-order LTI systems. *IEEE Trans. Autom. Control*, 56(9):2013–2025, 2011.

[66] Q. Liu, Z. Wang, X. He, and D. Zhou. A survey of event-based strategies on control and estimation. *Systems Science & Control Engineering*, 2(1):90–97, 2014.

[67] Z. Liu and Z. Chen. Reaching consensus in networks of agents via event-triggered control. *Journal of Information & Computational Science*, 8(3):393–402, 2011.

[68] Z. Liu, Z. Chen, and Z. Yuan. Event-triggered average-consensus of multi-agent systems with weighted and direct topology. *J. Syst. Sci. Complex*, 25(5):845–855, 2012.

[69] D. Liuzza, D. V. Dimarogonas, M. di Bernardo, K. H. Johansson, et al. Distributed model-based event-triggered control for synchronization of multi-agent systems. In *Proc. 9th IFAC Symposium on Nonlinear Control Systems*, pages 329–334, 2013.

[70] D. Luenberger and Y. Ye. *Linear and Nonlinear Programming*. Springer, 3 edition, 2008.

[71] J. Lunze and D. Lehmann. A state-feedback approach to event-based control. *Automatica*, 46(1):211–215, 2010.

[72] J. M. Maciejowski. *Predictive Control: with Constraints*. Pearson education, 2002.

[73] J. W. Marck and J. Sijs. Relevant sampling applied to event-based state-estimation. In *Proc. of the 2010 Fourth International Conference on Sensor Technologies and Applications*, pages 618–624, 2010.

[74] M. Mazo and P. Tabuada. Decentralized event-triggered control over wireless sensor/actuator networks. *IEEE Trans. Autom. Control*, 56(10):2456 –2461, 2011.

[75] M. Meinel, M. Ulbrich, and S. Albrecht. A class of distributed optimization methods with event-triggered communication. *Computational Optimization and Applications*, 57(3):517–553, 2014.

[76] X. Meng and T. Chen. Event-based stabilization over networks with transmission delays. *Journal of Control Science and Engineering*, 2012:1–8, 2012.

[77] X. Meng and T. Chen. Optimal sampling and performance comparison of periodic and event based impulse control. *IEEE Trans. Autom. Control*, 57(12):3252 – 3259, 2012.

[78] X. Meng and T. Chen. Event based agreement protocols for multi-agent networks. *Automatica*, 49(7):2123–2132, 2013.

[79] X. Meng and T. Chen. Event-driven communication for sampled-data control systems. In *Proc. of American Control Conference (ACC)*, pages 3002–3007, 2013.

[80] X. Meng and T. Chen. Event detection and control co-design of sampled-data systems. *Int. J. Control*, 87(4):777–786, 2014.

[81] X. Meng and T. Chen. Event triggered robust filter design for discrete-time systems. *IET Control Theory Appl.*, 8(2):104–113, 2014.

[82] X. Meng and T. Chen. Optimality and stability of event triggered consensus state estimation for wireless sensor networks. In *Proc. of American Control Conference (ACC)*, pages 3565–3570, 2014.

[83] X. Meng, B. Wang, T. Chen, and M. Darouach. Sensing and actuation strategies for event triggered stochastic optimal control. In *Proc. of IEEE 52nd Conf. on Decision and Control*, pages 3097–3102, 2013.

[84] M. Mesbahi and M. Egerstedt. *Graph Theoretic Methods in Multiagent Networks*. Princeton University Press, 2010.

[85] M. Miskowicz. Event-based sampling strategies in networked control systems. In *Proc. of 10th IEEE Workshop on Factory Communication Systems (WFCS)*, pages 1–10, 2014.

[86] B. Mohar. Eigenvalues, diameter, and mean distance in graphs. *Graphs and Combinatorics*, 7(1):53–64, 1991.

[87] A. Molin and S. Hirche. On the optimality of certainty equivalence for event-triggered control systems. *IEEE Trans. Autom. Control*, 58(2):470–474, 2013.

[88] V. Nguyen and Y. Suh. Improving estimation performance in networked control systems applying the send-on-delta transmission method. *Sensors*, 7(10):2128–2138, 2007.

[89] B. Øksendal. *Stochastic Differential Equations: An Introduction with Applications*. Springer, 6th edition, 2003.

[90] R. Olfati-Saber. Kalman-consensus filter: optimality, stability, and performance. In *Proceedings of the 48th IEEE Conference on Decision and Control*, pages 7036–7042, 2009.

[91] D. P. Palomar and M. Chiang. A tutorial on decomposition methods for network utility maximization. *Selected Areas in Communications, IEEE Journal on*, 24(8):1439–1451, 2006.

[92] D. P. Palomar and M. Chiang. Alternative distributed algorithms for network utility maximization: Framework and applications. *IEEE Trans. Autom. Control*, 52(12):2254–2269, 2007.

[93] A. Pawlowski, J. Guzman, F. Rodríguez, M. Berenguel, J. Sanchez, and S. Dormido. Simulation of greenhouse climate monitoring and control with wireless sensor network and event-based control. *Sensors*, 9(1):232–252, 2009.

[94] C. Peng and Q. Han. A novel event-triggered transmission scheme and control co-design for sampled-data control systems. *IEEE Trans. Autom. Control*, 58(10):2620–2626, 2013.

[95] C. Peng and T. Yang. Event-triggered communication and $\mathcal{H}_\infty$ control co-design for networked control systems. *Automatica*, 49(5):1326–1332, 2013.

[96] R. Poisel. *Modern Communications Jamming: Principles and Techniques*. Artech House, 2011.

[97] M. Rabi, K. Johansson, and M. Johansson. Optimal stopping for event-triggered sensing and actuation. In *Proc. of the 47th IEEE Conference on Decision and Control*, pages 3607–3612, 2008.

[98] M. Rabi, G. Moustakides, and J. Baras. Adaptive sampling for linear state estimation. *SIAM J. Control Optim.*, 50(2):672–702, 2012.

[99] C. Ramesh, H. Sandberg, and K. Johansson. Design of state-based schedulers for a network of control loops. *IEEE Trans. Autom. Control*, 58(8):1962–1975, 2013.

[100] J. B. Rawlings and D. Q. Mayne. *Model Predictive Control: Theory and Design*. Nob Hill Pub., 2009.

[101] W. Ren and R. Beard. *Distributed Consensus in Multi-Vehicle Cooperative Control: Theory and Applications*. Springer, 2008.

[102] W. Ren and Y. Cao. Convergence of sampled-data consensus algorithms for double-integrator dynamics. In *Proc. of the 47th IEEE Conference on Decision and Control*, pages 3965–3970, 2008.

[103] J. Sánchez, M. Guarnes, and S. Dormido. On the application of different event-based sampling strategies to the control of a simple industrial process. *Sensors*, 9(9):6795–6818, 2009.

[104] G. Seyboth, D. V. Dimarogonas, and K. H. Johansson. Event-based broadcasting for multi-agent average consensus. *Automatica*, 49(1):245–252, 2013.

[105] J. Sijs and M. Lazar. Event based state estimation with time synchronous updates. *IEEE Trans. Autom. Control*, 57(10):2650–2655, 2012.

[106] D. Simon. *Optimal State Estimation: Kalman, $\mathcal{H}_\infty$, and Nonlinear Approaches*. John Wiley & Sons, 2006.

[107] Y. Suh, V. Nguyen, and Y. Ro. Modified Kalman filter for networked monitoring systems employing a send-on-delta method. *Automatica*, 43(2):332–338, 2007.

[108] P. Tabuada. Event-triggered real-time scheduling of stabilizing control tasks. *IEEE Trans. Autom. Control*, 52(9):1680–1685, 2007.

[109] P. Tallapragada and N. Chopra. On event triggered tracking for nonlinear systems. *IEEE Trans. Autom. Control*, 58(9):2343–2348, 2013.

[110] S. Trimpe and R. D'Andrea. Event-based state estimation with variance-based triggering. In *Proc. of the 51st IEEE Conference on Decision and Control*, pages 6583–6590, Maui, Hawaii, USA, 2012.

[111] V. Vasyutynskyy and K. Kabitzsch. Event-based control: Overview and generic model. In *Proc. of 8th IEEE International Workshop on Factory Communication Systems (WFCS)*, pages 271–279, 2010.

[112] B. Wang, X. Meng, and T. Chen. Event based pulse-modulated control of linear stochastic systems. *IEEE Trans. Autom. Control*, 59(8):2144–2150, 2014.

[113] X. Wang and M. Lemmon. Event-triggering in distributed networked control systems. *IEEE Trans. Autom. Control*, 56(3):586–601, 2011.

[114] X. Wang and M. Lemmon. On event design in event-triggered feedback systems. *Automatica*, 47(10):2319–2322, 2011.

[115] E. Wei, A. Ozdaglar, and A. Jadbabaie. A distributed newton method for network utility maximization–i: Algorithm. *IEEE Trans. Autom. Control*, 58(9):2162–2175, 2013.

[116] J. Wu, Q. Jia, K. Johansson, and L. Shi. Event-based sensor data scheduling: trade-off between communication rate and estimation quality. *IEEE Trans. Autom. Control*, 58(4):1041–1046, 2013.

[117] F. Xiao, X. Meng, and T. Chen. Average sampled-data consensus driven by edge events. In *Proc. of 31st Chinese Control Conf.*, pages 6239–6244, 2012.

[118] D. Xie, D. Yuan, J. Lu, and Y. Zhang. Consensus control of second-order leader–follower multi-agent systems with event-triggered strategy. *Transactions of the Institute of Measurement and Control*, 35(4):426–436, 2013.

[119] X. Yin and D. Yue. Event-triggered tracking control for heterogeneous multi-agent systems with markov communication delays. *Journal of the Franklin Institute*, 350(5):1312–1334, 2013.

[120] H. Yu and P. Antsaklis. Event-triggered output feedback control for networked control systems using passivity: Achieving $\mathcal{L}_2$ stability in the presence of communication delays and signal quantization. *Automatica*, 49(1):30–38, 2013.

[121] H. Yu and P. Antsaklis. Output synchronization of networked passive systems with event-driven communication. *IEEE Trans. Autom. Control*, 59(3):750–756, 2014.

[122] D. Yue, E. Tian, and Q. Han. A delay system method for designing event-triggered controllers of networked control systems. *IEEE Trans. Autom. Control*, 58(2):475–481, 2013.

[123] X. Zhang and Q. Han. Network-based $\mathcal{H}_\infty$ filtering using a logic jumping-like trigger. *Automatica*, 49(5):1428–1435, 2013.

[124] Z. Zhang, F. Hao, L. Zhang, and L. Wang. Consensus of linear multi-agent systems via event-triggered control. *Int. J. Control*, 87(6):12431251, 2014.

[125] F. Zhao and L. Guibas. *Wireless Sensor Networks: An Information Processing Approach*. Morgan Kaufmann, 2004.

[126] M. Zhong and C. Cassandras. Asynchronous distributed optimization with event-driven communication. *IEEE Trans. Autom. Control*, 55(12):2735–2750, 2010.

[127] W. Zhu, Z. Jiang, and G. Feng. Event-based consensus of multi-agent systems with general linear models. *Automatica*, 50(2):552–558, 2014.